VE-PTP Inhibits GEF-H1 to Stabilize VE-cadherin Junctions in Endothelial Cells

BY

Vanessa V. Juettner
B.A., Cornell College, Mount Vernon, 2007
M.S., Colorado State University, Fort Collins, 2008

THESIS

Submitted as partial fulfillment of the requirements
for the degree of
Doctor of Philosophy in Cellular and Molecular Pharmacology
in the Graduate College of the
University of Illinois at Chicago, 2019

Chicago, Illinois

Defense Committee:
Dr. Asrar Malik, Chair and Advisor
Dr. Yulia Komarova
Dr. Dolly Mehta
Dr. Andrei Karginov
Dr. Jan Kitajewski, UIC Physiology and Biophysics

I dedicate this thesis to my husband and daughter for their unconditional love and support.

ACKNOWLEDGEMENTS

I would like to thank my advisor, Dr. Malik, for supporting my scientific development in the Pharmacology PhD program. I appreciate all of the opportunities for me to present my research at conferences, review research articles, and connect with established scientists in the field. Without these opportunities, I would not have gained the confidence and skills necessary to propel my career forward. Thank you also to my co-advisor, Dr. Komarova, who has guided me every step of the way and has been a constant source of support in my development as a scientist. Both Dr. Malik and Dr. Komarova have been tremendous in helping me balance motherhood and PhD candidacy. They both have shown me great understanding and compassion throughout my time in the Pharmacology department. I am forever grateful. Also, I would like to thank my committee members, Dr. Karginov, Dr. Mehta, and Dr. Kitajewski for their time, encouragement, and constructive feedback, which has helped to strengthen my research project.

There are many other people who have helped me immensely throughout my project. Dr. Toth and Ke in the imaging core have always been happy to take the time and help me with any issues or questions I have about my imaging experiments. Dr. Gao and Guilan have been a constant and friendly source of help if I needed anything for my studies or had any questions.

I would also like to thank the lab members of the Malik and Komarova labs. Both past and present lab members have always been ready to help if I needed anything. Whether it's sharing supplies, helping with an experiment, or answering questions, they are always happy to lend their support. The people that I've met and the friends that I've made during my time in the Pharmacology department will be with me always.

And finally, I would like to thank the most important people in my life – my family. My amazing husband who has always given me unconditional love and support, which has gotten me through the roughest of days. His faith in me and his unending encouragement have given me the fortitude to achieve my aspirations. My daughter, Lily, who brings so much joy and love to my life. Her smiles and hugs have lifted me up day after day. She has truly been my strength and my motivation. I am also forever thankful for my parents and my husband's parents, as well as our grandparents and siblings, who have always been there to give their help and support. I couldn't have asked for a more generous and loving family.

Contribution of Authors

Chapter 1 is a review of the literature of significance to my research question. Chapter 3 and 4 shows a series of my own currently unpublished experiments which will become a publication in the Journal of Cell Biology this year (2019). My advisors, A.B. Malik and Y.A. Komarova, contributed to conceiving the project, interpreting the data, and writing the manuscript. V.V. Juettner performed all of the experiments, except those specifically attributed to other authors. K. Kruse performed immunofluorescent staining and analysis; A. Dan performed micropillar array assays; V. Vu performed traction force microscopy; Y. Kahn generated VE-PTP deletion constructs for mammalian and bacterial expression; J. Le performed western blot; A.B. Malik, Y.A. Komarova, and D.E. Leckband provided critical discussion of the project. Chapter 5 represents the culmination of the research shown in this dissertation and my overall conclusions. The future directions of my research field and my research question are discussed.

LIST OF FIGURES

LIST OF ABBREVIATIONS

AJ	Adherens Junction
Ang-1	Angiopoetin-1
CFP	Cyan Fluorescent Protein
CHO	Chinese Hamster Ovary
CSK	c-Src tyrosine kinase
DEP-1	Density-enhanced phosphatase-1
DSP	Dual specificity protein tyrosine phosphatase
EC	Endothelial Cell
FLD	Fibronectin-Like Domain
EC-5	Extracellular Domain 5
FN	Fibronectin
FRET	Förster Resonance Energy Transfer
GAP	GTPase Activating Protein
GDI	Guanine Dissociation Inhibitor
GDP	Guanosine Diphosphate
GEF	Guanine Nucleotide Exchange Factor
GEF-H1	Guanine Nucleotide Exchange factor H1
GFP	Green Fluorescent Protein
GTP	Guanosine Triphosphate
HIF	Hypoxia-inducible Factor
HPAEC	Human Pulmonary Arterial Endothelial Cell
ICAM-1	Intracellular Adhesion Molecule-1
IF	Immunofluorescent
IP	Immunoprecipitation
KD	Knockdown
LPS	Lipopolysaccharide
MKP	MAP kinase phosphatase
MLCII	non-muscle Myosin II Light Chain
MLCK	Myosin Light Chain Kinase
MLCP	Myosin Light Chain Phosphatase
MLEC	Mouse Lung Endothelial Cell
MTM	Myotubularins
NOX	Nicotinamide adenine dinucleotide phosphate oxidase
NT	Non-Targeting
NRPTP	Non-receptor protein tyrosine phosphatase
PHD2	Prolyl Hydroxylase domain-containing protein 2
PI	Phosphatase Inactive
PRL	Phosphatases of the regenerating liver
PTEN	Phosphatase and tensin homologue
Pyk2	Proline-rich tyrosine kinase 2
RBC	Red Blood Cell
ROCK	Rho-associated coiled-coil forming protein kinase
RPTP	Receptor-like protein tyrosine phosphatase
SFK	Src family kinases

SHP2	Src homology 2-domain containing tyrosine phosphatase
Tiam1	T-cell Lymphoma Invasion and Metastasis-inducing Protein 1
TJ	Tight Junction
TNF	Tumor Necrosis Factors
TSad	T-cell specific adaptor
VCAM-1	Vascular adhesion molecule-1
VE-cadherin	Vascular Endothelial-cadherin
VEGF	Vascular Endothelial Growth Factor
VE-PTP	Vascular Endothelial Protein Tyrosine Phosphatase
WT	Wild-type
YFP	Yellow Fluorescent Protein

SUMMARY

Blood vessels are lined with an endothelial cell (EC) monolayer that forms a semi-permeable barrier between the blood and surrounding interstitium (Del Vecchio et al., 1987; Pappenheimer et al., 1951). ECs within a continuous endothelium are connected by interendothelial junctions which are responsible for regulating trans-endothelial protein flux and leukocyte trafficking (Feng et al., 1998; Fujita et al., 1991; Siflinger-Birnboim et al., 1987). They therefore contribute to maintaining tissue-fluid homeostasis and innate immune mechanisms (Broermann et al., 2011; Vestweber, 2012; Yeh et al., 2018; Zhao et al., 2017). Disruption of interendothelial junctions leads to increased endothelial permeability as seen in inflammatory states, resulting in increased flux of plasma protein into the tissue, edema formation, and trafficking of inflammatory cells (Broermann et al., 2011; Lee and Slutsky, 2010; Mamdouh et al., 2009).

Adherens junctions (AJs) are complexes formed between endothelial cells which are responsible for regulating the paracellular permeability pathway, and are composed of the adhesive protein Vascular Enodothelial (VE)-cadherin (Breviario et al., 1995; Lampugnani et al., 1995; Navarro et al., 1995). Phosphorylation and dephosphorylation of VE-cadherin on tyrosine residues located in its cytoplasmic domain (Esser et al., 1998; Lampugnani et al., 1997; Nawroth et al., 2002) causes the dissociation of p120-catenin and β-catenin from VE-cadherin, leading to increased VE-cadherin internalization, thus weakening the endothelial barrier (Baumeister et al., 2005; Chiasson et al., 2009; Potter et al., 2005; Xiao et al., 2005)

Vascular Endothelial Protein Tyrosine Phosphatase (VE-PTP) is a key EC-specific tyrosine phosphatase that binds VE-cadherin through its membrane proximal fibronectin-like domain at amino acids 1449-1619 (Nawroth et al., 2002). VE-PTP stabilizes the endothelial barrier through

supporting homotypic VE-cadherin adhesion, which contributes to keeping basal endothelial permeability low (Broermann et al., 2011; Nottebaum et al., 2008; Vockel and Vestweber, 2013; Wessel et al., 2014). Knockdown of VE-PTP increases endothelial permeability and leukocyte extravasation (Nottebaum et al., 2008) whereas preventing VE-PTP and VE-cadherin dissociation inhibits leukocyte extravasation and permeability (Broermann et al., 2011).

RhoGTPases also have an essential role in regulating endothelial integrity and the actin cytoskeleton, particularly Rac1 and RhoA. VE-cadherin outside-in signaling regulates the balance of Rac1 and RhoA to ensure the maintenance of the endothelial barrier. Rac1 induces actin polymerization whereas RhoA causes stress fiber formation and actomyosin contractility. Additionally, Rac1 counteracts RhoA activity and stabilizes VE-cadherin trans-interaction through suppression of actomyosin tension (Daneshjou et al., 2015). Therefore, the balance between RhoA and Rac1 activity is critical for VE-cadherin turnover.

In our studies, we have found that VE-PTP can regulate RhoA activity, but not Rac1 activity in the resting endothelium. RhoA signaling involves the activation of Rho-associated coiled-coil forming protein kinase (ROCK) which causes myosin II dephosphorylation and disassembly of the actomyosin cytoskeleton. This process promotes the tension that is applied to VE-cadherin adhesion.

While previous studies have focused on the relationship of VE-PTP and VE-cadherin in activated endothelial cells (Broermann et al., 2011; Nottebaum et al., 2008; Vockel and Vestweber, 2013), little is known about the role of VE-PTP in the resting endothelium. Although VE-PTP depletion in the endothelium increases endothelial permeability, it has minimal effect on VE-cadherin phosphorylation (Nottebaum et al., 2008). These findings raise the possibility that VE-PTP regulates basal endothelial permeability independently of its enzymatic activity. Here we

report a novel phosphatase-independent adaptor function of VE-PTP that is required to stabilize VE-cadherin junctions and restrict basal endothelial permeability.

In the first part of this thesis, we evaluated the role of VE-PTP in VE-cadherin internalization using the photo-convertable protein Dendra2 in the resting endothelium. We observed the effect of VE-PTP knockdown on endothelial permeability and VE-cadherin turnover at the AJ, then generated various VE-PTP constructs to determine the importance of VE-PTP domains in VE-cadherin internalization. We observed that VE-PTP knockdown increased VE-cadherin internalization and endothelial permeability, whereas overexpression of VE-PTP decreased VE-cadherin internalization. Deletion of VE-PTP's 17^{th} extracellular domain, however, did not result in decrease VE-cadherin internalization indicating that interaction with VE-cadherin is important for VE-PTP-dependent stabilization.

Additionally, we investigated the role of VE-PTP phosphatase activity on VE-cadherin internalization in the resting endothelium. We found that overexpression of phosphatase inactive VE-PTP decreased VE-cadherin internalization similar to wild-type VE-PTP. Treatment of a confluent, resting endothelium with a VE-PTP phosphatase inhibitor, AKB-9785, also had no effect on VE-cadherin internalization suggesting that VE-PTP phosphatase activity is not important in the unstimulated endothelium. Furthermore, we determined the importance of the entire VE-PTP cytosolic domain and discovered that this deletion resulted in no change in VE-cadherin stabilization suggesting a scaffolding function of VE-PTP.

In the second part of this thesis, we determine the role of VE-PTP in RhoGTPase activity. We show that VE-PTP binds directly to the RhoGEF, GEF-H1, and inhibits GEF-H1 activity in the resting endothelium. Using FRET biosensors for RhoA and VE-cadherin tension, we discovered that VE-PTP knockdown increased RhoA activity and the tension applied to VE-

cadherin in a confluent, unstimulated endothelium. GEF-H1 knockdown was able to rescue the VE-PTP phenotype in the RhoA and tension experiments as well as in VE-cadherin internalization experiments. Additionally, overexpression of WT and phosphatase inactive VE-PTP reduced RhoA activity and VE-cadherin tension in the resting endothelium. Interestingly, overexpression of phosphatase inactive VE-PTP in the endothelium stimulated with thrombin failed to retain its ability to reduce VE-cadherin tension, suggesting that VE-PTP's phosphatase activity is more important in the stimulated endothelium.

In summary, we describe a novel phosphatase-independent mechanism by which VE-PTP stabilizes VE-cadherin junctions. VE-PTP functions as a scaffold that binds and inhibits GEF-H1 activity. This limits RhoA-dependent tension across VE-cadherin junctions and reduces the VE-cadherin internalization rate to stabilize adherens junctions.

1. LITERATURE REVIEW

1.1 The Regulation of Endothelial Permeability and VE-cadherin Junctions

The endothelium lines the inner walls of the vasculature to form a semi-permeable barrier between the blood and surrounding tissue. This monolayer of endothelial cells controls the passive movement of fluids and proteinaceous solutes, as well as the inflammatory-mediated extravasation of leukocytes. The transport of proteins and leukocytes across the endothelium occurs either through the transcellular or paracellular pathway. The transcellular pathway is responsible for transport across the endothelial cell body via caveolae-mediated vesicular trafficking, whereas the paracellular pathway facilitates transport between neighboring endothelial cells(Yuan and Rigor, 2010). Under physiological settings, the passage of plasma proteins is predominantly mediated by the transcellular pathway, while passage of small molecules such as fluids and solutes utilize the paracellular pathway(Schulte et al., 2011; Woodfin et al., 2011). The interendothelial junctions which connect endothelial cells into a contiguous monolayer are responsible for the permeability of the paracellular route.

The two main types of interendothelial junctions are AJs and tight junctions (TJs). AJs are comprised of VE-cadherin adhesion complexes that restrict permeability of the endothelial vessel wall to proteins and macromolecules. TJs are less developed as compared to AJs, except within the brain and retinal barrier, which restrict the passage of smaller molecules (<1 kDa)(Liebner et al., 2000; Majno and Palade, 1961; Schulte et al., 2011; Woodfin et al., 2011). Increased permeability of the paracellular pathway is the leading cause of tissue edema and involves the flux of protein-rich fluid across the endothelial monolayer(Radeva and Waschke, 2018). Therefore, disruption of AJs is largely responsible for leakage of protein-rich fluids and the formation of interstitial edema.

VE-cadherin and its associated catenin proteins form the main adhesion complex of the AJs(Radeva and Waschke, 2018). VE-cadherin directly interacts with p120- and β-catenin proteins, which regulate the internalization and degradation of VE-cadherin, respectively. Specifically, β-catenin regulates VE-cadherin proteolysis while p120 catenin is responsible for VE-cadherin retention at the plasma membrane by inhibiting clathrin-mediated endocytosis(Chiasson et al., 2009; Davis et al., 2003; Miyashita and Ozawa, 2007; Xiao et al., 2005). Both p120- and β-catenin also regulate the attachment of the VE-cadherin complex to the actin cytoskeleton through interaction with α-catenin to stabilize VE-cadherin adhesions(Komarova et al., 2017).

Tyrosine phosphorylation of VE-cadherin and catenin proteins is a major determinant regulating the binding affinity of VE-cadherin to catenin proteins(Collares-Buzato et al., 1998; Matsuyoshi et al., 1992; Volberg et al., 1992; Young et al., 2003). Src family tyrosine kinases (c-Src, Lyn, Fyn, Yes) induce the phosphorylation of VE-cadherin-catenin complexes whereas tyrosine phosphatases (DEP-1, RPTPμ, and VE-PTP) act to reverse VE-cadherin phosphorylation and enhance or restore barrier function(Balsamo et al., 1998; Eliceiri et al., 1999; Han et al., 2013; Holsinger et al., 2002; Nottebaum et al., 2008; Piedra et al., 2003).

VE-PTP is the only known endothelial-specific protein tyrosine phosphatase that has been established as a key regulator of the endothelial barrier through its interaction with VE-cadherin(Broermann et al., 2011; Nawroth et al., 2002; Nottebaum et al., 2008). VE-PTP dephosphorylates VE-cadherin's tyrosine residues to stabilize VE-cadherin at the AJs and to decrease endothelial permeability(Allingham et al., 2007; Broermann et al., 2011; Monaghan-Benson and Burridge, 2013). Interestingly, VE-PTP also directly interacts with endothelial Tie2 tyrosine kinase receptor. VE-PTP dephosphorylates Tie2 to inhibit Ang1/Tie2 signaling and to

increase endothelial permeability(Fachinger et al., 1999; Frye et al., 2015). Induction of the Ang1/Tie2 pathway has been shown to prevent both inflammation and VEGF-induced vascular hyper-permeability(Frye et al., 2015; Thurston et al., 1999) indicating that Tie2-mediated signaling can enhance endothelial barrier function. Hence, depending upon intracellular localization and interacting partners, VE-PTP can play a dual role in the regulation of AJs and endothelial barrier function.

1.2. The Role of Tyrosine Phosphorylation of VE-cadherin and Associated Catenin Proteins in Regulating the Endothelial Barrier

1.2.1. Tyrosine Kinases

The first studies that describe a correlation between tyrosine phosphorylation of VE-cadherin and catenin proteins utilized permeability-inducing agents, such as vascular endothelial growth factor (VEGF), α-thrombin, and tumor necrosis factor (TNF)α(Andriopoulou et al., 1999; Esser et al., 1998). These agents demonstrate an ability to induce VE-cadherin tyrosine phosphorylation and destabilize the AJs causing an increase in endothelial permeability. Pro-angiogenic growth factor, VEGF, leads to tyrosine phosphorylation of VE-cadherin, β- and γ-catenin proteins and a subsequent increase in endothelial permeability(Esser et al., 1998). α-Thrombin and other permeability-inducing agents, also promote the overall tyrosine phosphorylation state of VE-cadherin, p120-, β- and γ-catenin proteins, thereby further providing evidence for tyrosine phosphorylation of constituents of VE-cadherin complexes in association with increased endothelial permeability (Andriopoulou et al., 1999; Angelini et al., 2006; Ukropec et al., 2000).

Specific phosphorylation sites of VE-cadherin have been identified through site-directed mutagenesis and the use of phospho-specific antibodies(Allingham et al., 2007; Monaghan-Benson and Burridge, 2013; Wallez et al., 2007). In a study by Allingham et al(Allingham et al., 2007) the specific tyrosine sites of VE-cadherin involved in leukocyte migration had been identified for the first time. Endothelial cells that were pre-treated with TNFα and sequentially incubated with human leukemic monocytes (THP-1 cells) demonstrated an increased level in VE-cadherin phosphorylation at both tyrosines (Y) 658 and 731 residues indicating that leukocyte trans-endothelial migration is associated with VE-cadherin phosphorylation. The role of these sites has been further addressed in subsequent studies where it has been shown that over-expression of GFP-tagged VE-cadherin phospho-defective mutants resulted in reduced trans-endothelial migration of myeloid cells(Allingham et al., 2007). Furthermore, mutation of both Y658 and Y731 residues to alanine prevented VEGF-induced permeability(Monaghan-Benson and Burridge, 2013) thus establishing a causal link between tyrosine phosphorylation of VE-cadherin and increased permeability of endothelial barrier. A study in Chinese hamster ovary (CHO) cells stably overexpressing VE-cadherin unveiled the phosphorylation of VE-cadherin's Y685 site upon stimulation of cells with VEGF or overexpression of constitutively active Src(Wallez et al., 2007) indicating Src as a major regulator of AJ stability. Phosphorylation of Y685 and Y731 was also confirmed *in vivo*. Interestingly, Y685 was found to be exclusively involved in vascular permeability induction, whereas Y731 was only involved in leukocyte extravasation, or binding.(Wessel et al., 2014) Furthermore, VE-cadherin is phosphorylated in Y658 and Y685 in veins, but not in arteries due to activation of Src in veins' response to shear stress. This study indicates that phosphorylation of VE-cadherin is not sufficient to increase endothelial permeability alone, but requires convergent signaling pathways induced by pro-

inflammatory mediators(Orsenigo et al., 2012). These studies established an important concept that phosphorylation of specific sites of VE-cadherin play a significant role in regulating vascular permeability and leukocyte transmigration in the context of responses to inflammation.

Numerous tyrosine kinases have been implicated in the regulation of endothelial barrier integrity through the phosphorylation of catenin proteins, constituents of the AJ complex. Src family kinases expressed in endothelial cells (c-Src, Lyn, Fyn and Yes) can each differentially phosphorylate the constituents of the VE-cadherin complex in response to permeability-inducing agents(Piedra et al., 2003; Wallez et al., 2007). Src phosphorylates both VE-cadherin at Y658 and β-catenin at Y654 via the C-terminal Src kinase SH2 domain to restrict binding to β-catenin or α-catenin, respectively, and hence destabilizes the AJs(Komarova et al., 2017; Lilien and Balsamo, 2005; Wallez et al., 2007). Both Fyn and Yes kinases phosphorylate β-catenin at Y142, which interferes with β-catenin interaction to both VE-cadherin and α-catenin(Piedra et al., 2003). In c-Src knockout mice, VEGF-induced phosphorylation of VE-cadherin was partially inhibited as compared to wild-type mice indicating a crucial role of c-Src in regulating VE-cadherin phosphorylation. Furthermore, inhibition of Src kinases with the selective inhibitor SKI-606, prevented VEGF-induced endothelial permeability exhibiting the role of Src family kinases (SFK) in opening the endothelial junction(Weis et al., 2004). Other constituent kinases of the AJs include c-Src tyrosine kinase (CSK) and proline-rich tyrosine kinase 2 (Pyk2). Similarly to SFK, Pyk2 induces increased endothelial permeability through VE-cadherin phosphorylation at Y658 and Y731(Cain et al., 2010) in response to TNFα. Although it remains a point of debate whether Pyk2 phosphorylates VE-cadherin directly or indirectly, *via* activation of c-Src(Allingham et al., 2007), the role of Pyk2 in mediating disruption of AJs is generally accepted. In contrast to Pyk2, CSK is recruited to VE-cadherin through binding to phosphorylated Tyr685 and can inhibit c-Src via

phosphorylation of Y527(Baumeister et al., 2005). This suggests negative feed-back loop regulation of c-Src that prevents the deleterious effect of protracted VE-cadherin phosphorylation. These studies began to demonstrate the complex nature of the intracellular signaling responsible for VE-cadherin tyrosine phosphorylation and the regulation of AJ integrity.

1.2.2 Tyrosine Phosphatases

VE-cadherin phosphorylation is reversed by protein tyrosine phosphatases (PTPs), which stabilize the VE-cadherin-catenin complex by opposing the effect of tyrosine kinases on constituents of the junctional complex(Nottebaum et al., 2008; Timmerman et al., 2012). Inhibitors used against tyrosine phosphatases impair the junctional integrity of endothelial cells at basal state(Young et al., 2003) suggesting that basal activities of PTPs are required for the maintenance of endothelial barrier function. Many phosphatases such as PTP1B, SH2-containing phosphotyrosine phosphatase (SHP2), protein tyrosine phosphatase receptor type M (RPTPμ), density-enhanced phosphatase-1 (DEP-1), and vascular endothelial protein tyrosine phosphatase (VE-PTP) are constituents of the VE-cadherin adhesion complex(Balsamo et al., 1998; Dejana et al., 2008; Nawroth et al., 2002; Nottebaum et al., 2008; Timmerman et al., 2012). Both RPTPμ and VE-PTP directly bind VE-cadherin(Nawroth et al., 2002; Sui et al., 2005) in order to continuously dephosphorylate VE-cadherin and thereby promote AJ stability. DEP-1 and SHP-2 associate indirectly with the VE-cadherin complex(Grazia Lampugnani et al., 2003; Ukropec et al., 2000). DEP-1 binds to p120- and β-catenin proteins, whereas SHP-2 binds selectively to β-catenin and induces reannealing of AJs post-injury. PTP1B is required for β-catenin dephosphorylation at Tyr654, which prevents its dissociation from VE-cadherin.

Among protein tyrosine phosphatases, VE-PTP is the only known phosphatase of which the expression is restricted to endothelial cells suggesting a tissue-specific function of this phosphatase (Baumer et al., 2006; Fachinger et al., 1999). The unique expression and function of VE-PTP has led to extensive interest in VE-PTP's role in endothelial barrier integrity.

1.3 VE-PTP

1.3.1. PTP Classification and Structure

VE-PTP belongs to the Class I receptor-like protein tyrosine phosphatases. Class I PTPs contain a distinct sequence motif, $HC(X)_5R$, and are separated into two general groups: Classical PTPs and Dual Specificity PTPs (Figure 1). Classical PTPs, which are highly substrate-selective, contain both receptor-like (RPTPs) and non-receptor (NRPTPs) protein tyrosine phosphatases. RPTPs localize at the plasma membrane whereas NRPTPs localize in the cytoplasm. Substrate selectivity of Classical PTPs is attributed to both the catalytic domain and flanking non-catalytic regions on the cytoplasmic side. The non-catalytic domains target the PTP to a certain location within the cell and facilitates substrate recognition and binding(Alonso et al., 2004; Tiganis and Bennett, 2007).

Twelve of the twenty-one RPTPs contain two adjacent cytosolic PTP domains - the membrane-proximal catalytic domain and more distal domain with weak or no catalytic activity - while the remaining nine members of RPTPs contain a single PTP domain. RPTP extracellular domains contain variations of cell adhesion molecule-like sequence motifs that are homologous to fibronectin III (FN3), immunoglobulin (Ig), and mephrin/A5/μ domains(Beltran and Bixby, 2003; Xu and Fisher, 2012). These domains involved in cell-cell or cell-matrix interactions tether the RPTP to specific intracellular locations where they dephosphorylate target proteins in order to

establish control of cell adhesion. VE-PTP and DEP-1 which contains numerous fibronectin extracellular repeats belong to RPTP subfamily (Figure 1)(Xu and Fisher, 2012).

VE-PTP is the murine homologue of human PTPβ (gene PTPRB). The major murine 11kb VE-PTP transcript, which is translated into a 1998 amino acid protein, was first identified through a PCR screening of genomic DNA and subsequent reverse transcription of the mRNA of mouse brain microvascular endothelial cells(Fachinger et al., 1999). VE-PTP protein is comprised of an extracellular region containing seventeen fibronectin III-like domains. A transmembrane segment links these extracellular domains to a single cytoplasmic tyrosine phosphatase VE-PTP domain(Krueger and Saito, 1992; Krueger et al., 1990) that is responsible for the phosphatase enzymatic activity (Figure 2).

Dual specificity PTPs (DSPs) contain a variety of PTPs which are less conserved and have minimal similarities in sequence aside from the $HC(X)_5R$ signature motif (Patterson et al., 2009; Tonks, 2006). Interestingly, DSPs have smaller catalytic domains and can facilitate dephosphorylation of serine and threonine residues as well as tyrosine residues, therefore exhibiting a broader substrate base. DSPs contain six subgroups based on sequence similarity, and include: Slingshots, mitogen-activated protein kinase phosphatases (MKPs), cell division cycle 14 (CDC14) phosphatases, Myotubularins (MTMs), phosphatase and tensin homologues (PTEN), phosphatases of generating liver (PRL), and Atypical DSPs (Patterson et al., 2009). Among the wide variety of DSPs, the most notable are the MAPK phosphatases (MKPs), which harbor high specificity for the localization of MAPK proteins and the dephosphorylation of MAPK tyrosine and threonine residues (Patterson et al., 2009; Schumacher et al., 2002; Tonks, 2006). These DSPs are therefore important regulators of the MAPK pathway.

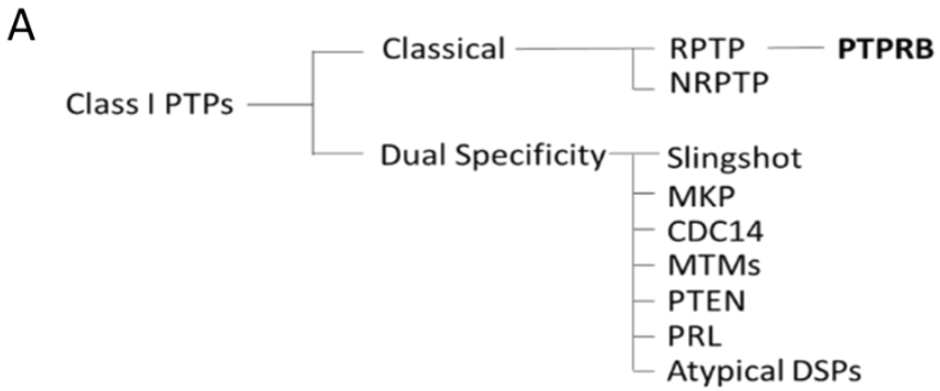

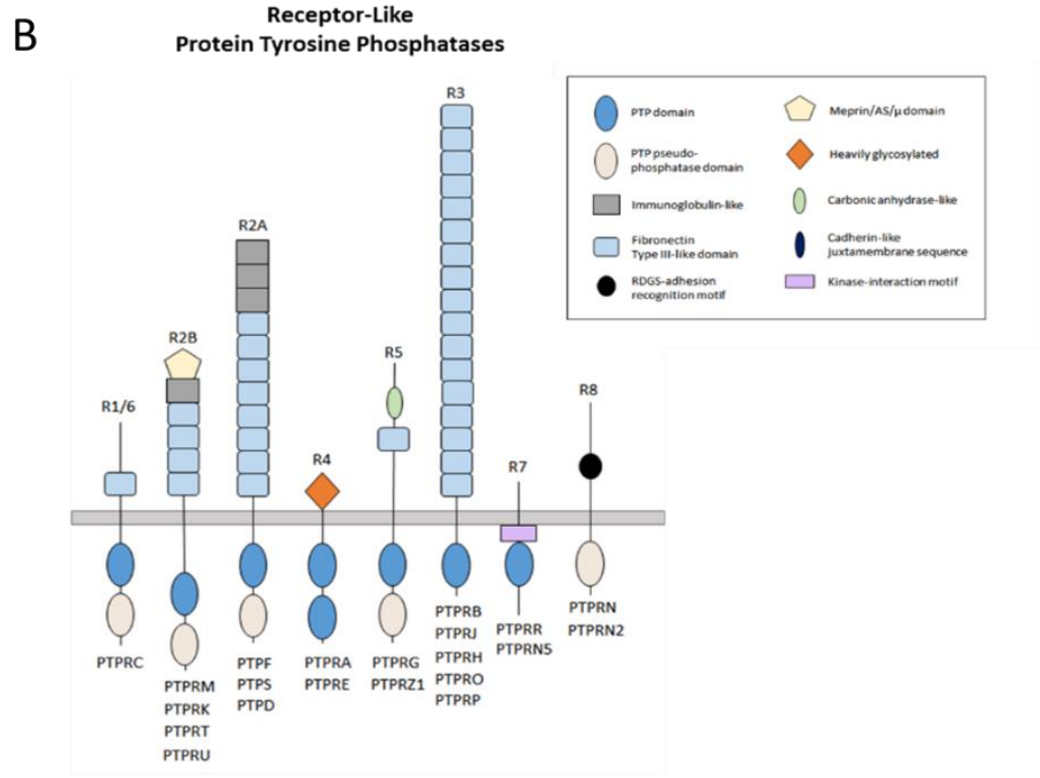

Figure 1. Protein Tyrosine Phosphatases. (A) Class I Protein Tyrosine Phosphatases containing classical and dual specificity PTPs. PTPRB (VE-PTP) is a Class I classical receptor-like PTP (RPTP), which typically localizes at the plasma membrane and is highly substrate-selective. (B) Representation of Classical RPTPs. The PTPs with two PTP domains have the catalytically active domain at the most proximal point (responsible for substrate selectivity), whereas the membrane distal PTP domain retains only residual activity (targets the PTP to specific cellular locations). [RPTP: receptor-like protein tyrosine phosphatase; NRPTP: non-receptor protein tyrosine phosphatase; DSP: Dual specificity; MKP: MAP kinase phosphatase; MTM: myotubularins; PTEN: phosphatase and tensin homologue; PRL: Phosphatases of the regenerating liver]

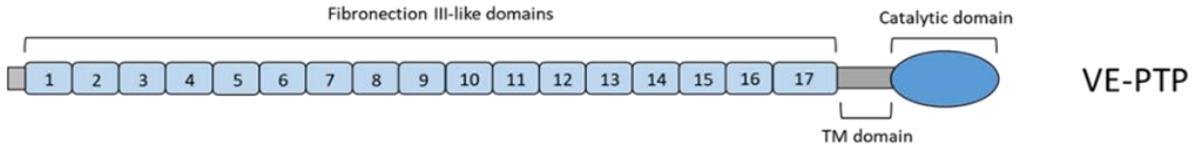

Figure 2. VE-PTP Structure. VE-PTP is comprised of 17 fibronectin (FN) III-like domains in its extracellular region, a transmembrane (TM) domain, and a cytoplasmic phosphatase domain.

1.3.2 VE-PTP Protein Expression Profile

VE-PTP is expressed in endothelial cells throughout the vascular system with higher expression in the brain, heart, lung, and kidney. It is exclusively found in the endothelial cells of large vessels (except for brain) rather than capillaries and post-capillary veins. In brain, VE-PTP is equally expressed in both large and small vessels(Dominguez et al., 2007; Fachinger et al., 1999). In the kidney, VE-PTP is prominently expressed in the arterial and glomerular vasculature (Takahashi et al., 2017). The endothelial cells within this vasculature experience high blood pressure and flow, and therefore require tighter AJs to maintain the integrity of endothelial barrier. This suggests that, in some vascular beds, VE-PTP plays an important role in the maintenance of vascular integrity under high pressure and shear stress. (Takahashi et al., 2017)

During embryonic development, expression of VE-PTP begins at day 9.5 (E9.5) of embryo development and reaches maximum expression level at E17. By E15.5, VE-PTP is present in all organs with the highest level of expression in the lung(Fachinger et al., 1999). Mice lacking VE-PTP have formed normal blood vessels (vasculogenesis), however, by E9.5, the yolk sac exhibits defective vessel remodeling due to a failure to extend the vascular scaffold in the higher order arteries, veins, and capillaries(Baumer et al., 2006; Dominguez et al., 2007). VE-PTP is therefore essential for blood vessel remodeling, but dispensable for vasculogenesis(Baumer et al., 2006; Carra et al., 2012).

1.4 VE-PTP-Dependent Regulation of AJ stability

1.4.1. Interaction with VE-cadherin

VE-PTP stabilizes the AJs through dephosphorylating VE-cadherin adhesion which are formed through trans-dimerization of molecules located at the surface of opposite cells(Broermann et al.,

2011; Nawroth et al., 2002; Nottebaum et al., 2008; Vockel and Vestweber, 2013). VE-cadherin contains 5 extracellular domains (EC1-5), a single transmembrane domain, and an intracellular domain containing several tyrosine sites, which upon phosphorylation, influence interaction with associated catenin proteins. For example, phosphorylation of Y658 and Y731 results in dissociation of p120 and β/γ catenins from VE-cadherin, respectively (Figure 2). VE-PTP interacts with VE-cadherin through the membrane-proximal, extracellular domain(Nawroth et al., 2002). Specifically, the seventeenth fibronectin III-like repeat of VE-PTP interacts with the fifth ectodomain of VE-cadherin. VE-PTP dephosphorylates VE-cadherin at tyrosine residues 658 and 685, with conflicting reports regarding Y731(Allingham et al., 2007; Gong et al., 2015; Monaghan-Benson and Burridge, 2013; Nawroth et al., 2002; Wessel et al., 2014) and thereby limits the endocytosis of VE-cadherin from the AJs(Gong et al., 2015).

The role of VE-PTP in regulating the stability of VE-cadherin adhesion was further elucidated in studies of leukocyte trans-endothelial migration(Allingham et al., 2007; Nottebaum et al., 2008; Vockel and Vestweber, 2013). The trans-endothelial migration of leukocytes, in response to inflammatory stimuli, is an active process accompanied by opening of inter-endothelial junctions(Carman and Springer, 2004). Transient opening of the AJs allows transmigration of leukocytes without excessive endothelial leakage(Nourshargh et al., 2010; Vestweber, 2008). A study done by Allingham determined that leukocyte engagement of intracellular adhesion molecule-1 (ICAM-1) induces activation of Pyk2 and Src, leading to VE-cadherin phosphorylation at Y658 and Y731 thereby destabilizing AJs and allowing leukocyte trans-endothelial migration(Allingham et al., 2007) . In another study done by Vockel and Vestweber (Vockel and Vestweber, 2013), the mechanism by which leukocyte adhesion as well as activation of VEGFR2 signaling leads to phosphorylation of VE-cadherin was investigated(Vockel and Vestweber, 2013).

VEGFA binding to VEGFR2 induces auto-phosphorylation of the receptor at Tyr949, which is a binding site for T-cell specific adaptor (TSad).(Li et al., 2016) Leukocyte binding to vascular adhesion molecule-1 (VCAM-1) at endothelial cell surface leads to activation of Rac1 and subsequent activation of NOX (nicotinamide adenine dinucleotide phosphate oxidase) (Vockel and Vestweber, 2013). NOX generates reactive oxygen species (ROS) such as superoxide and hydrogen peroxidase, which are responsible for activating the protein kinase Pyk2 (Vockel and Vestweber, 2013). Pyk2 phosphorylates VE-PTP at Y1891 which leads to binding of VE-PTP to the SH2 domain of Src and activates Src (Soni et al., 2017). Src phosphorylates VE-cadherin, and therefore increases endothelial permeability(Soni et al., 2017; Vockel and Vestweber, 2013).

Loss of VE-PTP *in vitro* enhances endothelial permeability and increases leukocyte transmigration, which was shown to be largely due to increases in VE-cadherin, β-catenin, and γ-catenin tyrosine phosphorylation(Nottebaum et al., 2008). Interestingly, in quiescent endothelial monolayers, knockdown of VE-PTP only increases γ-catenin phosphorylation and does not significantly increase the tyrosine phosphorylation levels of VE-cadherin and β-catenin, thus implicating γ-catenin as an essential component of the cadherin-catenin complex in maintaining the endothelial barrier(Nottebaum et al., 2008). A study using VE-cadherin Y685F and Y731F mutant knock-in mice, has shown that VE-cadherin phosphorylation at Y685 in response to VEGF or histamine is responsible for increased endothelial permeability, whereas leukocyte transmigration depends on phosphorylation of Y731(Wessel et al., 2014). Knockdown of VE-PTP in bEnd.5 cells causes the phosphorylation of VE-cadherin at Y685, but not at Y731 indicating that VE-PTP regulates vascular permeability through Y685 dephosphorylation,(Wessel et al., 2014) and possibly regulates leukocyte diapedesis through the dephosphorylation of γ-catenin.(Nottebaum et al., 2008; Vestweber et al., 2014)

Stabilizing the interaction between VE-PTP and VE-cadherin promotes endothelial barrier function (Broermann et al., 2011). In an elegant study done by Broermann et al.,(Broermann et al., 2011) the VE-PTP and VE-cadherin interaction was modulated using a transgenic murine knock-in model. In this model, endogenous VE-cadherin is replaced by engineered VE-cadherin-FKBP and VE-PTP-FKB* in endothelial cells. Upon administration of a non-immunogenic rapamycin analog (rapalog), VE-cadherin and VE-PTP are experimentally linked through FKBP/ FKB dimerization. Stabilizing VE-PTP and VE-cadherin interaction enabled inhibition of both increased lung vascular permeability and leukocyte extravasation in a model of acute lung injury, hence reinforcing the importance of the VE-PTP complex with VE-cadherin in regulating endothelial barrier function(Broermann et al., 2011).

In another model of acute lung injury, our group has demonstrated the therapeutic benefits of hypoxic stress, which causes upregulation of VE-PTP expression.(Gong et al., 2015) This study has identified VE-PTP as a HIF-2α target, which drives VE-PTP expression during hypoxic stress. Induction of VE-PTP expression with an inhibitor of prolyl hydroxylase domain-containing protein 2 (PHD2), ameliorates vascular leakage in lung associated with the onset of polymicrobial sepsis. Through this study, the HIF-2α-VE-PTP pathway was established as an adaptive anti-inflammatory response to inflammatory diseases such as acute respiratory distress syndrome(Gong et al., 2015).

In summary, the interaction of VE-PTP with VE-cadherin is essential to maintain tissue-fluid homeostasis in inflammatory lung diseases. VE-PTP counterbalances the kinase activities by dephosphorylating VE-cadherin and associated catenin proteins, and preventing disassembly of AJs, thereby mitigating vascular leakage and leukocyte infiltration in lung. VE-PTP

transcription is also upregulated as a part of acute hypoxic stress response, hence implicating VE-PTP as part of an adaptive response in inflammatory lung disease.

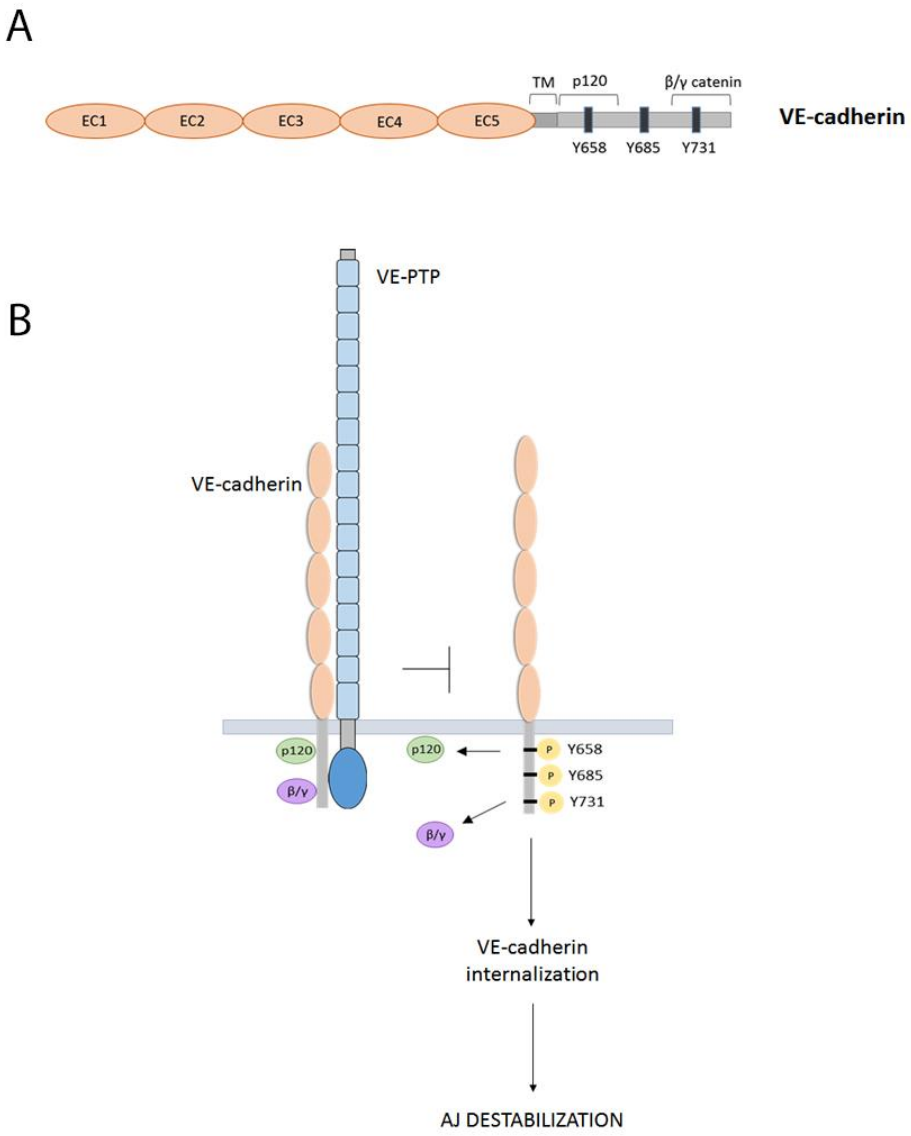

Figure 3. VE-PTP interacts with VE-cadherin to regulate the endothelial barrier function. (A) Structure of VE-cadherin. VE-cadherin contains 5 extracellular domains (EC1-5), a TM domain, and intracellular domain containing tyrosine (Y) sites that influence the interaction of catenin proteins (p120, β, γ). (B) VE-PTP interacts with VE-cadherin through its fibronectin 17 (FN17) extracellular domain and dephosphorylates VE-cadherin at Y658, Y685, and Y731. Phosphorylation of Y658 and Y731 results in VE-cadherin internalization due to p120 catenin dissociation and degradation due to β-catenin dissociation, thereby leading to AJ destabilization. VEGF acts to dissociate VE-PTP from VE-cadherin by a mechanism outlined in Figure 3. [FN, fibronectin type III-like domain]

1.5 The Role of RhoGTPases, Rac1 and RhoA, in the Endothelial Barrier

1.5.1. RhoGTPases

Rho (Ras homologous) GTPases are a subfamily of the ras-sarcoma (Ras)-related superfamily (Johnson and Chen, 2012; Rojas et al., 2012; Wennerberg et al., 2005). RhoA, Rac1, and Cdc42 are the most widely studied among the 20 members of the Rho subfamily and are important regulators of the actin cytoskeleton and VE-cadherin adhesion (Bishop and Hall, 2000; Braga et al., 1997). RhoGTPases transition between active and inactive states and act as biological switches. In the active state, RhoGTPases are guanine triphosphate (GTP)-bound and in their inactive state, they are guanine diphosphate (GDP)-bound (Vetter and Wittinghofer, 2001). GTP-bound RhoGTPases can induce a downstream cascade ultimately resulting in a specific physiological response, whereas GDP-bound RhoGTPases do not.

In this thesis, investigation was focused on RhoA and Rac1 due to their established interplay. Interaction of RhoA or Rac1 with actin-binding proteins causes the formation of stress fibers or lamellopodia, respectively (Nobes and Hall, 1995; Ridley and Hall, 1992). In the migrating cell, Rac1 is therefore at the leading edge causing lamellopodia protrusion and RhoA is at the back end inducing contractility (Raftopoulou and Hall, 2004).

1.5.2 GAPS and GEFs

The upstream regulators of the GTPase cycle include: guanine nucleotide exchange factors (GEFs), GTPase activating proteins (GAPs), and guanine nucleotide dissociation inhibitors (GDIs) (Bishop and Hall, 2000). GEFs facilitate the exchange of GDP for GTP by increasing the release rate of GDP, therefore inducing RhoGTPase activity. GAPs induce the hydrolysis of GTP and therefore inhibit RhoGTPase function (Bishop and Hall, 2000). GDIs bind to the inactive, GDP-

bound GTPase and prevent GTP binding, therefore having an inhibitory role on GTPase function (van Buul et al., 2014).

1.5.3 The RhoA and Rac1 Relationship

The relationship between RhoA and Rac1 in VE-cadherin junctional integrity has been vastly studied. RhoA and Rac1 have been shown to work cooperatively to regulate cell migration and cadherin adhesion (Braga et al., 1997; Kurokawa and Matsuda, 2005), but have also been shown to have an antagonistic relationship such as in the case of cadherin "outside-in signaling" (Komarova et al., 2017).

VE-cadherin adhesion has exhibited an ability to recruit Rac1 through upstream effectors PI3K (128) and T-cell lymphoma invasion and metastasis-inducing protein 1 (Tiam1), and is activated through RacGEF, Vav2 (Lampugnani et al., 2002; Liu et al., 2013), which stimulates Rac1 activity. Rac1 activity then induces the expression of p190RhoGAP (Herbrand and Ahmadian, 2006; Wildenberg et al., 2006), which causes a reduction of RhoA activity. This general pathway has been implicated in mediating the stabilization of the adherens junctions. Previous studies in our lab have supported the importance of Rac1 and RhoA in the mechanical tension applied to VE-cadherin adhesion at mature adherens junctions. It was shown that Rac1 facilitated the inhibition of RhoA-mediated actomyosin contractility, which resulted in decreased tension across VE-cadherin adhesion (Daneshjou et al., 2015).

RhoA responds to inflammatory stimuli through stress fiber formation and junctional remodeling (Stockton et al., 2010; van Nieuw Amerongen et al., 2007). Pro-inflammatory agents, such as VEGF or thrombin, activate effectors such as GEF-H1 and p115RhoGEF (Birukova et al., 2006; Kozasa et al., 1998), GEFs which activate RhoA. The activation of RhoA therefore induces

downstream events which include the activation of Rho-associated coiled coil forming protein kinase (ROCK) I and II. ROCK inhibits myosin light chain phosphatase (MLCP) causing an increase in the phosphorylation state of non-muscle myosin II light chain (MLCII) due to myosin light chain kinase (MLCK) activity (van Nieuw Amerongen et al., 2000). This mechanism leads to actomyosin contraction which pulls on the VE-cadherin junction eventually causing an increase in endothelial permeability.

1.5.4 GEF-H1

In this thesis, GEF-H1 was identified as a VE-PTP interacting protein. GEF-H1 is a microtubule-associated guanine nucleotide exchange factor (Birkenfeld et al., 2008; Birukova et al., 2006), which promotes the exchange of RhoA GDP to GTP leading to the activation of RhoA (Patel and Karginov, 2014). Several studies have established that GEF-H1 release from the microtubules is a consistent mechanism in RhoA activation (Aijaz et al., 2005; Bakal et al., 2005; Birukova et al., 2006; Zenke et al., 2004), therefore GEF-H1 may be the principle regulator in connecting cytoskeletal dynamics to RhoA-dependent signaling.

In the epithelium, GEF-H1 activation causes disassembly of the epithelial barrier by activating RhoA signaling and inducing actomyosin contraction which disrupts the epithelial junctional complexes (Samarin et al., 2007). This has also been demonstrated in the lung endothelial cells where RhoA causes destabilization of the endothelial barrier due to microtubule polymerization (Birukova et al., 2004). GEF-H1 depletion as well as GEF-H1 dominant negative overexpression in the endothelium had a barrier protective effect on endothelial permeability establishing GEF-H1 as a prominent player in RhoA-dependent endothelial barrier function (Birukova et al., 2006).

GEF-H1 has four main domains. The N-terminal domain contains a zinc finger region. Mutation at the C53R residue or complete deletion of the zinc finger domain prevents GEF-H1 binding to microtubules and therefore induces GEF-H1 activation. The Dbl-homology (DH) domain is a conserved 200 amino acid region that is responsible for GEF-H1's enzymatic activity and physically interacts with RhoA. Mutations in this domain result in a non-catalytic GEF-H1 which inhibit GEF-H1-regulated RhoA pathways. The plextrin homology domain (PH) domain is found C-terminal to the DH domain and plays a role in GEF activity regulation through interacting with the DH domain and binding to phospholipids. Additionally, this domain targets GEF-H1 to different cellular compartments and further enables microtubule binding. The coiled coil domain is at the C-terminal end of GEF-H1 and is a helical structure which promotes GEF-H1 mechanical stability and enables protein-protein interaction. The C-terminus proline-rich regions and 14-3-3 binding sites contribute to the regulation of GEF-H1 catalytic activity (Birkenfeld et al., 2008).

Protein-protein interaction and phosphorylation on serine and threonine residues are the primary means of regulating GEF-H1 activity (Birkenfeld et al., 2008; Callow et al., 2005; Fujishiro et al., 2008; Kakiashvili et al., 2009; Patel and Karginov, 2014; von Thun et al., 2013; Yamahashi et al., 2011; Zenke et al., 2004). Kinases such as Pak1 phosphorylate serine 885 and cause 14-3-3 recruitment to GEF-H1 (Birkenfeld et al., 2007; Zenke et al., 2004), which can inhibit GEF-H1 activity. Conversely, phosphorylation of threonine 678 by ERK1/2 promotes GEF-H1 catalytic activity (Fujishiro et al., 2008).

Studies show that when not bound to microtubules, GEF-H1 is active and in its open conformation (Birkenfeld et al., 2008). In the closed conformation, GEF-H1 microtubule binding inhibits GEF-H1 activity through GEF-H1's N-terminus and PH domain, thereby blocking the DH domain from binding RhoA (Birkenfeld et al., 2008). The C-terminus of GEF-H1 has been shown

to be critical for full GEF-H1 inhibition, where deletion of the C-terminus results in increased GEF-H1 activity (Zenke et al., 2004). In addition to GEF-H1 inhibition through microtubule binding, GEF-H1 can be inhibited through protein-protein interaction through microtubule-associated and junctional proteins (Birukova et al., 2006; Krendel et al., 2002; Ren et al., 1998). For example, GEF-H1 binds to the TJ protein cingulin in epithelial cells where it inhibits RhoA activity at TJs (Aijaz et al., 2005).

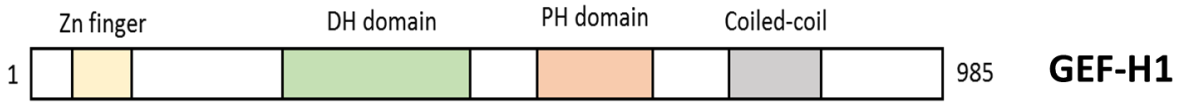

Figure 4. Structure of GEF-H1.
GEF-H1, a GEF for RhoA, is 985 amino acids long and contains a Zinc finger domain, a DH domain, a PH domain, and a coiled-coil region.

1.6 STATEMENT OF AIMS

AIM 1. To determine the role of VE-PTP on VE-cadherin internalization in a confluent, resting endothelium. Using the photo-convertible, fluorescent protein VE-cadherin-Dendra2 and various VE-PTP DNA constructs, we investigated the importance of VE-PTP's domains and enzymatic activity in VE-cadherin internalization.

AIM 2. To investigate VE-PTP's role in RhoA activity and VE-cadherin tension. Using mass spec analysis, we determined that VE-PTP binds to the RhoGEF, GEF-H1. With Förster resonance energy transfer (FRET)-based biosensors for RhoA and tension, we elucidated the relationship between VE-PTP and GEF-H1 in regulating RhoA activity and the tension applied to VE-cadherin at the AJ.

2. MATERIALS AND METHODS

2.1. DNA Constructs

For mammalian expression: VE-cadherin–Dendra2 was inserted into a pCDNA3 vector (Daneshjou et al., 2015) at 5'KpnI and 3'-EcoRI restriction sites for VE-cadherin and sites 5'-EcoRI and 3'-Xhol for Dendra2; the FRET-based RhoA and Rac1 biosensors are in a pTriEx plasmid with a hybrid promoter (MacNevin et al., 2016; Pertz et al., 2006) was a gift from K. Hahn (University of North Carolina School of Medicine, Chapel Hill, NC). VE-cadherin tension (VE-t) FRET-based biosensor was in a pLPCX plasmid with a CMV promoter. The tension sensor module (TSmod) was placed into mouse VE-cadherin cytoplasmic domains (Conway et al., 2013). CFP-tagged murine full length VE-PTP aa 1-1998 (WT VE-PTP) was cloned from mVE-PTP cDNA (Winderlich et al., 2009), a gift from Vestweber (Max Planck Institute for Molecular Biomedicine, Münster, Germany), into pAmCyan1-C1 (Clontech cat. # PT3478-5 or #632441) at flanking 5'/3' Sal I restriction sites. CFP-tagged deletion mutant VE-PTP 1422-1998 aa (Δ16FN) was generated from WT VE-PTP and inserted into pAmCyan1-C1 at 5'-Bgl II and 3'-EcoRI restriction sites. CFP-tagged deletion mutant VE-PTP aa 1-1650 (ΔC) and CFP-tagged deletion mutant VE-PTP 1611-1998 aa (ΔN) was generated from WT VE-PTP and inserted into pAmCyan1-C1 at 5'-BspEl and 3'-Xhol sites. Plum-tagged deletion mutant VE-PTP 1422-1998 aa was generated from CFP-tagged Δ16FN and inserted into pPlum-C1 vector at 5'-Bgl II and 3'-EcoRI. pPlum-C1 vector was constructed using the pAmCyan1-C1 vector as the backbone, where cDNA for the mPlum protein (Clontech cat#632527) replaced cDNA for the AmCyan1 protein. CFP-tagged VE-PTP phosphatase inactive mutant (VE-PTP PI) with a D/A mutation at 1871 aa was generated from WT VE-PTP using site-directed mutagenesis. CFP-tagged deletion mutant VE-PTP 1651-1998 aa was generated from WT VE-PTP and inserted into pAmCyan1-C1 at 5'-

BspEI and 3'-XhoI restriction sites. Plum-tagged deletion mutant VE-PTP 1422-1998 aa was generated from CFP-tagged Δ16FN and inserted into pPlum-C1 vector at 5'-Bgl II and 3'-EcoRI.

For bacteria expression and purification: GST-GEF-H1 deletion mutants 1-236 aa, 237-464 aa, 462-570 aa, and 570-985 aa were in pGEX-KG vector (Pathak et al., 2012) and was provided by Dr. Celine DerMardirossian (The Scripps Research Institute, La Jolla, CA). GST-GEFH1 aa 572-985 was used to generate the panel of GST-GEF-H1 C-terminal constructs (572-876 aa, 731-876 aa, 731-925 aa, and 731-985 aa) by subcloning corresponding regions into pGEX-KG at 5'- EcoRI and 3'-HindIII restriction sites. Histidine-tagged cytoplasmic VE-PTP domain aa 1651-1998 was generated by subcloning the cytoplasmic domain (amino acids 1651-1998) of VE-PTP into pNH-TRXT (Addgene, plasmid#26106) at 5'-EcoRI and 3'-HindIII restriction sites.

2.2. Cell culture, transfection, and treatment

Primary human pulmonary arterial endothelial cells (HPAEC) from six different donors were used at passage 3-6 for all experiments. Cells were grown in EBM-2 cell culture medium supplemented with 10% FBS and EGM-2 bullet kit (Lonza) and maintained at 37°C with 5% CO^2. For imaging, HPAECs were plated on gelatin-coated (0.2%) glass-bottom coverslips and were transfected at 70–80% confluency with siRNA (200nM) using Genlantis Transfection Kit and 48hr later, they were transfected with DNA plasmids using X-tremeGENE transfection reagent (Roche). Post-confluent endothelial cells were used for live-cell imaging 24 hours after DNA plasmid transfection (72 hours after siRNA treatment). In the experiments that did not involve siRNA treatment, the cells were transfected with DNA plasmids at 90% confluence and used for the experiments between 24 and 48 hrs post-transfection.

In AKB-9785 studies, HPAECs were treated with different concentrations (0-50μM) of the inhibitor for 1 hour in serum-free media. Cells were either collected for Western blot (ThermoFisher) or imaged immediately after treatment.

To test the role of RhoA activity in VE-cadherin internalization, Rho Activator I, CN-01 (Cytoskeleton, Inc., 50uM) and Rockout (Rho kinase inhibitor, 50μM) were used to activate or inhibit the Rho pathway, respectively.

To test the phospho-profile of VE-cadherin in the presence of the various VE-PTP constructs, CHO cells were infected with GFP-VE-cadherin and transfected with the VE-PTP construct simultaneously. The resulting lysates were analyzed with Western blot and probed with VE-cadherin (Santa Cruz, sc-6458, anti-goat) and VE-cadherin phospho-tyrosine antibodies for Tyr658 (ThermoFisher, 44-1144G, anti-rabbit) and Tyr685 (Abcam, ab119785, anti-rabbit).

2.3. Immunofluorescent (IF) staining

HPAEC post-confluent monolayers were stained as previously described (Kruse et al., 2018). Briefly, cells were washed with warm HBSS buffer containing both Ca^{2+} and Mg^{2+}, fixed with 4% formaldehyde or a mixture of 4% formaldehyde and 0.1% glutaraldehyde (for tubulin staining) for 15 minutes at room temperature, permeabilized with 0.1% Triton X-100 for 15 minutes, and blocked using 3% BSA for 1 hour. The samples were incubated with primary antibodies against the protein of interest (VE-cadherin [Santa Cruz, sc-6458, anti-goat]; cingulin [Novus Biologicals, NBP1-89602, anti-rabbit]; GEF-H1 [Abcam, ab90783, anti-mouse] , tubulin [Sigma Aldrich, T8328, anti-mouse]) or Alexa 647 phalloidin at 1:100 overnight at 4^0 C and

thereafter with secondary antibodies 1:100 at room temperature for 1 hour. Cells were mounted using Fluoromount-G (Southern Biotech).

2.4. Immunostaining Analysis

To analyze VE-cadherin, GEF-H1, and cingulin at AJs, a Z-projected image (max intensity) of the in-focus frames were generated. VE-cadherin junctional area was measured using a threshold function to select only junctional VE-cadherin. VE-cadherin thresholded images were also used to generate a binary mask in order to determine the area and average intensity (accumulation) of GEF-H1 and cingulin at AJs. The VE-cadherin mask was multiplied by the GEF-H1 or cingulin channels to remove any non-junctional protein.

For analyses of MTs and actin cytoskeleton, a Z-projected images (max intensity) of the in-focus frames for either the MTs or the actin were generated. The total areas of either MTs or actin were measure using a thresholded images. The total MT or actin areas were normalized to the cell area.

2.5. Live-cell imaging

HPAECs were imaged in phenol red–free EGM-2 media supplemented with 10% FBS and heated on a stage heater (Temp control 37^{oC}; Carl Zeiss) at 37°C. Time-lapse images were generated using an LSM 710 confocal microscope (Carl Zeiss) containing a 63×, 1.4 NA oil immersion objective lenses, Ar ion and HeNe dual lasers. Image analysis was done using Meta-Morph software and images were prepared using Adobe Photoshop.

In order to study VE-cadherin dynamics, HPAECs co-expressing VE-cadherin–Dendra2 and CFP-tagged VE-PTP were simultaneously imaged in green (λ = 488 nm) and red (λ = 543 nm) fluorescent states of Dendra2. VE-cad-Dendra2 undergoes an emission shift from 488nm (green) to 543nm (red) after irradiation using a 405nm laser at 8-12% power (Daneshjou et al., 2015; Kruse et al., 2018). Images were acquired every 5 seconds. Through the analysis of red fluorescent decay and green fluorescent recovery within a circular irradiation zone, we determined the rates of VE-cadherin internalization from the AJ and the recruitment of VE-cadherin molecules to the AJ, respectively. The AJs exhibiting a slower VE-cadherin internalization rate was considered to be more stable. For FRET imaging, 16-bit z-stack images were acquired for CFP (λ= 458 nm; band pass 500/20 nm), FRET (λ= 458 nm; long pass 530 nm), and YFP (λ= 514 nm; long pass 530 nm) as previously described (Daneshjou et al., 2015; Kruse et al., 2018).

2.6. Image processing

In VE-cadherin–Dendra2 studies, the fluorescent intensities of 488- (green) and 543-nm (red) maximum emission spectra were quantified inside the photoconversion zone. The changes in fluorescent integrated intensities over time were analyzed in MetaMorph. Data obtained in Metamorph were fit to exponential decay and exponential rise-to-max curves for red and green fluorescence, respectively, in Sigmaplot. Rate constants were calculated from exponential curves and signify VE-cadherin internalization (at 543 nm) and recruitment (at 488 nm).

FRET processing was performed in either Metamorph or ImageJ. A binary mask was generated using a maximized and thresholded image of YFP z-stack, where outside the cell fluorescence has a value of 0 and inside the cell has a value of 1. A ratio image (FRET/CFP) was

created by separately multiplying the FRET and CFP z-stack images by the YFP binary mask. FRET was then divided by CFP to generate a ratio. The region used for quantification consisted of a thick area between two endothelial cells (i.e. junction, overlapping membrane). The activity of RhoA and the tension applied to VE-cadherin were expressed as a FRET/CFP ratio.

2.7. Protein Purification

His-tagged VE-PTP and GST-tagged GEF-H1 constructs were transformed into BL21-competent bacterial cells. Proteins were induced with IPTG for 4 hours at 30^{o}C. Bacterial pellets were resuspended and lysed (50mM Tris, 150mM NaCl, 5mM imidazole, pH 7.5) prior to incubation with NiNTA-His beads or GST beads for 1 hour. Proteins were purified using column purification. Expression of purified protein was confirmed on Coomassie-stained SDS gel.

2.8. Binding Assay

To confirm direct binding between VE-PTP and GEF-H1, a binding assay was performed. Briefly, binding buffers containing 20 mM Tris-HCl, pH 7.5, 100 mM, 1 mM mercaptoethanol, and 1% Triton X-100 (Lansbergen et al., 2004) were used for binding assay experiments. 10μg of GST-tagged GEF-H1 and 10μg of His-tagged VE-PTP purified proteins were incubated with binding buffer at 4^{o}C for 90 minutes. His-tagged VE-PTP was pulled down using HisPur Ni-NTA beads, run on SDS-PAGE, and probed with GST (Santa Cruz, sc-374171, anti-mouse) or His antibody (ThermoFisher Sci, 4E3D10H2/E3, anti-mouse).

2.9. Mass Spectrometry Analysis

To determine VE-PTP binding partners, CFP-VE-PTP was overexpressed in HPAECs and an immunoprecipitation (IP) was performed using an anti-GFP antibody (Thermofisher Sci, GF28R, anti-mouse). The resulting precipitates were run on an SDS gel, was stained with Coomassie, and analyzed using proteomic analysis (Harvard Medical School Taplin Mass Spectrometry Facility).

2.10. RhoA G17A Pulldown

The level of GEF-H1 activity was determined as previously described (Kruse et al., 2018). 1 mL of HPAECs lysates from cells treated with siRNA or overexpressing DNA construct, were incubated with 40uL of nucleotide-free GST-tagged RhoA G17A attached to beads (Abcam, ab211183) for 2 hrs. The beads were centrifuged and washed 3X in lysis buffer. Captured proteins on RhoA G17A beads were separated by electrophoresis and detected with GEF-H1 antibody (Abcam, ab155785, anti-rabbit) using western blot.

2.11. Immunoprecipitation

HPAECs were grown to confluency in 100mm dishes and were treated with siRNA as previously described. 300ug of protein lysate was diluted to 300uL with RIPA buffer (150 mM NaCl, 1.0% IGEPAL® CA-630, 0.5% sodium deoxycholate, 0.1% SDS, 50 mM Tris, pH 8.0) containing protease/phosphatase inhibitor cocktail. 1ug of antibody was added followed by overnight incubation. 40uL of protein A/G beads were added and incubated for 1-2hours at 4^{o}C.

The beads were spun down and washed 3 times with RIPA buffer. The sample buffer was added and the analyzed with Western blot.

2.12. Permeability Assay

HPAECs were seeded on 12-well transwell inserts and were incubated in phenol red-free EGM-2 media. The cells were transfected with either siRNA or DNA construct as previously described. 72 hours after siRNA transfection or 24 hours after DNA construct transfection, the cells were washed and the media was replaced with FITC-albumin (0.5 mg/ml) in phenol red-free EGM-2 in the top chamber. Samples from the bottom chamber were collected at timepoints 0, 30, 60, and 120 minutes and analyzed for fluorescence with a PHERAstarFS spectrofluorometer.

2.13. Micropipette Experiments

2.13.1 Cell Isolation and Modification

Erythrocyte surfaces used to probe adhesion (cadherin-mediated) were modified covalently with immunoglobulin Fc-tagged human VE-cadherin ectodomains (Tabdili et al., 2012b). Human erythrocytes were collected from healthy subjects by informed consent. The erythrocyte surfaces were modified with anti-hexahistidine or -Fc antibodies, as described (Kofler and Wick, 1977). The immobilized antibodies were used to capture Fc- or hexahistidine-tagged VE-cadherin ectodomains.

Mouse lung endothelial cells were isolated from the lungs of wild-type VE-PTP$^{flox/flox}$ mice and VE-PTP$^{-/-}$ knockout mice as previously described (Quaggin, 2017). VE-PTP knockout transgenic mice exhibited the following genotype: PTPRB$^{flox/flox}$, rosa26rtTA$^{+/+}$, tetOCre$^{+/-}$.

PTPRB gene encoding VE-PTP was deleted in utero by adding tetracycline intro drinking water starting at E13.

2.13.2. Treatment of Red Blood Cells with VE-cadherin Ectodomains

Fc was tagged on the C-terminus of E-cadherin exctodomains and were oriented on red blood cells (RBCs) with anti-Fc antibody (Aviva Systems Biology).

2.13.3. Quantification of Cadherin Surface Expression Levels

Flow cytometry measurements were used to measure the VE-cadherin densities on cell surfaces (cadherin/μm2)(Chien et al., 2008). VE-cadherin-expressing cells were labeled with primary, anti-VE-cadherin antibody. The secondary antibody is fluorescein isothiocyanate (FITC) – conjugated anti-IgG. The labeling of antibody was done in PBS containing 1% BSA at pH 7.4. To prevent cell aggregation, calcium was removed in step-in order. To measure the fluorescence intensities of labeled cells, an LSR II flow cytometer was used (BD Biosciences). Calibrated FITC-labeled beads were used to generate a calibration curve for the fluorescence intensity (Bands Laboratories, Inc., Fishers, IN).

2.13.4. Micropipette Measurements of Cell Binding Kinetics.

Opposing micropipettes were used to control interacting pairs of cells. The intracellular binding probability was quantified as adhesion frequency measurements indicated as a function of cadherin contact time.

The binding probability P(t) is the number of binding events (nb) ratio to the total cell-cell touches (NT), nb/NT, which is a function of the cell-to-cell bond number. In these experiments, a cadherin-expressing cell and a red blood cell with His-tagged VE-cadherin were partially aspirated into glass micropipettes. The experimental chamber was filled with L15 medium (Invitrogen Carlsbad, CA) supplemented with 1 w/v% BSA and 2mM $CaCl_2$ and diluted with deionized water (1:1), which ensures the RBC stays rounded. Cells were analyzed with a Zeiss Axiovert 200 microscope (X100 oil immersion objective lens). Images were taken with a high resolution (1080 x 720 pixels) Manta G201B camera (AVT Technologies). Manipuation of contact time was done with automated piezo-electric controllers which constantly induce cell contact at defined time intervals. The area of cell contact was controlled at 6 ± 1 μm^2. Binding events were the result of RBC surface deformation during the separation and the recoil of the bonds. Each pair of cells was tested for 50 cell-cell touches (NT = 50), and each contact time indicates 3 different cell pair measurements. The mean and standard error of each set of tests was determined with the Bernoulli distribution (Shashikanth et al., 2015).

Analysis of the binding probability, P(t), for these experiments is as follows:

$P(t) = 1 - exp(-(mRmLAcK2D(1 - exp(-kofft))))$(Eq. 1) mL and mR (ligand and receptor surface densities [number/μm^2]) on two cells, Ac is contact area (μm^2), K2D is the 2D binding affinity (μm^2), and k_{off} is the off rate (s^{-1}). The ligand densities (number/um2) and contact areas are known. Two-dimensional affinity K2D and k_{off} for cadherin trans-bonds were estimated from Equation 1 fits to the data correlated to the first, trans-binding step (i.e. the rise to P1)(Chesla et al., 1998).

2.14. Micropillar Arrays

The micropillar methodology was used to quantify the imbalance in cellular traction forces when cells are in a cluster. Because the net force on the cell must be zero, the traction force must be balanced with the tension on cell junctions. Micropillars enables definition of the exact forces at the cell junction whereas FRET biosensor provides a relative indication of changes in force.

VE-PTP$^{flox/flox}$ (WT) and VE-PTP$^{-/-}$ (VE-PTP KO) MLECs were immunofluorescent stained by permeabilization with 0.1% (v/v) Triton X-100 in PBS for 4 min and blocked with 1% (w/v) bovine serum albumin in PBS for 1 h. Primary and secondary antibody for β-catenin (Sigma, catalog # C7207, 1:40 dilution; goat anti-mouse IgG Alexa Fluor 488 (Life Technologies, 1:200 dilution)) was performed for 1 h each at room temperature. Samples were mounted with Fluoromount G onto micropillars stained with DiD and coated with fibronectin and stored at 4C until imaging. Images of the micropillar tip positions and endothelial junctions were taken on a Zeiss Axiovert.Z1 epifluorescence microscope with a 40× oil immersion objective (Institute for Genomic Biology, UIUC). Mechanical force calculations were only done using cell doublets and linear triplets.

Junction area was calculated using ImageJ v1.51k (National Institutes of Health) from the β-catenin immunostaining. Traction force analysis was performed using a custom MATLAB program written for MATLAB R2007a (Cohen et al., 2013).

The traction force map was calculated using beam bending theory for small cantilever deflections:

$$F=k*x;\ k=(3EI/L^3);\ I=(\pi d^4/64)$$

where **F** is the force exerted on the free end of the cantilever; **k** is the spring constant; **x** is the deflection; **E** is the bulk elastic modulus; **I** is the area moment of inertia; **L** is the length of the cantilever; and **d** is the diameter of the cantilever. Knowing the displacement (**x**) map and the spring constant (22 nN), a traction force (**F**) map can be generated.

The junction stress for each junction was calculated with the equation, where junction area is calculated from β-catenin immunostaining:

$$Stress = Force/Area$$

When cell junction tension is divided by cell junction area, this provides a measure of stress at cell junctions. This stress is the force acting on a unit element of cell junction; this is the equivalent readout as the tension from the FRET biosensor.

2.15. Traction force microscopy

Traction force microscopy (TFM) measurements were performed on polyacrylamide hydrogels with Young's moduli 40kPa (Tse and Engler, 2010). Proteins were immobilized on

Sulfo-SANPAH-activated gels. This was done by incubating overnight at 4°C with fibronectin (0.1 mg/ml) or PLL (0.2 mg/ml) in immobilization buffer (100 mM HEPES, 100 mM NaCl, and 5 mM CaCl2 at pH 8) (Tabdili et al., 2012a). Substrates were rinsed two times with 1× phosphate buffered saline (PBS), and sterilized by irradiation (365 nm), for at least 15 min, before seeding cells. Harvesting of MLECs was done using 3.5 mM EDTA in PBS containing 1% (w/v) BSA (Takeichi and Nakagawa, 2001). MLECs were seeded at 5000–8000 cells/ml onto hydrogels, and were allowed to adhere and spread for 6 h at 37°C in 5% CO^2 on polyacrylamide gels containing embedded fluorescent microspheres. Fiduciary bead displacements were determined with absolute basal RMS traction force (BTF), and were relative to the traction-free bead positions after cell lysis (Butler et al., 2002). The bead displacement maps determined the traction maps and the RMS traction stresses (Pa; N/m2) (Butler et al., 2002; Muhamed et al., 2016).

2.16. Statistical Analysis

Statistical significance was analyzed using GraphPad Prism. Unpaired t-tests were performed for two experimental groups and 1-way ANOVA was performed for three or more experimental groups. The following p-values are used: *, $p < 0.05$; **, $p < 0.01$; *** $p < 0.001$.

3. THE ROLE OF VE-PTP ON VE-CADHERIN INTERNALIZATION IN THE QUIESCENT ENDOTHELIAL MONOLAYER

3.1. *VE-PTP reduces VE-cadherin internalization in the quiescent endothelium*

VE-PTP acts to stabilize the endothelial monolayer through decreasing endothelial permeability (Nottebaum et al., 2008). Many studies have focused on VE-PTP's role in the stimulated endothelium, however no studies have focused on the role of VE-PTP in the quiescent endothelium. We observed increased endothelial permeability in response to siRNA-mediated knockdown (KD) of VE-PTP in ECs (Figure 5), consistent with VE-PTP's key role in stabilizing VE-cadherin junctions and restricting basal endothelial permeability (Nottebaum et al., 2008). Since the rate of VE-cadherin internalization is a key determinant of junctional permeability (Gavard and Gutkind, 2006; Gong et al., 2014; Hou et al., 2011; Vandenbroucke St Amant et al., 2012), we addressed the role of VE-PTP in regulating VE-cadherin dynamics in quiescent endothelial monolayers. Here we used the irreversible, photo-convertible fluorescent protein Dendra2 attached to the C-terminus of VE-cadherin (VE-cad-Dendra2) (Chudakov et al., 2007; Daneshjou et al., 2015). Irradiation of Dendra2 using a 405 nm laser induces an emission shift from 488nm to 543nm (Chudakov et al., 2007), which was used to monitor VE-cadherin dynamics only within the irradiation zone. We observed that VE-PTP depletion increased the VE-cadherin internalization rate as compared to cells treated with non-targeting (NT) siRNA. This occurred without a change in VE-cadherin recruitment rate to AJs (Figure 6). Consistent with faster internalization rate of VE-cadherin and increased permeability of VE-PTP-deleted cells, we also observed reduced VE-cadherin junctional area, however the overall VE-cadherin protein expression however did not change (Figure 7). These results show that VE-PTP regulation of VE-

cadherin internalization in quiescent endothelial cell monolayers stabilizes VE-cadherin junctions while reducing endothelial permeability.

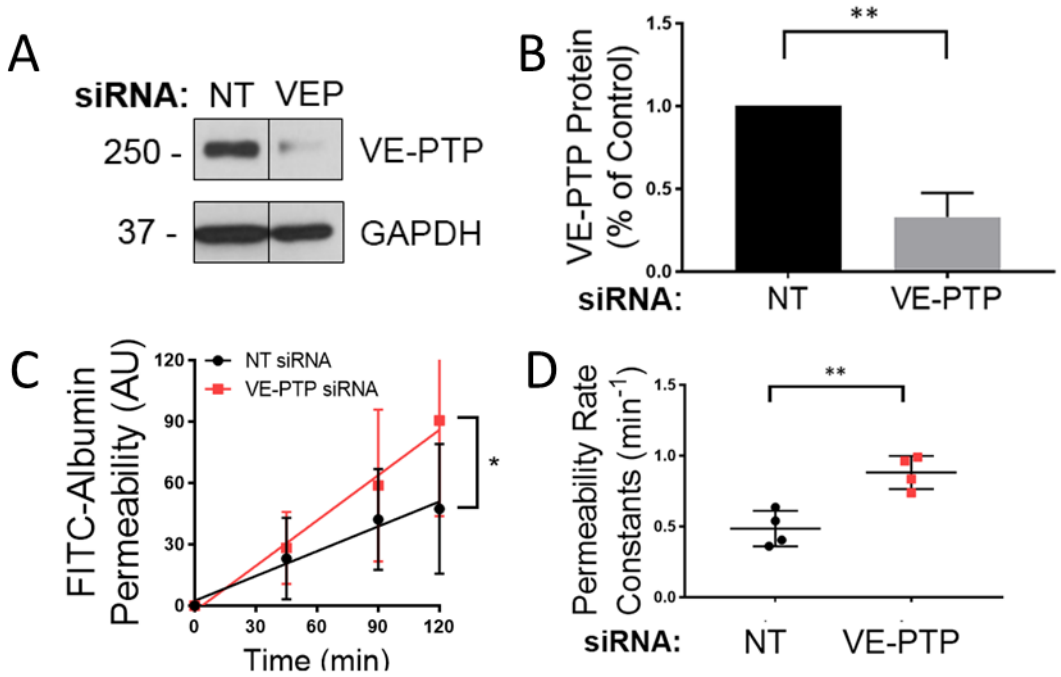

Figure 5. Knockdown of VE-PTP increases endothelial cell permeability.
(A-B) WB analysis of VE-PTP protein expression in HPAECs treated with NT and VE-PTP siRNA (A) and quantification normalized to GAPDH (loading control) in (B). mean ± SEM, n=3, **p<0.05 (C) Permeability of HPAEC monolayers to FITC-conjugated albumin tracer after treatment with NT (non-targeting, control) siRNA or VE-PTP siRNA; mean ± SEM, n=3-4 independent experiments; *, p<0.05, unpaired *t*-test. (D) Endothelial permeability rate constants of 0.48 ± 0.06 min^{-1} and 0.88 ± 0.05 min^{-1} in cells from C treated with NT siRNA or VE-PTP siRNA, respectively; mean ± SEM; n=3-4; **, p<0.001, unpaired *t*-test.

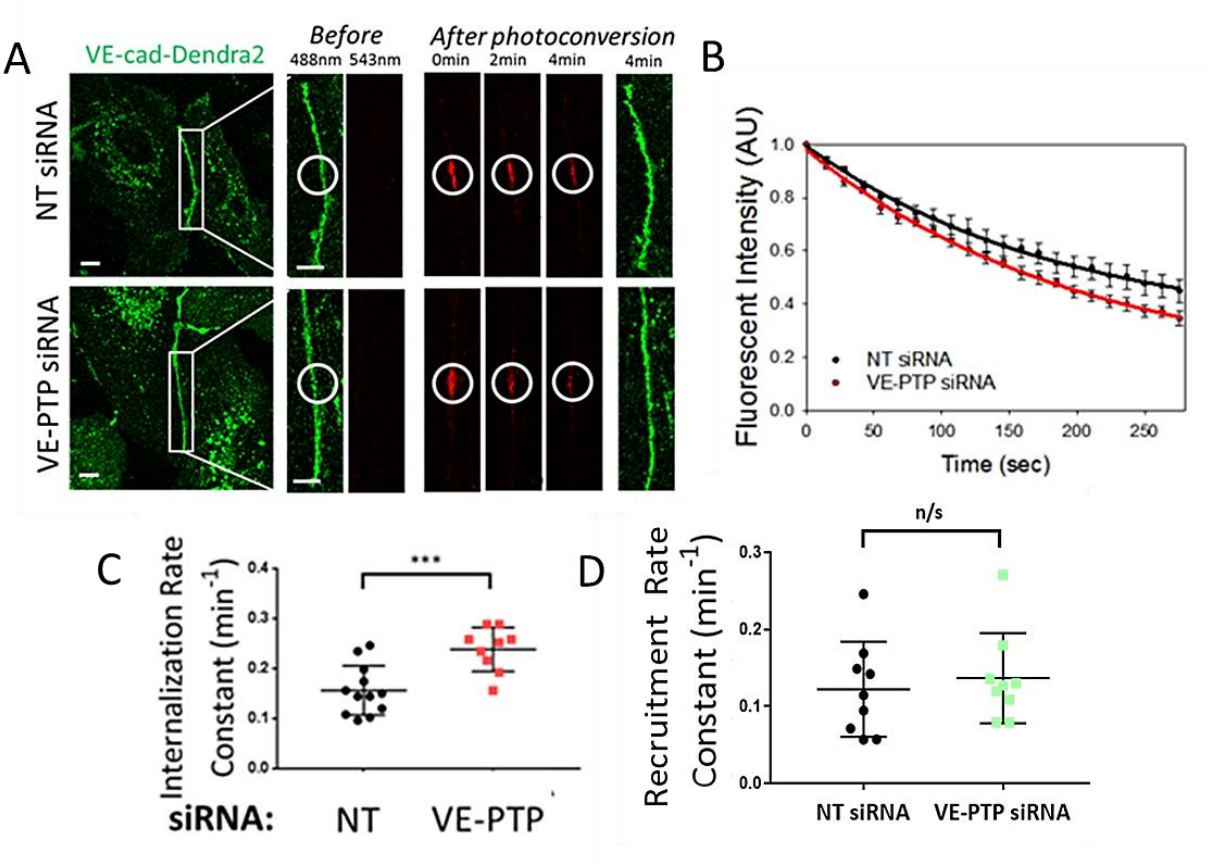

Figure 6. Knockdown of VE-PTP increases VE-cadherin internalization rate.
(A) Time-lapse images of VE-cadherin-Dendra2 emitting green fluorescence before photo-conversion and red fluorescence after photo-conversion within a selected region (indicated by circle) in HPAECs treated with NT siRNA or VE-PTP siRNA. Scale bar, 5μm. (B) VE-cadherin internalization rate (decay in red fluorescence within photo-conversion zone in A) in NT siRNA and VE-PTP siRNA-treated HPAECs; mean ± SEM; n=9-12 junctions from 4 independent experiments. (C) Internalization rate constants of 0.15±0.01 min^{-1} and 0.23 ± 0.01 min^{-1} from data in B in cells treated with NT siRNA or VE-PTP siRNA, respectively; mean ± SEM; n=9-12 junctions from 4 independent experiments; ***, $p<0.0001$, unpaired *t*-test. (D) Recruitment rate constants of VE-cadherin-Dendra2 to AJs in HPAECs treated with NT or VE-PTP siRNA were 0.12 ± 0.02 min^{-1} and 0.13 ± 0.01 min^{-1} respectively; mean ± SEM; n=9, unpaired *t*-test.

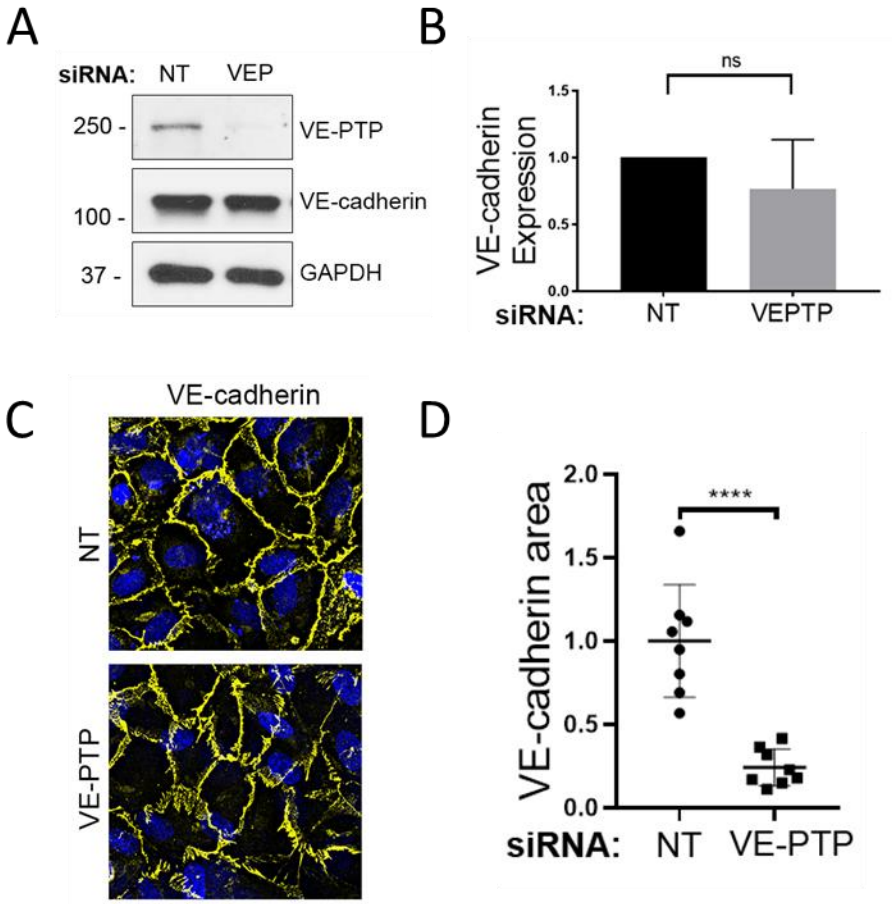

Figure 7. VE-PTP knockdown reduces VE-cadherin junctional area, but not protein expression.

(A-B) WB analysis of VE-cadherin protein expression in HPAECs treated with NT and VE-PTP siRNA (A) and quantification normalized to GAPDH (loading control) (B). VE-cadherin level did not significantly change; n=3, ns, not significant; unpaired *t*-test. (C) Immunofluorescent images of VE-cadherin in confluent HPAEC monolayer treated with NT siRNA and VE-PTP siRNA. Scale bar, 10 μm. (D) Analysis of VE-cadherin junctional area from data in C; mean ± SEM; ****p<0.0001, unpaired *t*-test.

The VE-PTP extracellular domain consists of 17 fibronectin-like domains (FLD), of which the most proximal, seventeenth FLD, interacts with the VE-cadherin extracellular domain 5 (EC5) (Nawroth et al., 2002). We used deletion mutants lacking sixteen (Δ16FN) or all FLDs (ΔN) in addition to full-length (WT) VE-PTP (Figure 8-9) to identify the VE-PTP extracellular domain regulating VE-cadherin internalization. Overexpression of WT or Δ16FN VE-PTP markedly reduced VE-cadherin internalization rate compared to overexpressing control fluorescent tag alone, whereas overexpression of ΔN mutant, which accumulated poorly at AJs, had no effect on VE-cadherin dynamics. However, overexpression of WT VE-PTP had no effect on the VE-cadherin recruitment rate (Figure 10). These data show that the seventeenth FLD, interacting with VE-cadherin, is essential for stabilizing AJs through preventing VE-cadherin internalization.

As VE-PTP is known to promote the adhesion of Chinese hamster ovary (CHO) cells to VE-cadherin-coated surfaces (Nawroth et al., 2002), we addressed the possibility that VE-PTP may regulate the binding affinity of VE-cadherin *trans*-interaction and thus control stability of VE-cadherin junctions. Thus, we carried out a dual micropipette experiment in which VE-cadherin *trans*-interaction was measured between red blood cells (RBCs) expressing human VE-cadherin-Fc fragment and mouse lung endothelial cells (MLEC) isolated from either VE-PTP$^{flox/flox}$ (WT) or *VE-PTP*$^{-/-}$ (KO) mice (Quaggin, 2017; Souma et al., 2018). *VE-PTP*$^{-/-}$ MLECs showed no significant effect on binding affinity (k_A) or off-rate (k_{off}) of VE-cadherin *trans*-interaction (Figure 11). Thus, although interaction between VE-PTP and VE-cadherin is required for stabilizing AJs, VE-PTP does not allosterically regulate VE-cadherin *trans*-interaction.

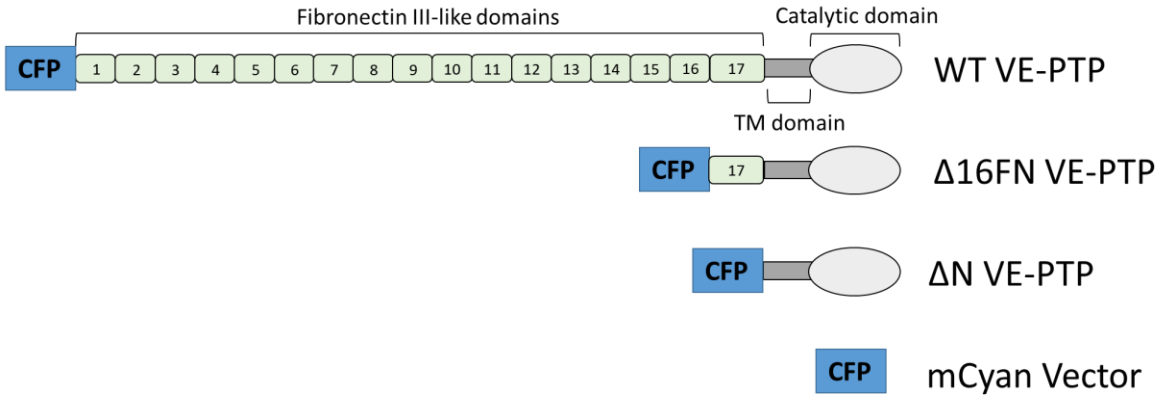

Figure 8. VE-PTP deletion mutants investigating the extracellular domain.
Schematic representation of VE-PTP mutants used in Figure 10; mCyan (control), full-length (WT) VE-PTP, Δ16FN VE-PTP mutant (lacking FN1-16 but capable of binding to VE-cadherin via intact 17th FN domain), or ΔN VE-PTP mutant (lacking entire extracellular VE-PTP domain).

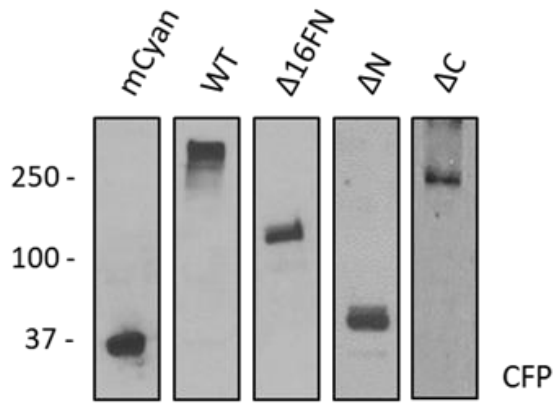

Figure 9. VE-PTP Constructs.
(A) WB analysis of VE-PTP mutants; mCyan (control), full-length (WT) VE-PTP, Δ16FN VE-PTP (lacking FN1-16) mutant, ΔN VE-PTP (lacking extracellular domain), and ΔC VE-PTP (lacking cytosolic domain) mutants overexpressed in HPAECs.

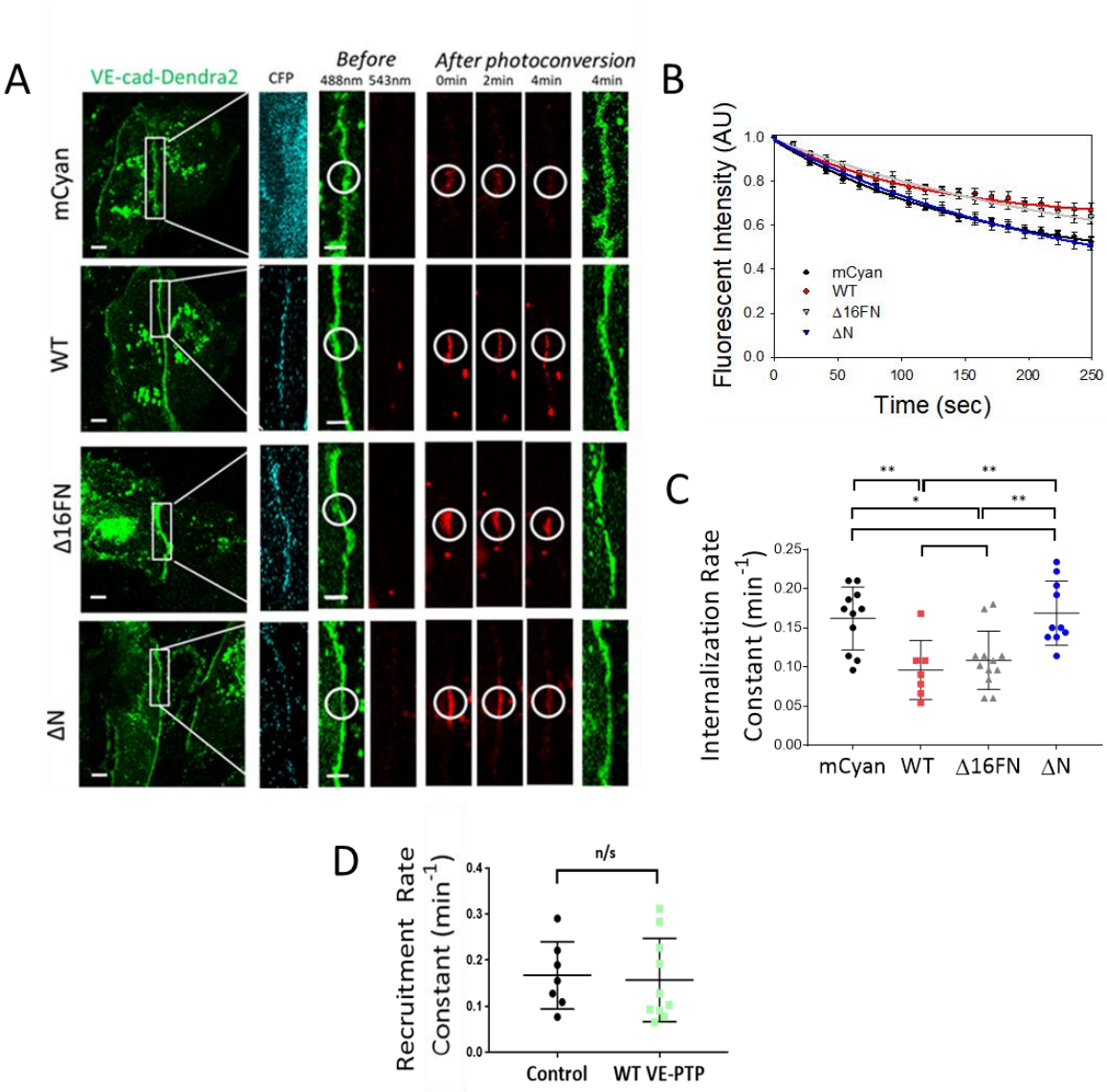

Figure 10. **VE-PTP stabilizes the endothelial barrier through decreasing VE-cadherin internalization rate, but not VE-cadherin recruitment rate.**

(A) Time lapse images of VE-cadherin-Dendra2 in HPAECs over-expressing constructs in F. Scale bar, 5μm. (B) VE-cadherin internalization rates from AJs in HPAECs transfected with constructs in A; mean ± SEM; n=7-12 junctions from 4 independent experiments. (C) Internalization rate constants from data in B in cells overexpressing mCyan (0.16 ± 0.012 min^{-1}); WT VE-PTP (0.09 ± 0.01 min^{-1}); Δ16FN (0.10 ± 0.01 min^{-1}); or ΔN (0.16 ± 0.01 min^{-1}); mean ± SEM; n=7-12 junctions from 4 independent experiments; *, $p<0.05$, **, $p<0.001$, one-way ANOVA. (D) Recruitment rate constants were 0.16 ± 0.02 sec^{-1} and 0.15 ± 0.02 sec^{-1} in control and WT VE-PTP overexpressing cells; mean ± SEM; n=7-10, ns, not significant; unpaired *t*-test.

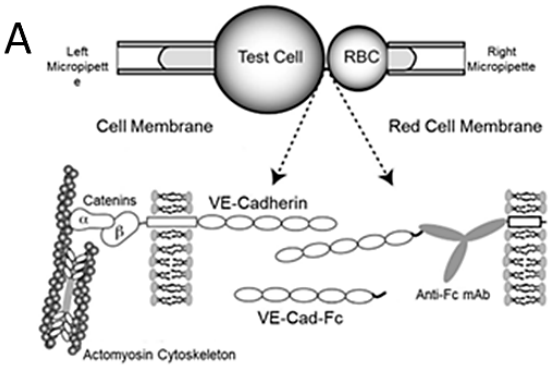

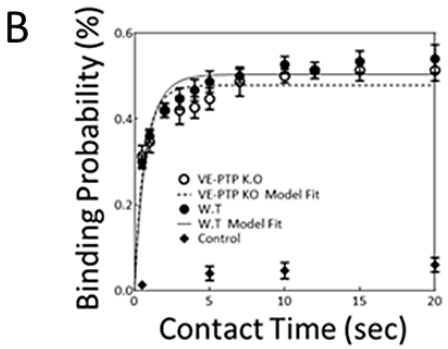

C

Left Micropipette (cad/um²)	Right Micropipette (cad/um²)	K_A (x 10^{-5} um²)	K_{off} (sec^{-1})
MLEC W.T (95)	RBC-VE-Cadherin (54)	1.9 ± 0.4	1.0 ± 0.2
MLEC VE-PTP KO (81)	RBC-VE-Cadherin (54)	2.1 ± 0.5	1.2 ± 0.3

Figure 11. Deletion of VE-PTP does not affect VE-cadherin binding probability.
(A) Schematic representation of micropipette experiments. (B) Binding probability of VE-cadherin *trans*-interaction in WT and VE-PTP KO mouse lung endothelial cells (MLEC). RBCs without immobilized VE-cad-Fc served as control. The solid, dashed lines are weighted; nonlinear least squares fit of the data. (C) Table of VE-cadherin kinetics in WT and VE-PTP KO endothelial cells; n=54 per group.

3.2. VE-PTP cytosolic domain but not phosphatase activity is required for stabilization of VE-cadherin junctions

Studies have shown that VE-PTP knockdown or inhibition of phosphatase activity does not result in VE-cadherin phosphorylation in the resting endothelial monolayers (Gurnik et al., 2016; Nawroth et al., 2002). We therefore determined whether VE-PTP's phosphatase activity is required for VE-PTP mediated stabilization of VE-cadherin junctions. Hence, we used the VE-PTP phosphatase inactive (PI) mutant containing a D/A (aspartic acid to alanine) point mutation at amino acid 1871 (Figure 12). VE-PTP PI overexpression reduced VE-cadherin internalization rate to the level seen in WT VE-PTP expressing cells (Figure 13), indicating that the VE-PTP catalytic activity in the resting monolayer is not required for regulation of VE-PTP-dependent VE-cadherin internalization. Similarly, the VE-PTP phosphatase inhibitor, AKB-9785 (Gurnik et al., 2016; Shen et al., 2014), had no effect on either VE-cadherin phosphorylation or internalization rates (Figure 14-15) consistent with VE-PTP-mediated stabilization of VE-cadherin junctions in the quiescent endothelium occurring independent of VE-PTP phosphatase activity. To determine whether the cytosolic domain of VE-PTP was required for stabilization of VE-cadherin, we overexpressed VE-PTP deletion mutant lacking the cytosolic domain (ΔC). Overexpression of ΔC VE-PTP mutant had no effect on VE-cadherin internalization rate in contrast to full-length VE-PTP (Figure 13). These studies collectively show that the cytosolic domain of VE-PTP, but not its phosphatase activity, is important for stabilizing VE-cadherin junctions.

The observed effects of the VE-PTP mutants on VE-cadherin internalization importantly corresponded to their effects on endothelial permeability. Overexpression of VE-PTP mutants stabilizing VE-cadherin junctions reduced endothelial permeability as compared to mCyan control (Figure 16). Stabilization of VE-cadherin junctions occurred without any apparent changes in VE-

cadherin phosphorylation (Figure 17) thus reinforcing our findings that stabilization of VE-cadherin junctions did not require VE-PTP phosphatase activity.

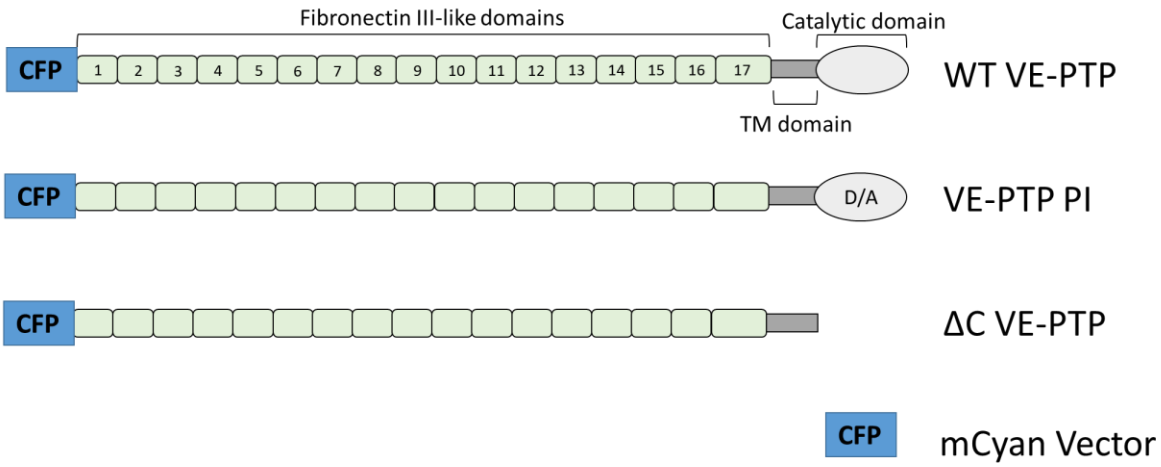

Figure 12. VE-PTP constructs investigating VE-PTP intracellular domain.
Schematic representation of VE-PTP mutants overexpressed in HPAECs; mCyan, WT VE-PTP, VE-PTP PI (phosphatase inactive) and VE-PTP ΔC (lacking cytoplasmic domain) mutants.

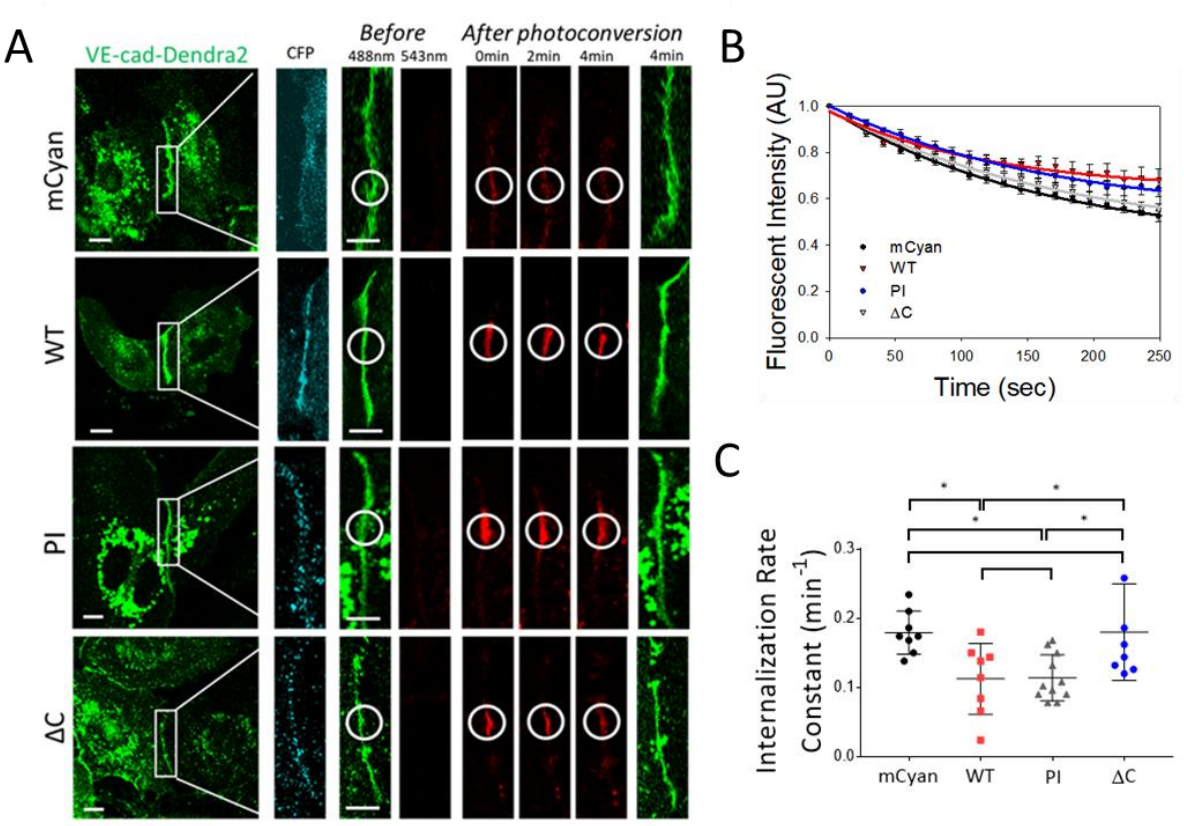

Figure 13. VE-PTP phosphatase activity is not required for stabilization of VE-cadherin junctions.

(A) Time lapse images of VE-cadherin-Dendra2 in HPAECs over-expressing constructs in Figure 12. Scale bars, 5μm (B) VE-cadherin internalization from AJs in HPAECs over-expressing constructs in Figure 12; mean ± SEM; n=8-11 junctions from 3-4 independent experiments. (C) Internalization rate constants calculated from B in cells overexpressing mCyan (0.17 ± 0.01 min^{-1}); WT (0.11 ± 0.01 min^{-1}); VE-PTP PI (0.11 ± 0.01 min^{-1}), and ΔC VE-PTP (0.18 ± 0.02 min^{-1}); mean ± SEM; n=8-11 from 3-4 independent experiments; *, $p<0.05$, one-way ANOVA.

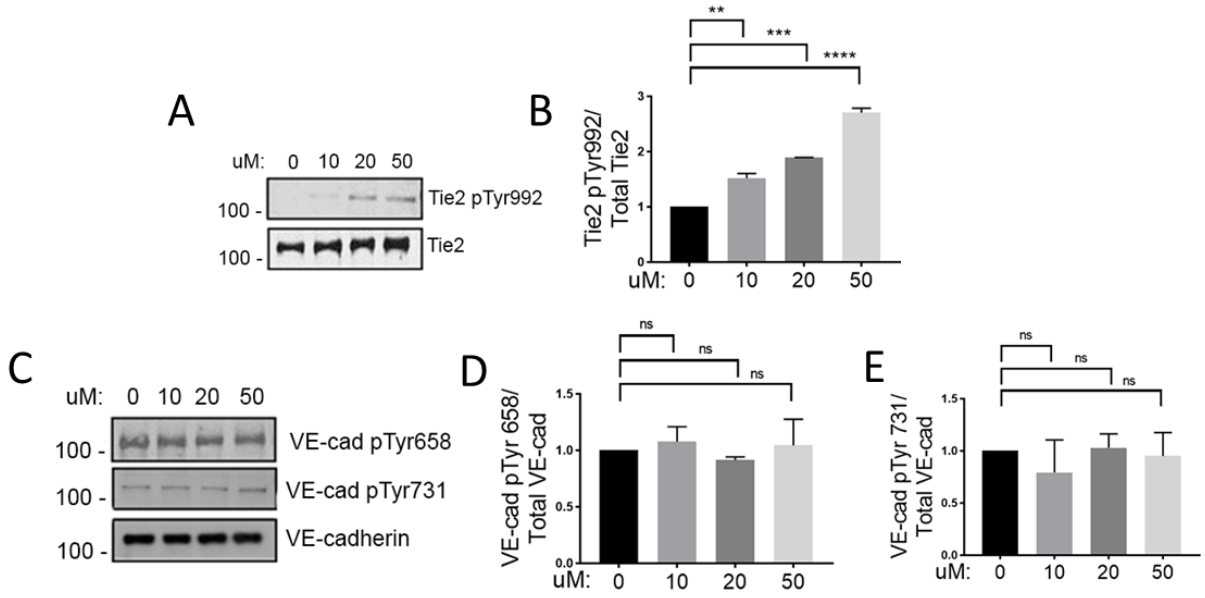

Figure 14. Inhibition of phosphatase activity with AKB-9785 does not affect VE-cadherin tyrosine phosphorylation in the basal state.

(A-E) Results of WB analyses of Tie-2 phosphorylation at Y992 and VE-cadherin phosphorylation at Y658 (VE-PTP-dependent) and Y731 (VE-PTP-independent; control) in HPAECs treated with indicated concentrations of AKB-9785. Inhibition of VE-PTP phosphatase activity with AKB-9785 increases Tie2 tyrosine phosphorylation at Y992, consistent with Tie2 activation as previously described (Frye et al., 2015; Shen et al., 2014) but has no effect on VE-cadherin phosphorylation at selected tyrosine residues. Quantifications are shown in (B) and (D-E); mean ± SEM, n=2, **, $p<0.001$, ***, $p<0.005$, ****, $p<0.0001$; ns, not significant; one-way ANOVA.

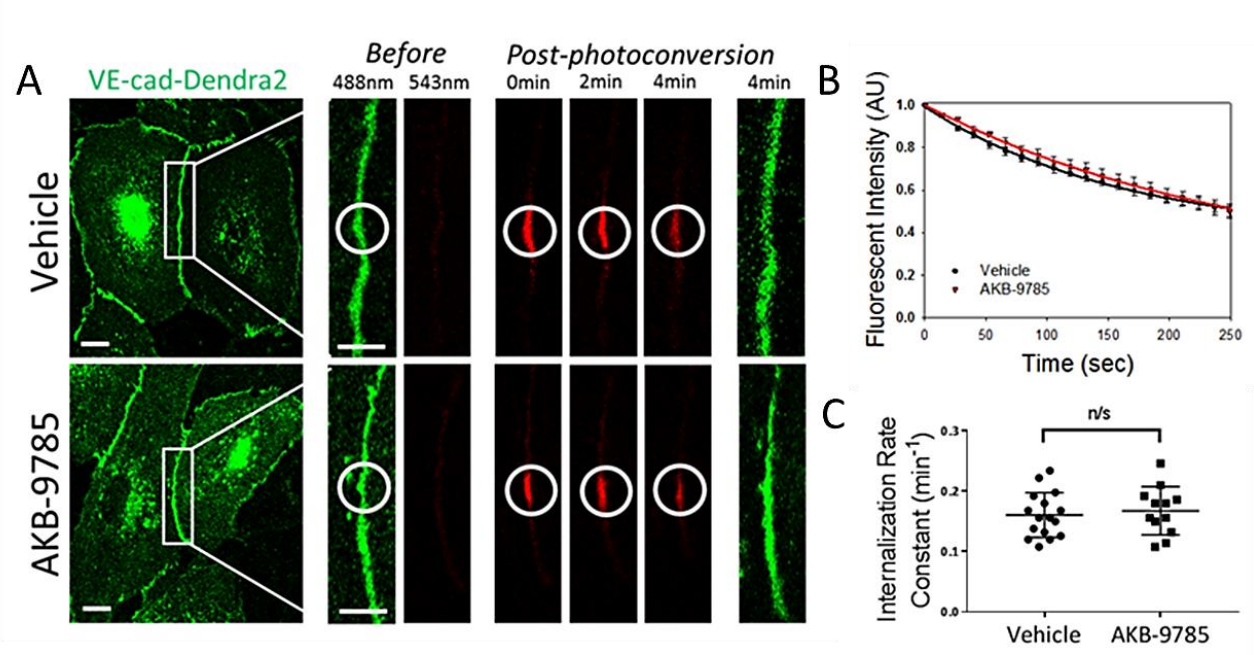

Figure 15. Inhibition of VE-PTP phosphatase activity with AKB-9785 fails to alter VE-cadherin internalization rate at AJs.

(A) Time lapse images of VE-cadherin-Dendra2 in HPAECs treated with vehicle or 50µM AKB-9785. Scale bars, 5 µm. (B) VE-cadherin internalization from AJs from data in A; mean ± SEM, n=12-16. (C) Internalization rate constants calculated from B were 0.16 ± 0.01 min^{-1} and 0.17 ± 0.01 min^{-1} in vehicle and 50uM AKB-9785 treated cells; mean ± SEM; n=12-16; ns, not significant; unpaired *t*-test.

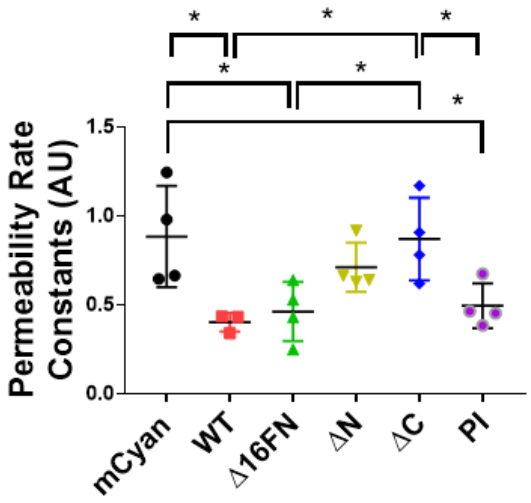

Figure 16. VE-PTP reduces endothelial permeability. Permeability rate constants of HPAEC monolayers overexpressing VE-PTP mutants to FITC-conjugated albumin tracer; mean ± SEM; *, $p<0.05$ by one-way ANOVA.

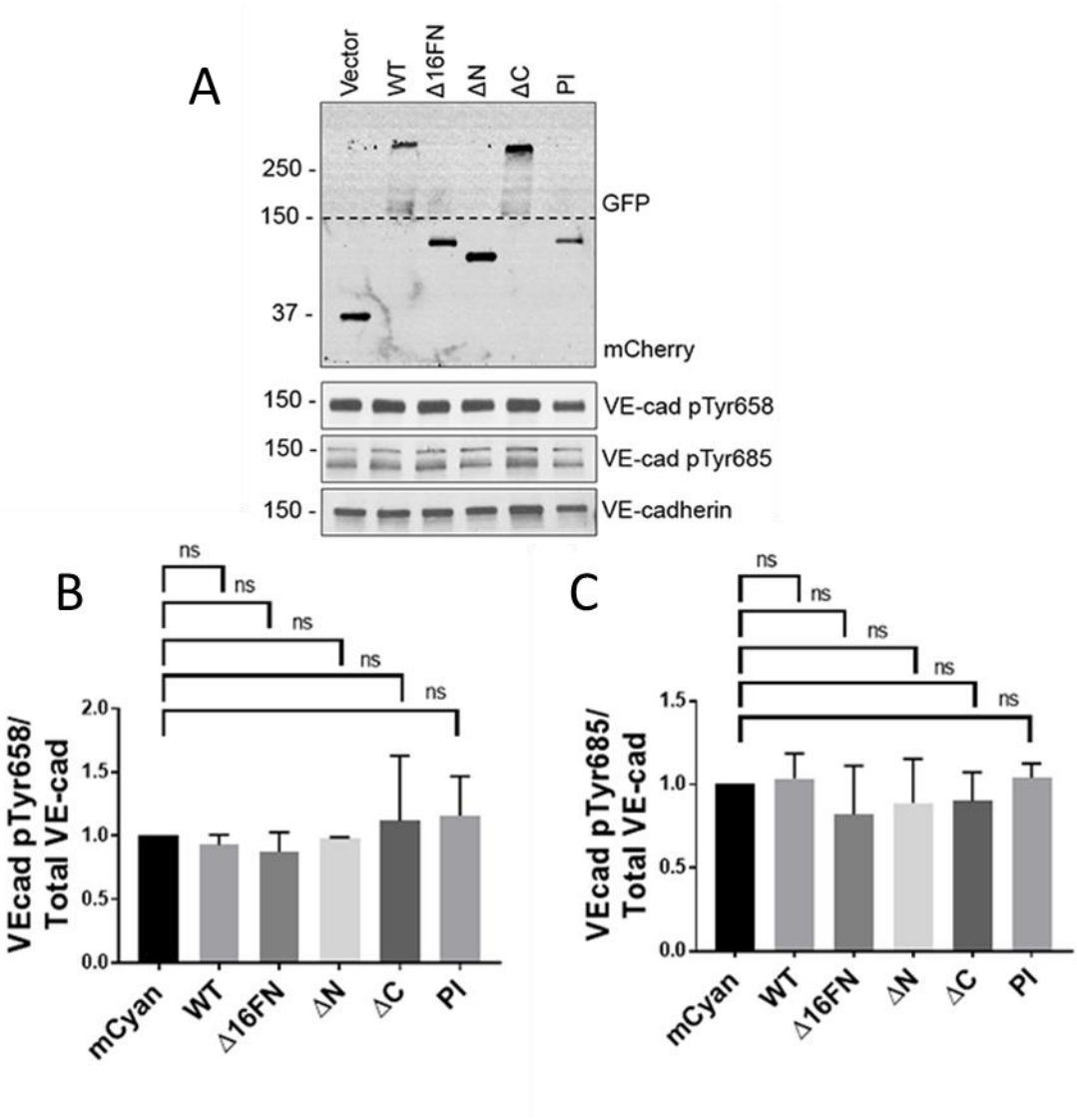

Figure 17. VE-PTP constructs have no effect on VE-cadherin phosphorylation state.
(A-C) Effect of VE-PTP mutants on tyrosine phosphorylation of VE-cadherin overexpressed in CHO-K1 cells. WB analysis with abs against VE-cadherin, phospho-specific Y658 and Y685 VE-cadherin, GFP or mRFP for detection of CFP-tagged or plum-tagged VE-PTP mutants, respectively (A) and quantification (B-C)); n=2; ns, not significant; unpaired *t*-test.

4. VE-PTP AS A RHOA MODULATOR

4.1. VE-PTP interacts with GEF-H1

We next addressed the possibility that VE-PTP controls VE-cadherin internalization through regulation of RhoGTPase signaling, which was described by us as an essential VE-cadherin junction-stabilizing signal pathway (Daneshjou et al., 2015). To identify the RhoGTPase signaling pathway regulated by VE-PTP, we performed mass spectrometry of immunoprecipitated (IP) VE-PTP protein complexes from endothelial cell lysates. We identified ARHGEF2, also known as GEF-H1, as the primary RhoGTPase bound to VE-PTP. Reverse immunoprecipitation studies in which GEF-H1 co-precipitated with VE-PTP and *vice versa* confirmed this interaction (Figure 18). To determine GEF-H1 domains involved in interacting with VE-PTP, we performed binding experiments using bacteria purified GST-tagged GEF-H1 deletion mutants and cytosolic domain of His-tagged VE-PTP (Figure 19). The cytoplasmic domain of VE-PTP (aa1651-1998) interacted with the C-terminal domain of GEF-H1 (aa572-985) (Figure 20). Further deletions of GEF-H1 C-terminus showed that the most proximal domain (925-985 aa) was the primary VE-PTP interacting site.

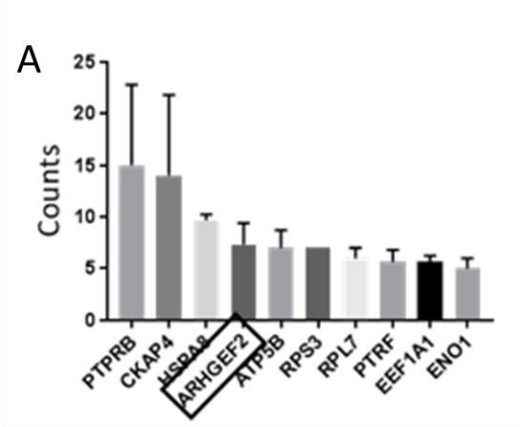

B

	Gene	Protein	Avg Counts
1	PTPRB	Protein Tyrosine Phosphatase, Receptor Type B	15
2	CKAP4	Cytoskeletal assoc protein 4	14
3	HSPA8	Heat shock protein 8	10
4	ARHGEF2	Rho/Rac Guanine Nucleotide Exchange Factor 2	7
5	ATP5B	ATP Synthase F1 Subunit Beta	7
6	RPS3	Ribosomal Protein 3	7
7	RPL7	Ribosomal Protein 7	6
8	PTRF	Caveolae Associated Protein 1	6
9	EEF1A1	Eukaryotic Translation Elongation Factor 1 Alpha 1	5
10	ENO1	Enolase 1	5

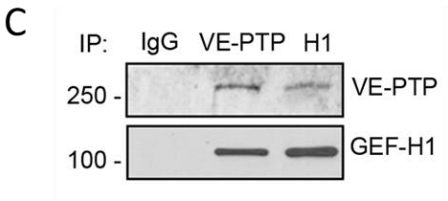

Figure 18. GEF-H1 is a VE-PTP binding partner.
(A) The histogram demonstrating abundance of unique peptides found by mass spectrometry (MS). Gene names are indicated. Number of counts shown on the bars. See Materials and Methods for more details. (B) Table of unique peptides found by MS with corresponding gene and protein names. Myosin, an apparent VE-PTP binding protein, is excluded from analysis. (C) Reverse immunoprecipitation of endogenous VE-PTP or GEF-H1 proteins from HPAEC lysates. Blots were probed for GEF-H1 and VE-PTP.

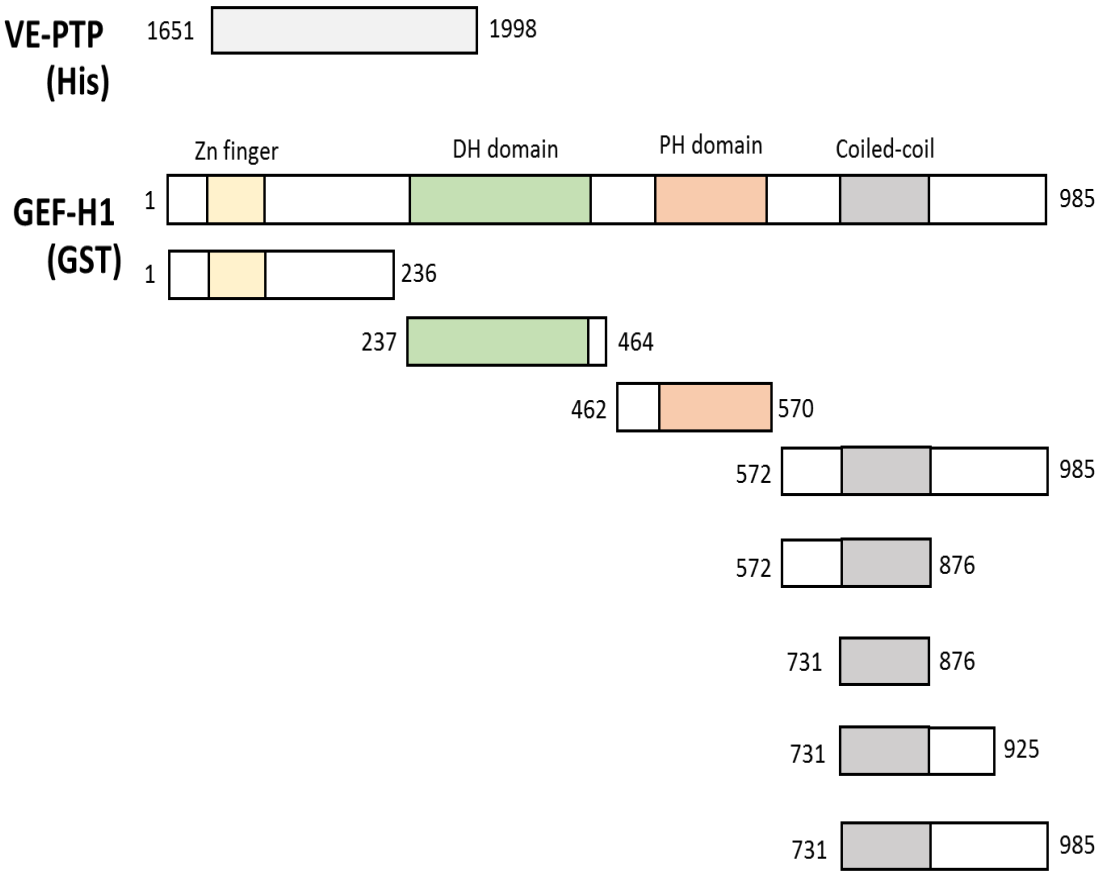

Figure 19. GEF-H1 and VE-PTP Constructs used for Binding Assay.
Schematic representation of indicated His-tagged C-terminus VE-PTP and GST-tagged GEF-H1 deletion mutants.

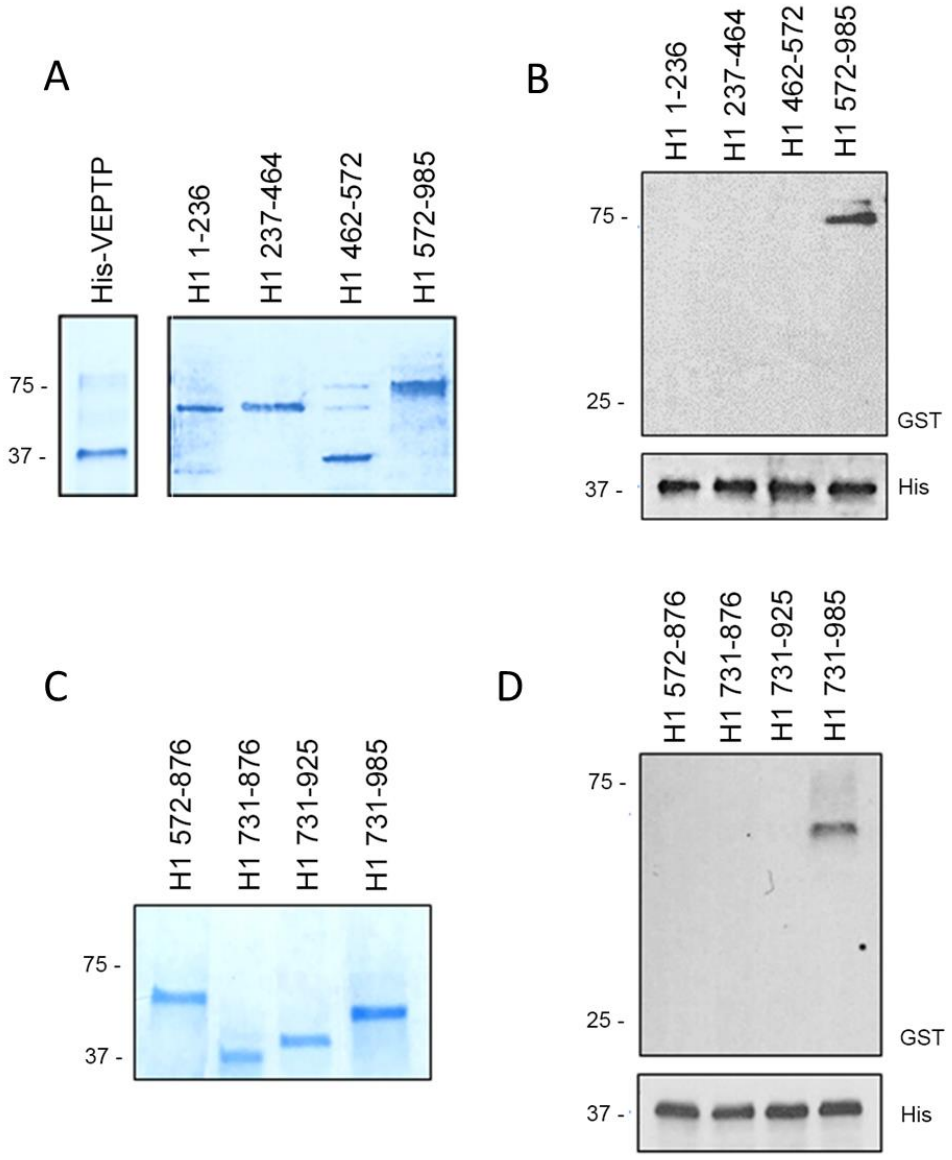

Figure 20. VE-PTP interacts with C-terminus of GEF-H1.

(A-D) Domain interaction of GEF-H1 tested in pull-down experiments. Gel electrophoresis stained with Coomassie Blue of bacteria purified proteins indicated on the left. Direct interactions between cytosolic domain of His-VE-PTP (aa1651-1998) and various GEF-H1 deletion mutants (right) detected by Western Blot analysis.

4.2. VE-PTP inhibits GEF-H1 binding to RhoA and reduces RhoA activity at AJs

GEF-H1 is a guanine nucleotide exchange factor promoting the exchange of RhoA GDP to GTP leading to the activation of RhoA (Krendel et al., 2002; Nalbant et al., 2009; Ren et al., 1998). Therefore, we surmised that GEF-H1 binding to VE-PTP regulates GEF activity, and RhoA signaling at AJs to control the stability of VE-cadherin junctions. Using nucleotide-free RhoA (G17A), the mutant exhibiting highest binding to active RhoGEFs, we determined the amount of RhoA-bound GEF-H1 in endothelial cells treated with control siRNA or VE-PTP siRNA. VE-PTP depletion markedly increased GEF-H1 binding to nucleotide-free RhoA, indicative of increased GEF-H1 activity, as compared to control cells (Figure 21). Furthermore, GEF-H1 tyrosine phosphorylation was undetectable in cells treated with either control or VE-PTP siRNA (data not shown) suggesting that VE-PTP did not regulate GEF-H1 phosphorylation. These data suggest that the interaction between VE-PTP and GEF-H1 reduces GEF-H1 binding to RhoA and thereby GEF-H1 function.

Depletion of VE-PTP also significantly decreased GEF-H1 accumulation at AJs (Figure 22) that occurred without a change in GEF-H1 protein expression (Figure 22). We also observed that overexpressing WT VE-PTP restored GEF-H1 accumulation at AJs in VE-PTP-depleted endothelial monolayers (Figure 23). But this was not seen in ECs overexpressing the VE-PTP ΔC mutant lacking the GEF-H1 interacting domain (Figure 23). Thus, the VE-PTP's cytosolic domain was essential for VE-PTP-dependent accumulation of GEF-H1 at AJs.

Since GEF-H1 inhibition may also occur through the binding to microtubules and the TJ protein cingulin (Aijaz et al., 2005; Ren et al., 1998; Schossleitner et al., 2016; Tsai et al., 2008), we addressed the possibility that depletion of VE-PTP could influence intracellular distribution of cingulin or cause reorganization of the microtubule cytoskeleton. However, depletion of VE-PTP

had no effect on the expression or distribution of cingulin in endothelial cells (Figure 24), suggesting that cingulin was not responsible for inhibiting GEF-H1. Depletion of VE-PTP however reorganized cortical F-actin into stress fibers accompanied by reduced F-actin area (Figure 25). Loss of cortical actin was likely a result of destabilization of VE-cadherin junctions (Komarova et al., 2012). VE-PTP depletion was also accompanied by reorganization of microtubules which became aligned with F-actin fibers (Figure 25); however, this occurred without a change in the microtubule area (Figure 25), suggesting that reorganization of microtubule cytoskeleton is unlikely to be responsible for GEF-H1 activation in VE-PTP-depleted cells.

Next, we investigated the role of VE-PTP in regulating RhoA and Rac1 activities specifically at AJs using Förster Resonance Energy Transfer (FRET)-based biosensors for RhoA (Pertz et al., 2006) or Rac1 (MacNevin et al., 2016). Knockdown of VE-PTP increased RhoA activity at AJs while there was no effect in the cytosol (Figure 26). This change in RhoA activity seen in VE-PTP depleted cells was not accompanied by change in Rac1 activity (Figure 27) showing that VE-PTP is solely responsible for RhoA signaling at AJs. Overexpression of WT VE-PTP and the C-terminus domain of VE-PTP (aa1651-1998), which both bind GEF H1, in ECs depleted of VE-PTP significantly reduced RhoA activity at AJs (Figure 28). However, VE-PTP ΔC mutant lacking GEF H1 interacting domain failed to reduce RhoA activity at AJs (Figure 28). Furthermore, knockdown of GEF-H1 decreased RhoA activity at AJs in both control and VE-PTP depleted ECs (Figure 26, 29). Although some reduction in cytosolic RhoA activity was seen in GEF-H1 depleted cells, the change was not significant (Figure 26). These results show that VE-PTP inhibits GEF-H1 activation and reduces RhoA signaling at the level of AJs in the quiescent endothelium.

We also observed that overexpression of WT VE-PTP reduced GEF-H1 binding to RhoA (Figure 30) that was accompanied by reduced RhoA activity at AJs as compared to control ECs expressing fluorescent tag (Figure 31). In addition, overexpression of VE-PTP PI mutant reduced RhoA activity at AJs (Figure 31), consistent with the central observation that VE-PTP phosphatase activity did not regulate VE-cadherin dynamics at AJs. Consistent with the proposed role of VE-PTP in modulating RhoA signaling, overexpression of the VE-PTP PI mutant had no effect on Rac1 activity at AJs (Figure 32). Together, these data demonstrate that VE-PTP reduced RhoA activity at AJs without altering Rac1 activity, and thereby stabilized VE-cadherin junctions.

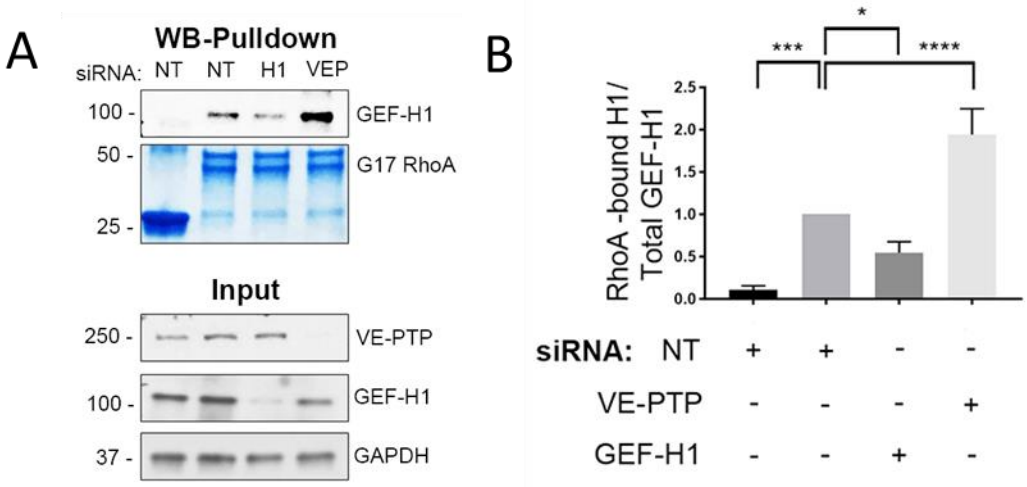

Figure 21. VE-PTP reduces GEF-H1 binding to RhoA.
(A-B) Interaction of GEF-H1 with GST-RhoA (G17A) in HPAECs treated with NT siRNA, or VE-PTP siRNA. The resulting precipitates were probed for GEF-H1 (A) and quantification of data (B); mean ± SEM; n=3; **, p<0.001; unpaired *t*-test.

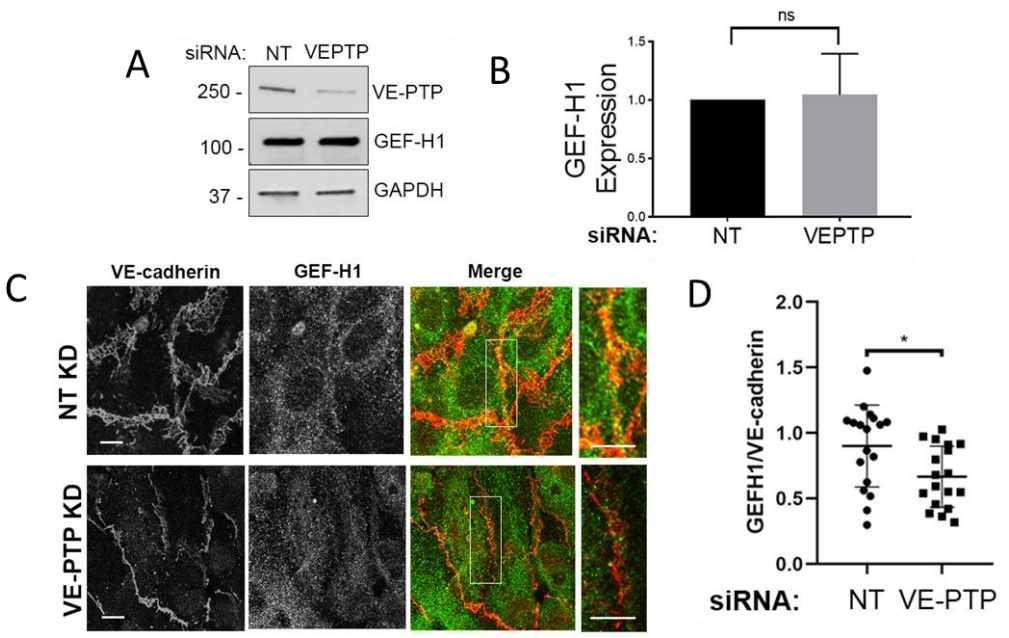

Figure 22. VE-PTP KD reduces GEF-H1 at the AJ.
(A-B) WB analysis of GEF-H1 expression in HPAECs treated with NT siRNA or VE-PTP siRNA; GAPDH, loading control (A); and data quantification (B), n=3, ns, not significant; unpaired *t*-test (C) Immunofluorescent images of VE-cadherin (red), GEF-H1 (green), and GEF-H1 junctional expression at AJs (greyscale) after VE-cadherin mask was applied in confluent HPAEC monolayer treated with NT siRNA and VE-PTP siRNA. Scale bar, 10 μm. (D) Analysis of GEF-H1 expression at VE-cadherin junctions from data in C; mean ± SEM, n=18 images per group from 2 independent experiments.

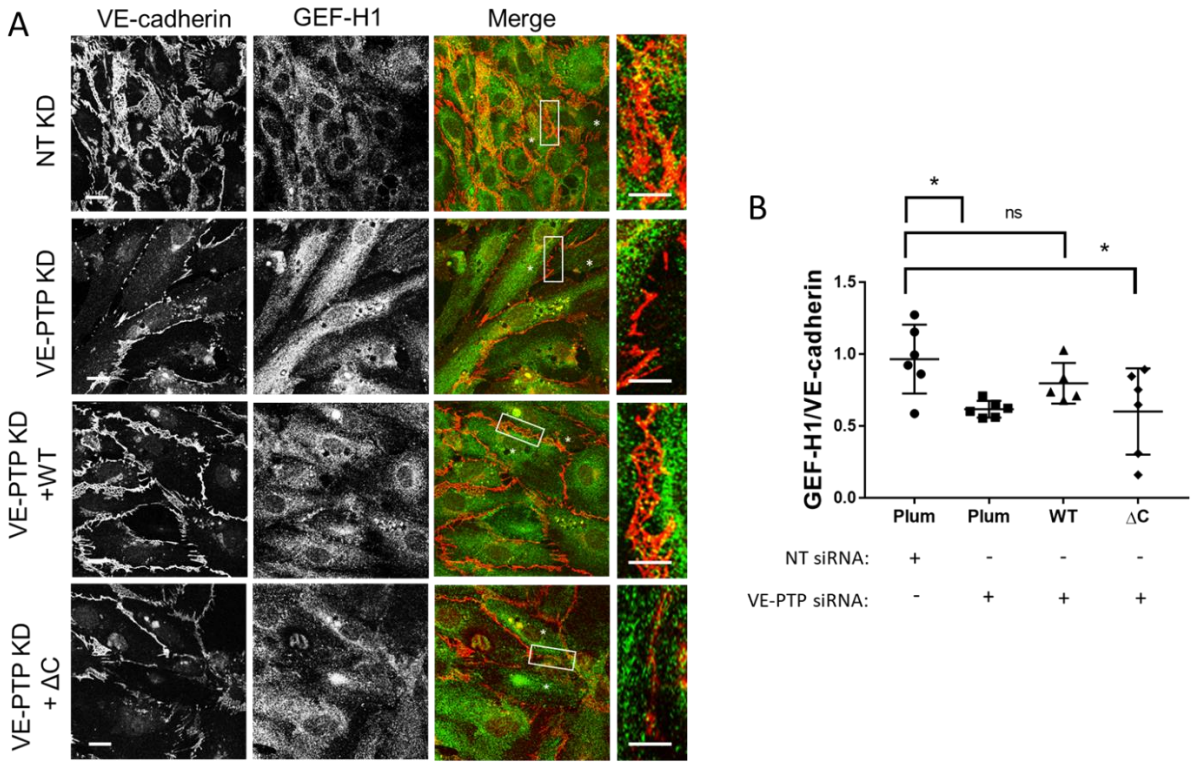

Figure 23. VE-PTP's cytosolic domain was essential for VE-PTP-dependent accumulation of GEF-H1 at AJs

(A) Immunofluorescent images of VE-cadherin (red) and GEF-H1 (red), in confluent HPAEC monolayer treated with NT siRNA or VE-PTP siRNA and overexpressing either mCyan (vector control), VE-PTP WT, or VE-PTP ΔC. *denotes transfected cells. Scale bar, 10 μm. (B) Analysis of GEF-H1 expression at VE-cadherin junctions from data in E; mean ± SEM, n=5-6 images per group; one-way ANOVA; $p<0.05$; ns, not significant.

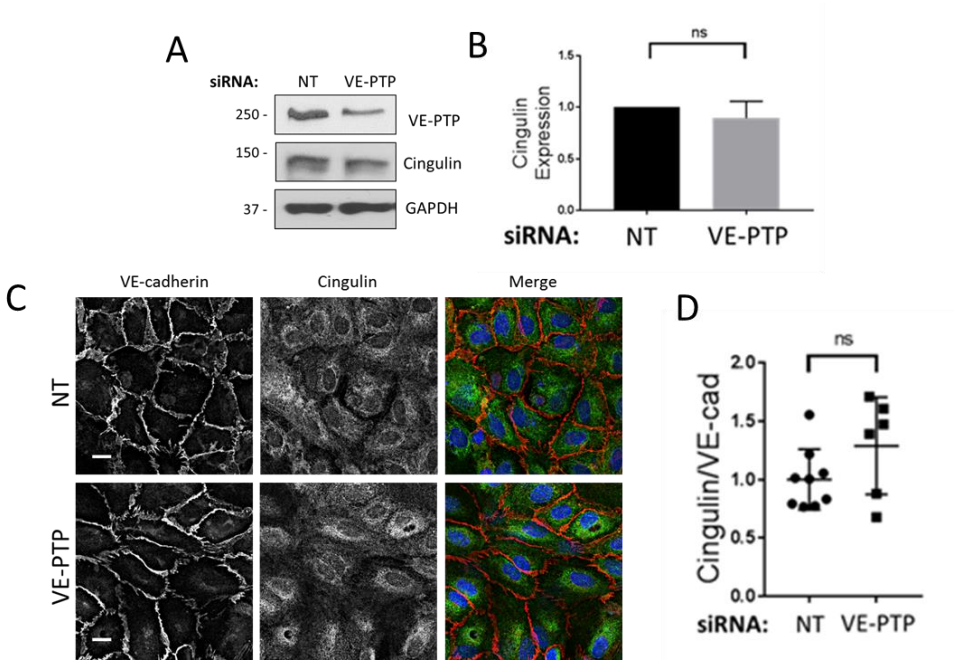

Figure 24. VE-PTP KD has no effect on cingulin expression.
(A-B) WB analysis of cingulin in HPAECs treated with NT siRNA or VE-PTP siRNA; GAPDH, loading control (A) and data quantification (B). mean ± SEM; n=3; ns, not significant; unpaired t-test. (C-D) Immunofluorescent staining for VE-cadherin (red) and cingulin (green), in HPAECs treated with NT siRNA or VE-PTP siRNA (C) and data quantification (D). Scale bar, 10μm. n=6-8 fields from 3 independent experiments; ns, not significant; unpaired *t*-test.

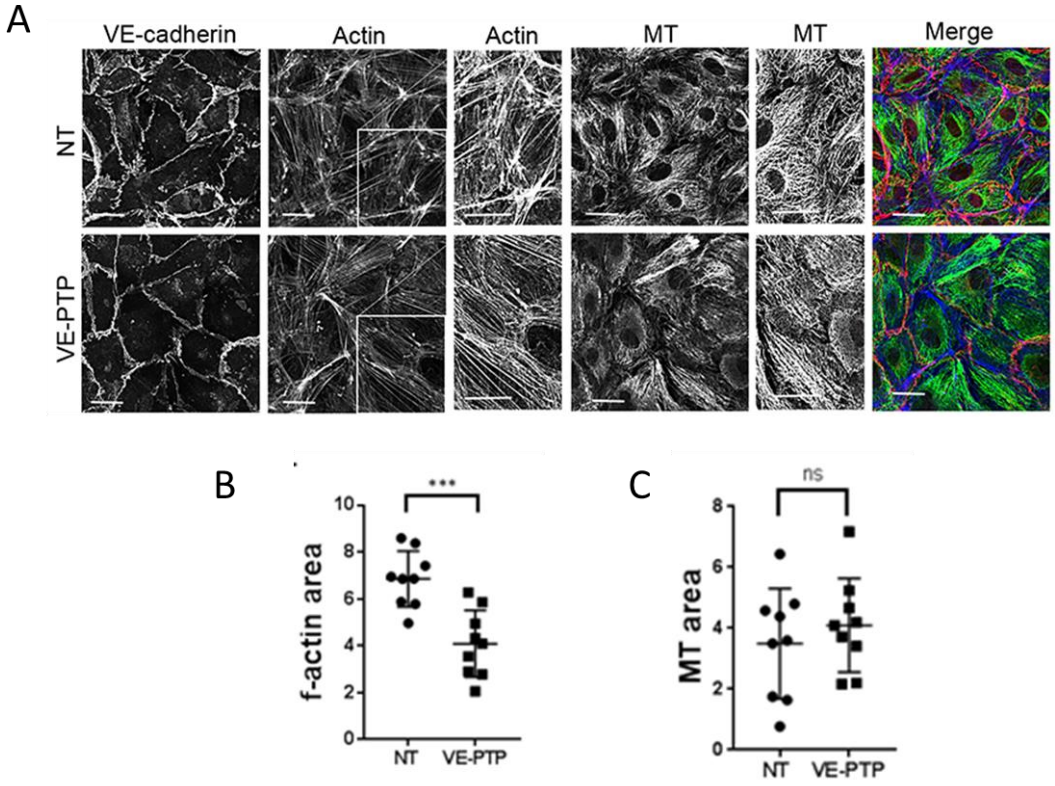

Figure 25. VE-PTP KD reduces f-actin area.
(A) Immunofluorescent staining for VE-cadherin (red), actin (blue), microtubules (green) in HPAECs treated with NT siRNA or VE-PTP siRNA. Scale bar, 10 μm. (B-C) Analysis of f-actin (B), and microtubule (C) areas normalized to the cell area; mean ± SEM; n=18 images from 2 independent experiments; ***p<0.001; unpaired *t* test. Scale bar, 10 μm

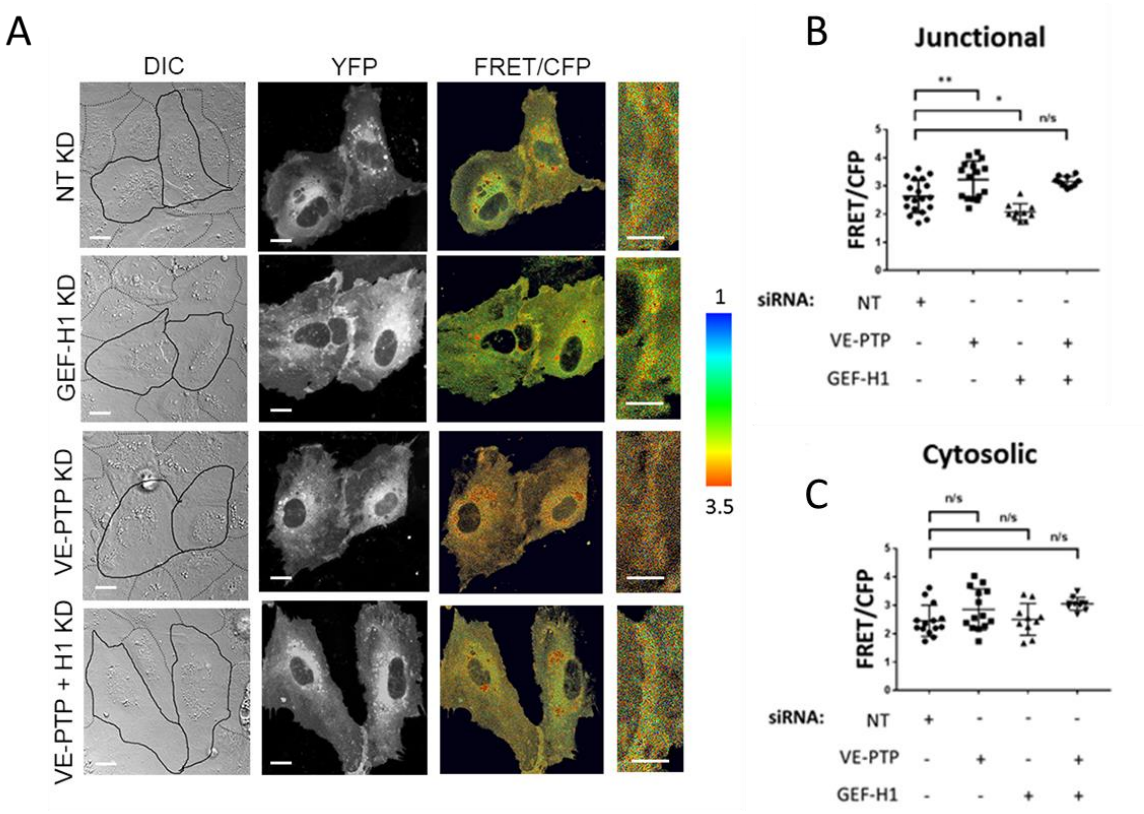

Figure 26. VE-PTP reduces RhoA activity at the AJ.
(A) DIC and confocal images of biosensor (YFP) and RhoA activity (FRET/CFP) in HPAECs treated with NT siRNA, or siRNA against VE-PTP, GEF-H1, or both proteins. The ratiometric images were scaled from 1 to 3.5 and color coded as indicated on right. Warmer colors denote higher RhoA activity. Scale bars, 5μm. (B-C) Relative RhoA activity at the AJs (B) or in cytosol (C) of cells in C; mean ± SEM; n=10-19 junctions from 3 independent experiments; *, $p<0.05$, **, $p<0.001$; one-way ANOVA.

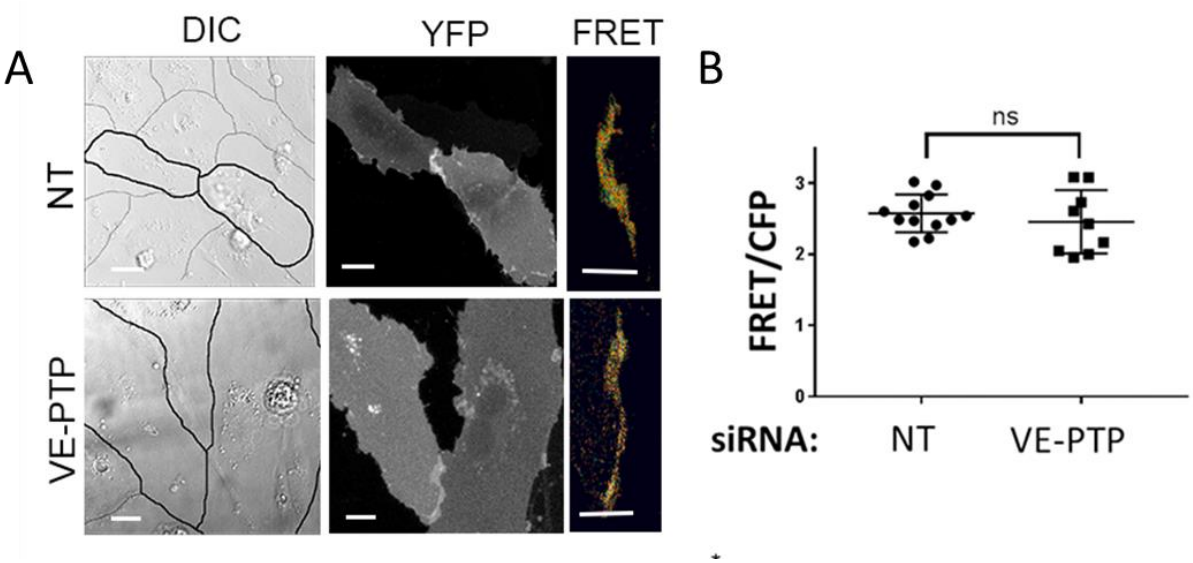

Figure 27. VE-PTP has no effect on Rac1 activity. Rac1 activity at VE-cadherin junctions in HPAECs treated with NT or VE-PTP siRNA, n=3, ns, not significant; unpaired *t*-test.

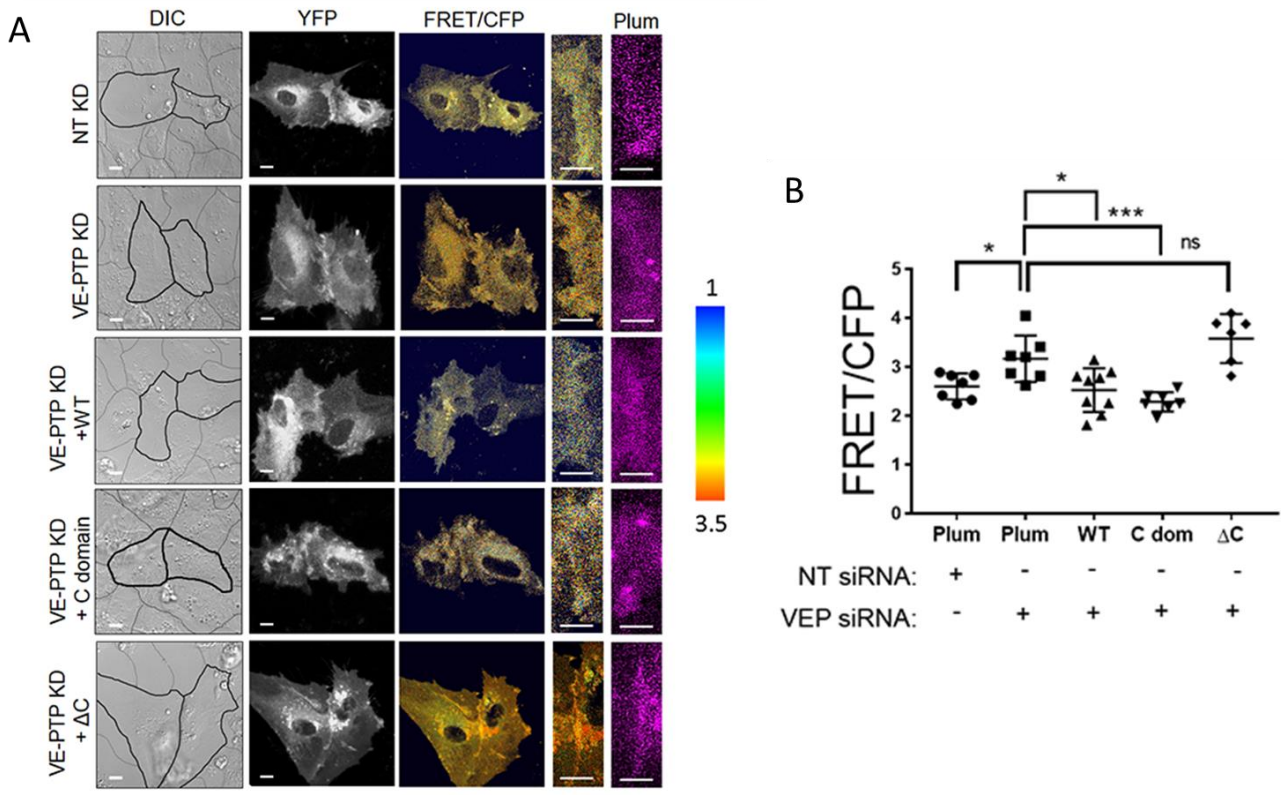

Figure 28. VE-PTP's C domain is essential for reducing RhoA activity at the AJs. (A) RhoA FRET of HPAECs in confluent monolayer treated with NT siRNA or VE-PTP siRNA and overexpressing either mCyan (control), VE-PTP WT, VE-PTP C domain, or VE-PTP ΔC. Scale bar, 5 µm. (B) Quantification of data in (A); n=6-9 junctions from 2 independent experiments. ns, not significant; *, $p<0.05$, ***, $p<0.0001$; unpaired t-test

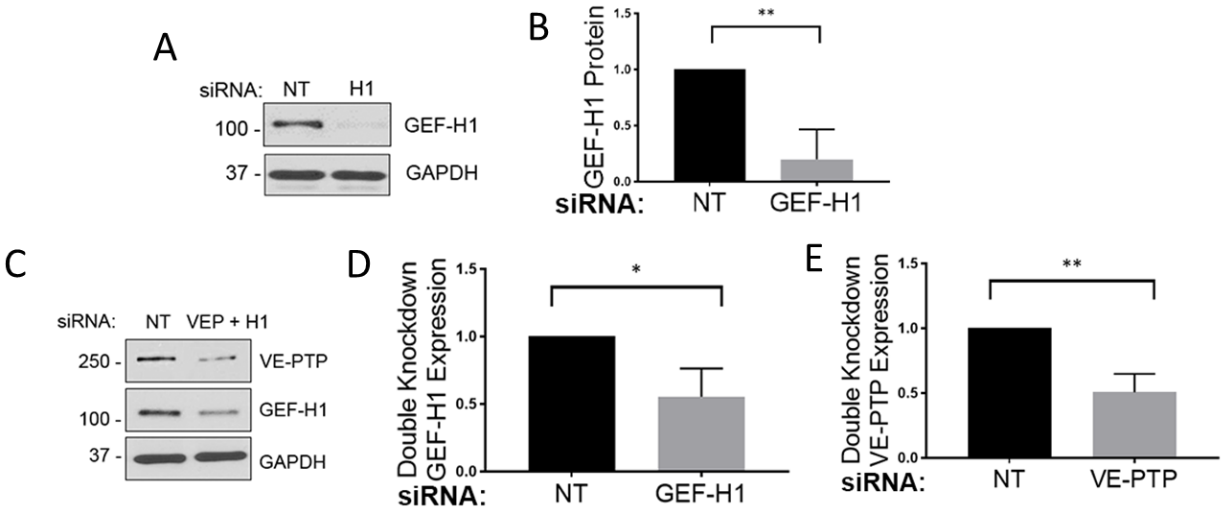

Figure 29. GEF-H1 knockdown alone and in combination with VE-PTP KD.
(A-E) WB analyses of VE-PTP, and GEF-H1 expression in HPAECs treated with NT siRNA, GEF-H1 siRNA, or VE-PTP and GEF-H1 siRNA; GAPDH, loading control. (B, D, E) Quantification of data in A and C; mean ± SEM; n=3; *, $p<0.05$, **, $p<0.001$; unpaired *t*-test.

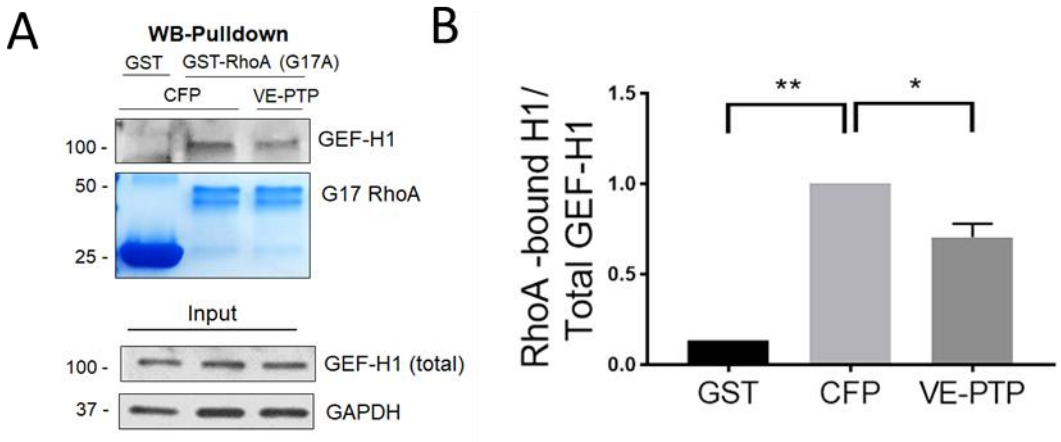

Figure 30. VE-PTP reduces GEF-H1 activity.
Interaction of GEF-H1 with GST-RhoA (G17A) in HPAECs overexpressing CFP or CFP-VE-PTP. The resulting precipitates were probed for GEF-H1 using WB analysis (A) and quantification of data (B). GST precipitates from CFP-expressing cells used as a control; n=2; *$p<0.05$, **$p<0.001$; one-way ANOVA.

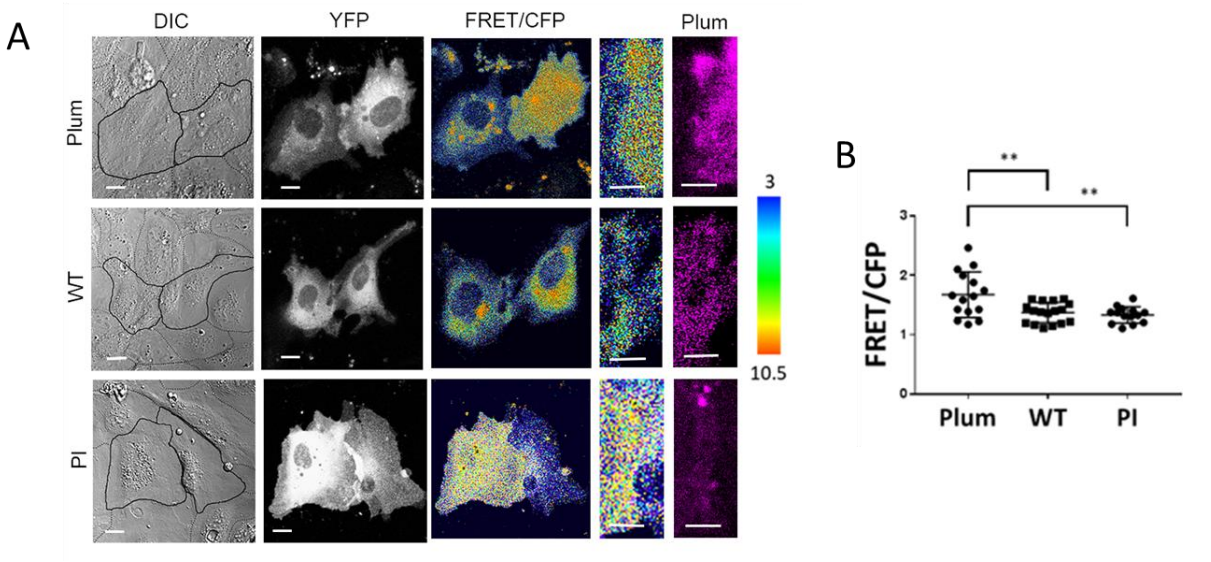

Figure 31. VE-PTP reduces RhoA activity at the AJ.
(A) DIC and confocal images of biosensor (YFP) and RhoA activity (FRET/CFP) in HPAECs expressing mPlum (control), or mPlum-VE-PTP (WT), or mPlum-VE-PTP PI (PI). The ratiometric images were scaled from 3 to 10.5 and color coded as indicated on right. Scale bars, 5μm. (B) Relative RhoA activity at AJs of cells shown in H; mean ± SEM; n=14-17 junctions from 3 independent experiments; **p<0.001; one-way ANOVA.

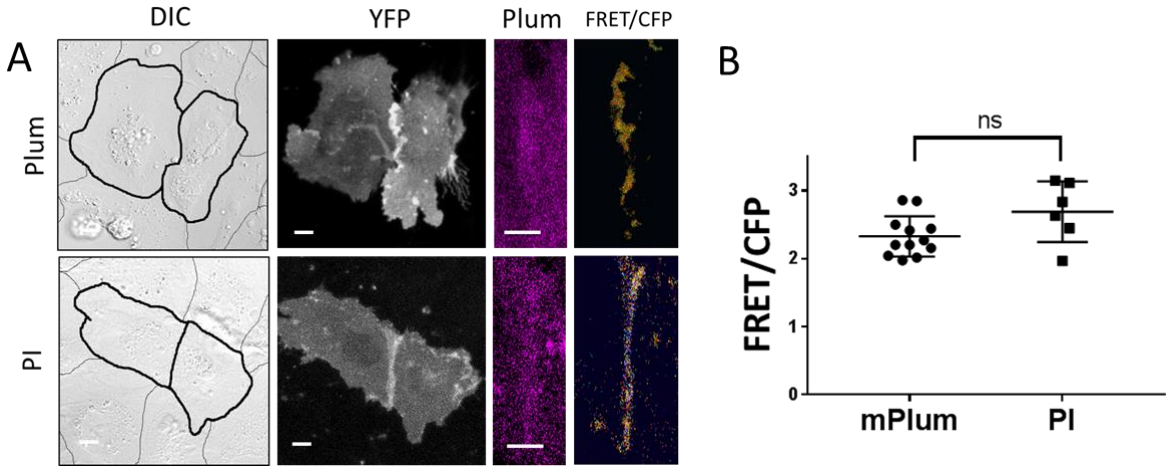

Figure 32. VE-PTP has no effect on Rac1 activity.
Rac1 activity at VE-cadherin junctions in HPAECs overexpressing mPlum or Plum-VE-PTP PI, n=6-10 junctions from 3 independent experiments; ns, not significant; unpaired t-test.

4.3. VE-PTP relieves tension across VE-cadherin junctions

Since RhoA activation increases tension applied across VE-cadherin junctions (Daneshjou et al., 2015), we addressed whether VE-PTP-dependent inhibition of GEF-H1 activity would reduce actomyosin-mediated tension and thereby enhance endothelial barrier function. To quantify tension changes at AJs, we used the VE-cadherin FRET-based tension biosensor (Conway et al., 2013). VE-PTP knockdown increased the tension applied at AJs compared to endothelial monolayers treated with control siRNA (Figure 33). Consistent with the role of VE-PTP in reducing GEF-H1 binding to RhoA, we observed that knockdown of GEF-H1 reduced the tension across VE-cadherin junctions in control and VE-PTP-depleted endothelial cells (Figure 33). Furthermore, we observed that overexpression of VE-PTP PI (like WT VE-PTP) also reduced the tension applied to VE-cadherin in quiescent monolayers (Figure 34), reinforcing the observation that VE-PTP phosphatase activity is not required to regulate RhoA activity at AJs).

Overexpression of WT VE-PTP significantly reduced the tension across VE-cadherin junctions induced by α-thrombin (Figure 35), which is known to activate RhoA signaling (van Nieuw Amerongen et al., 2000). Although WT and PI mutants were expressed and accumulated at AJs to the same extent (Figure 36), overexpression of PI mutant, however, had no significant effect on the tension applied to AJs in endothelial cell monolayers challenged with α-thrombin (Figure 34-35). These data further support the distinct functions of VE-PTP in resting quiescent endothelium *vs*. the endothelium activated with pro-inflammatory stimulus.

To reinforce the tension changes occurring at AJs as measured by the biosensor described above, we also determined the role of VE-PTP in modulating stress across AJs measured alternatively using the micropillar array assay (Yang et al., 2011). This measurement is very similar to that obtained with the VE-cadherin biosensor described above (see materials and

methods); however, it allows us to determine forces applied to AJs in absolute units. We observed that *VE-PTP*$^{-/-}$ mouse lung endothelial cells exhibited an increase in stress at AJs as compared to VE-PTP$^{flox/flox}$ (WT) endothelial cells (Figure 37), thus reinforcing our results with the VE-cadherin biosensor. Furthermore, analysis of traction forces using the bead displacement assay demonstrated that VE-PTP deletion had no effect on development of tension in single endothelial cells (Figure 37) consistent with the tension-reducing function of VE-PTP at VE-cadherin junctions described above.

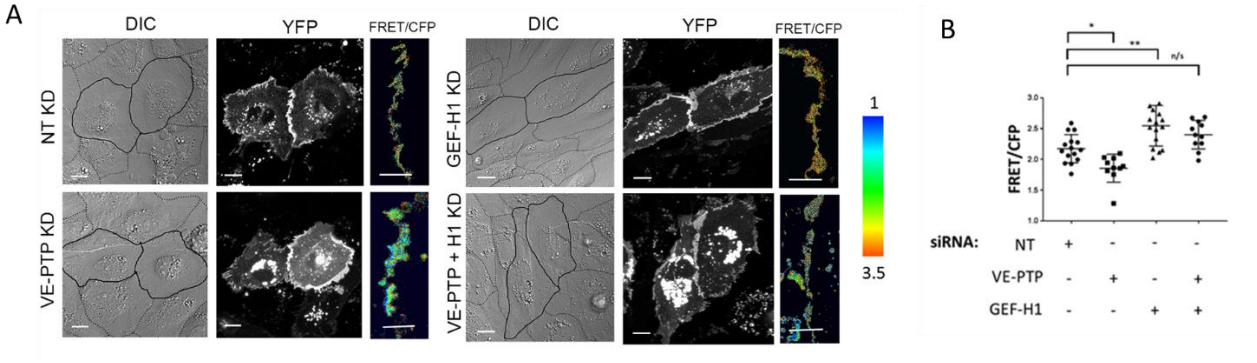

Figure 33. VE-PTP relieves the tension across VE-cadherin junctions.
(A) DIC and confocal images of VE-cadherin biosensor (YFP) and VE-cadherin tension (FRET/CFP) in HPAECs depleted of VE-PTP, GEF-H1, or both. The ratiometric images scaled from 1 to 3.5 and color coded as indicated on right. Warmer colors denote low tension. Scale bars, 5 μm.(B) Relative tension at AJs for groups in A. Higher values denote lower tension; mean ± SEM; n=10-15 junctions from 3 independent experiments; *, $p<0.05$, **, $p<0.001$; one-way ANOVA.

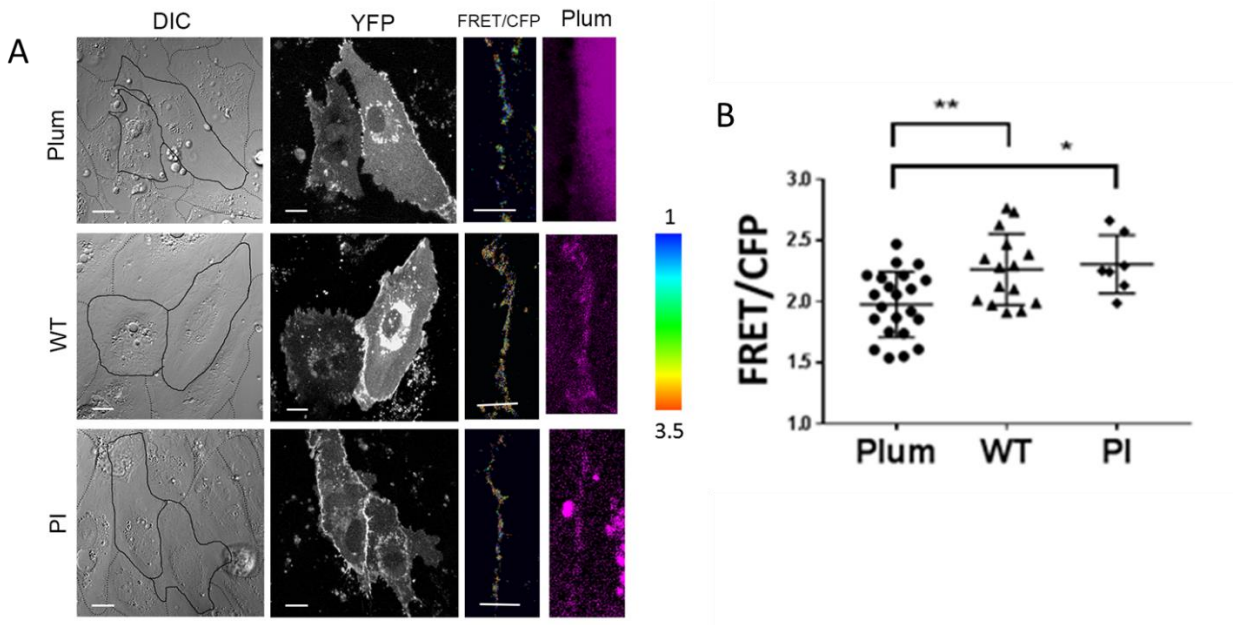

Figure 34. VE-PTP reduces the tension across VE-cadherin junctions independent of phosphatase activity.

(A) DIC and confocal images of VE-cadherin biosensor (YFP) and VE-cadherin tension (FRET/CFP) in HPAECs overexpressing mPlum (control), mPlum-VE-PTP (WT) or mPlum-VE-PTP PI (PI). The ratiometric images are scaled as in A. Scale bars, 5 μm. (B) Relative tension at AJs for groups in A; mean ± SEM; n=8-16 junctions from 3 independent experiments; *, $p<0.05$, **, $p<0.001$; one-way ANOVA.

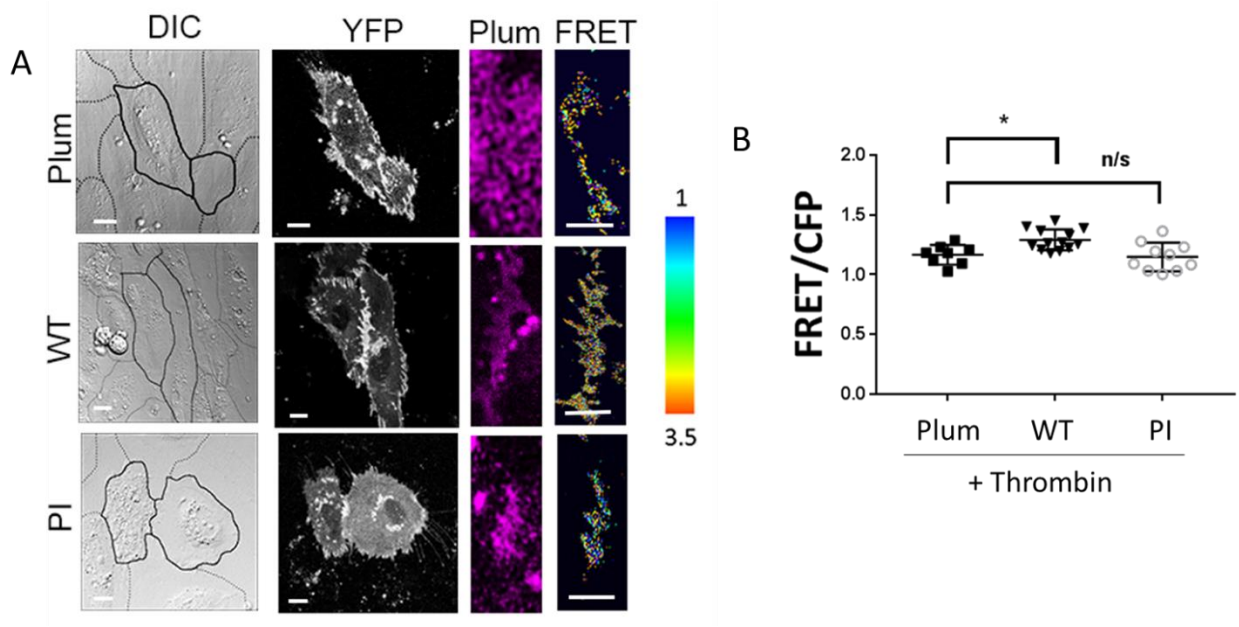

Figure 35. VE-PTP phosphatase is important in the stimulated endothelium.
(A) Tension across VE-cadherin junctions in HPAECs overexpressing mPlum, mPlum-VE-PTP (WT) or mPlum-VE-PTP PI (PI) and treated with 50nM human α-thrombin for 15 min. DIC, VE-cadherin tension biosensor (YFP), VE-PTP (magenta), and FRET/CFP (color coded) images are shown. The ratiometric images scaled from 1 to 3.5 and color coded as indicated on right. Warmer colors denote low tension. Scale bar, 5 µm. (B) Quantification of data in H; n=8-12 junctions from 3 independent experiments; *, $p<0.05$; one-way ANOVA.

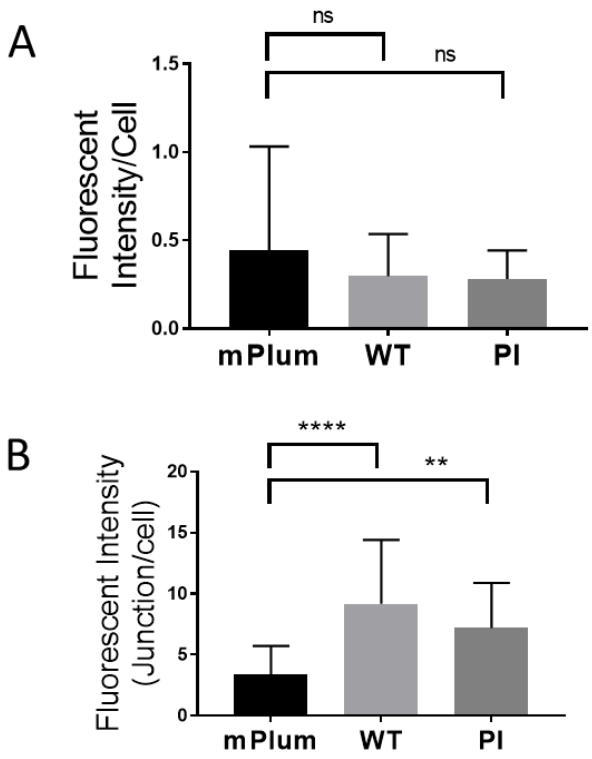

Figure 36. VE-PTP construct expression in HPAECs localizes to the AJ.
Expression levels of mPlum, WT or PI in HPAECs used in FRET studies. Fluorescent intensity per cell (A) and at the junction normalized to total mPlum fluorescence (B); n=21-32 from 9 experiments; **, $p<0.001$, ****, $p<0.0001$; one-way ANOVA.

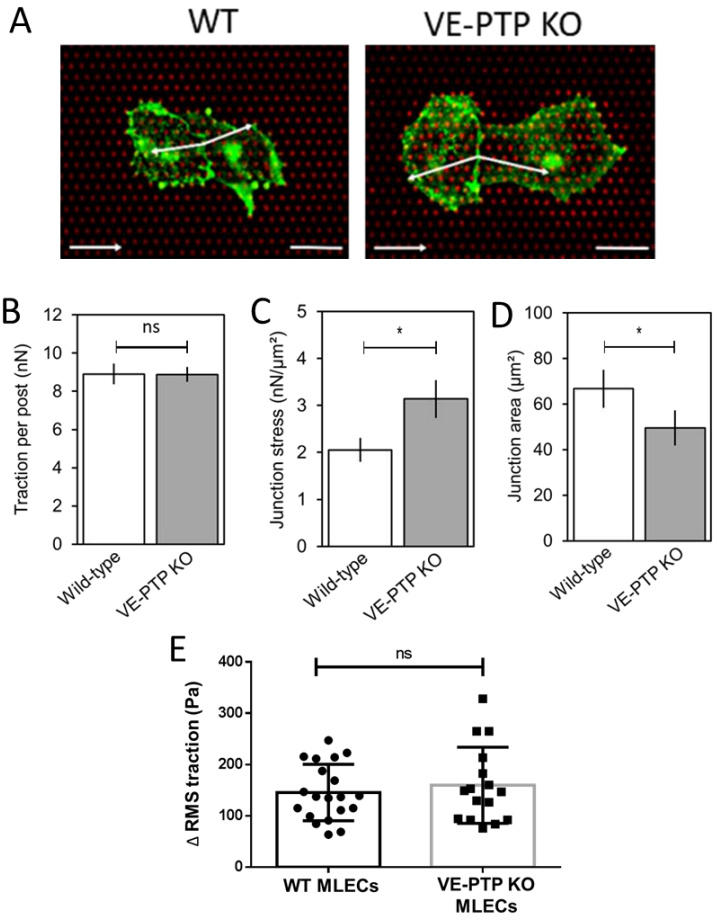

Figure 37. VE-PTP reduces EC stress and does not affect tension development in single cells. (A) Stress at AJs determined by micropillar array assay. Fluorescent images of WT (VE-PTP$^{flox/flox}$) and VE-PTP KO mouse lung endothelial cells (MLECs) grown on fibronectin-coated micropillar posts (red). Junctions were visualized with β-catenin staining (green). Sum of traction forces shown by vectors (see Materials and Methods). Scale bar, 30 µm; force bar, 100 nN. (B-D) Quantification of junction stress, area, and traction. VE-PTP knockout mouse cells show increase junctional stress and reduced junctional area. n = 12-14; Stress values were 2.05 ± 0.25 nN/µm^2 and 3.13 ± 0.40 nN/µm in WT and VE-PTP KO MLEC; mean ± SEM; *, $p<0.05$ by unpaired t-test. (E) Bar graph indicating traction changes (ΔRMS traction, Pa) exerted by WT MLECs and VE-PTP KO MLECs plated on 40-kPA gels coated with fibronectin (n=20 for WT MLECs, n=16 for VE-PTP KO MLECs). Two-tailed *t*-test show no significant differences.

4.4. GEF-H1 knockdown or overexpression of VE-PTP cytosolic domain restores VE-cadherin internalization rates in VE-PTP deficient cells

To determine the specific role of GEF-H1 (ARHGEF2) in mediating stabilization of VE-cadherin junctions, we measured VE-cadherin internalization rates in endothelial monolayers depleted of GEF-H1 and in monolayers depleted of other relevant RhoGEFs. Knockdown of GEF-H1 significantly reduced VE-cadherin internalization rate compared to cells treated with control siRNA (Figure 38). In contrast, knockdown of ARHGEF1 (p115RhoGEF), ARHGEF18 (p114RhoGEF), or ARHGEF28 (p190RhoGEF), also known to regulate RhoA activity (Abiko et al., 2015; Gebbink et al., 1997; Hart et al., 1998; Holinstat et al., 2003; Kozasa et al., 1998; Niu et al., 2003; Tornavaca et al., 2015), did not show reduction in VE-cadherin internalization rates (Figure 39). Furthermore, GEF-H1 depletion reduced VE-cadherin internalization rate and permeability values in the background of VE-PTP deficiency (Figure 38, 40).

To investigate the role of VE-PTP interaction with GEF-H1 in regulating VE-cadherin dynamics at AJs, we determined the effects of overexpressing the VE-PTP cytosolic domain (C domain) which interacts with GEF-H1 *in vitro* (Figure 20). We found that overexpression of the VE-PTP C domain significantly reduced GEF-H1 binding to RhoA in endothelial monolayers depleted of VE-PTP (Figure 41). Furthermore, it reduced the VE-cadherin internalization rate and endothelial permeability to albumin in VE-PTP-depleted endothelial cells (Figure 42-43) indicating a causal link between VE-PTP and GEF-H1 in regulating the stability of VE-cadherin junctions and the endothelial barrier. To establish the relationship between RhoA signaling and VE-cadherin dynamics at AJs, we also pharmacologically activated Rho signaling or inhibited ROCK. Activation of Rho with CN-01 increased VE-cadherin internalization rates whereas inhibition of Rho signaling with Rockout (ROCK inhibitor) decreased VE-cadherin internalization

rates in quiescent confluent monolayers (Figure 44). The data therefore show a connection between RhoA signaling and VE-cadherin internalization rate. These findings are consistent with the proposed model that VE-PTP stabilizes VE-cadherin junctions and reduces endothelial permeability through the inhibition of GEF-H1, RhoA activity, and tension, thereby decreasing the rate of VE-cadherin internalization.

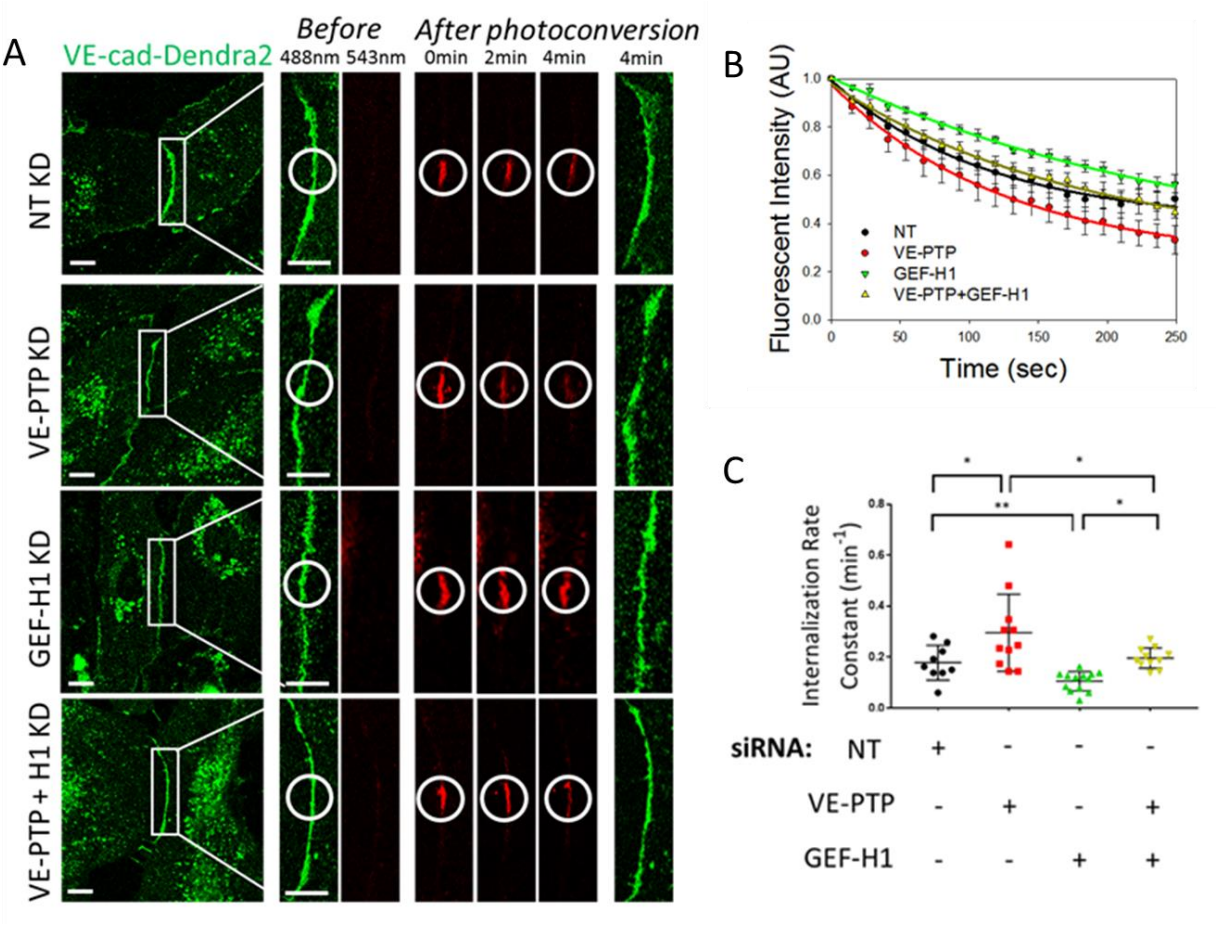

Figure 38. GEF-H1 knockdown restores VE-cadherin internalization rate in VE-PTP-depleted endothelial monolayers.

(A) VE-cadherin-Dendra2 before (green) and after (red) photoconversion in HPAECs depleted of VE-PTP, GEF-H1, or VE-PTP and GEF-H1 simultaneously. Scale bars, 5μm. (B) VE-cadherin internalization from AJs from data in A; mean ± SEM; n=9-13 junctions from 3 independent experiments. (C) Internalization rate constants calculated from B were 0.17 ± 0.02 min^{-1} in NT siRNA treated cells, 0.29 ± 0.04 min^{-1} and 0.10 ± 0.01 min^{-1} in VE-PTP and GEF-H1 depleted cells, or 0.19 ± 0.01 min^{-1} after simultaneous depletion of VE-PTP and GEF H1; mean ± SEM; n=9-13 junctions from 3 independent experiments; *, $p<0.05$, **, $p<0.001$; one-way ANOVA.

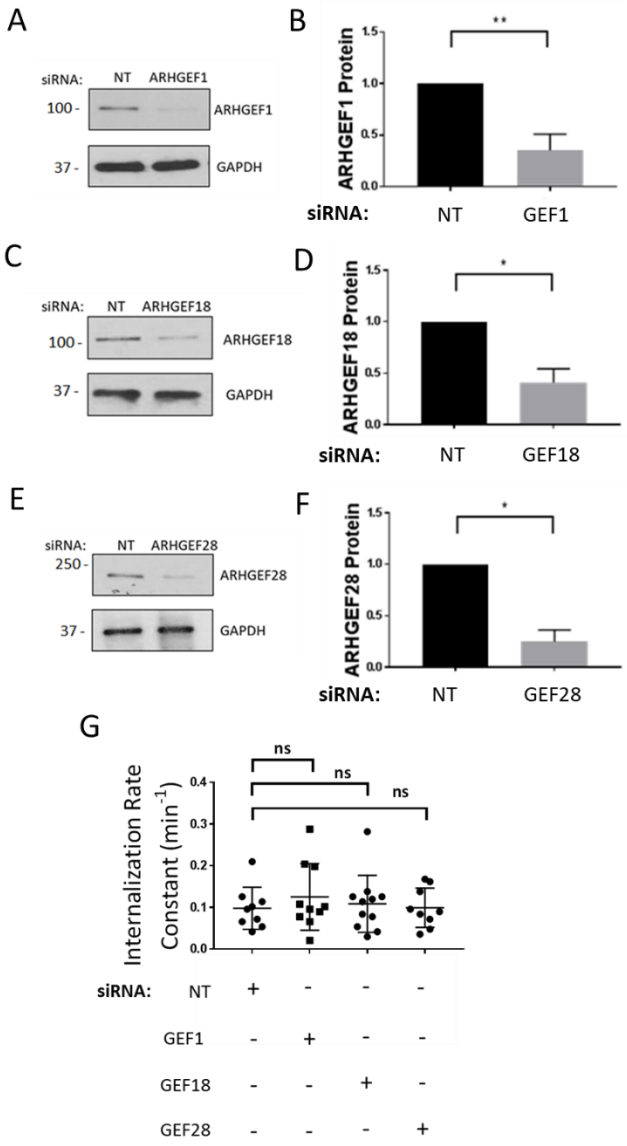

Figure 39. Knockdown of various RhoGEFs and their contribution in regulating VE-cadherin internalization rates at AJs.
(A,C,E) WB analysis and (B,D,F) data quantification of ARHGEF1, ARHGEF18, and ARHGEF28 in HPAECs depleted of these proteins, n=2-3; *, $p<0.05$, **, $p<0.001$, unpaired *t*-test. (G) VE-cadherin-Dendra2 internalization rate constants in HPAECs monolayers treated as indicated; mean ± SEM; n=9-11 junctions from 3 independent experiments; ns, not significant; one-way ANOVA.

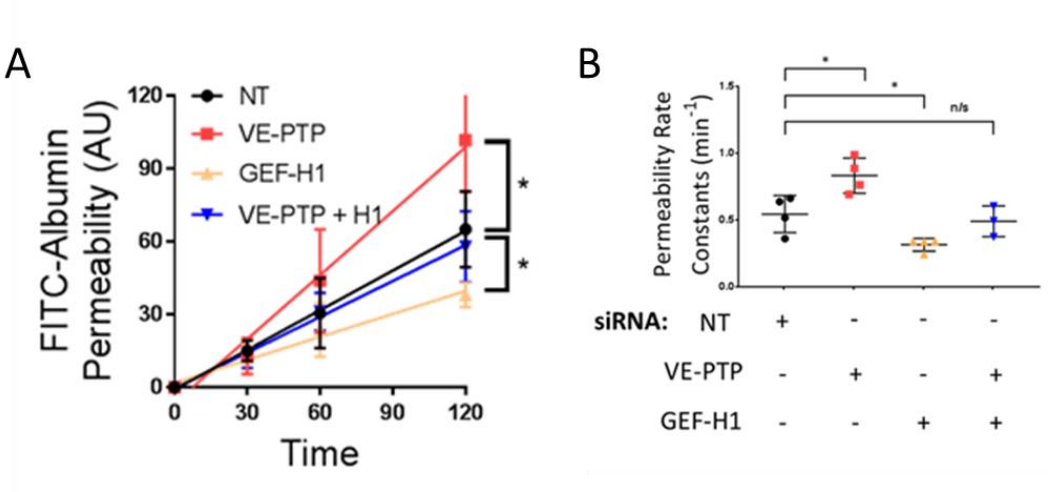

Figure 40. GEF-H1 restores permeability in VE-PTP-depleted endothelial monolayers. (A) Permeability of HPAEC monolayers to FITC-conjugated albumin in HPAECs depleted of VE-PTP, GEF-H1, or VE-PTP and GEF-H1 simultaneously; n=3-4. *, $p<0.05$; one-way ANOVA. (B) Permeability rate constants from A were 0.54 ± 0.06 min^{-1} in NT siRNA-treated cells, 0.83 ± 0.06 min^{-1} and 0.31 ± 0.02 min^{-1} after VE-PTP and GEF H1 depletion, or 0.49 ± 0.06 min^{-1} after simultaneous depletion of VE-PTP and GEF H1; mean ± SEM; n=3-4, *, $p<0.05$; one-way ANOVA.

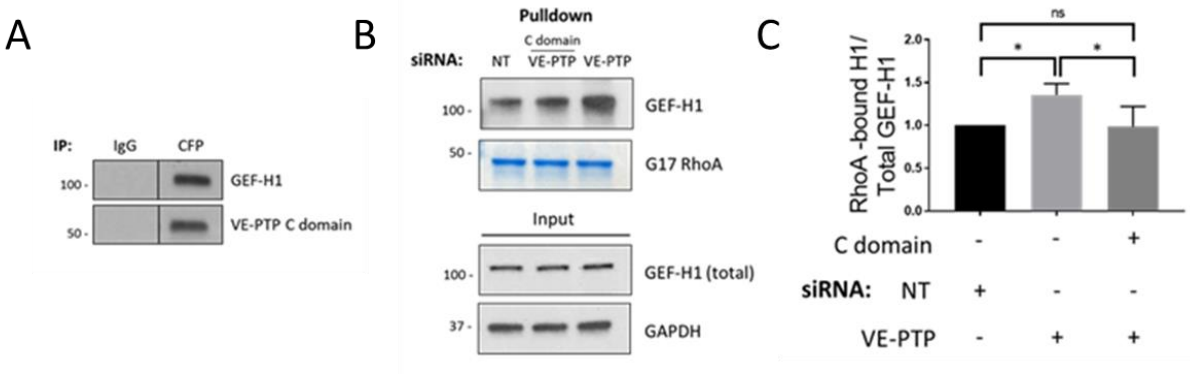

Figure 41. VE-PTP cytosolic domain rescues GEF-H1 activity in VE-PTP-depleted endothelial monolayers.

(A) Immunoprecipitation of CFP-tagged VE-PTP C domain from HPAEC lysates. Blots were probed for GEF-H1 and CFP (B) Interaction of GEF-H1 with GST-RhoA (G17A) in HPAECs treated with NT siRNA, or depleted of VE-PTP with and without overexpression of VE-PTP cytosolic (C) domain. The resulting precipitates were probed for GEF-H1. (C) Analysis of interaction from data in B. mean ± SEM; n=3; *, $p<0.05$; one-way ANOVA.

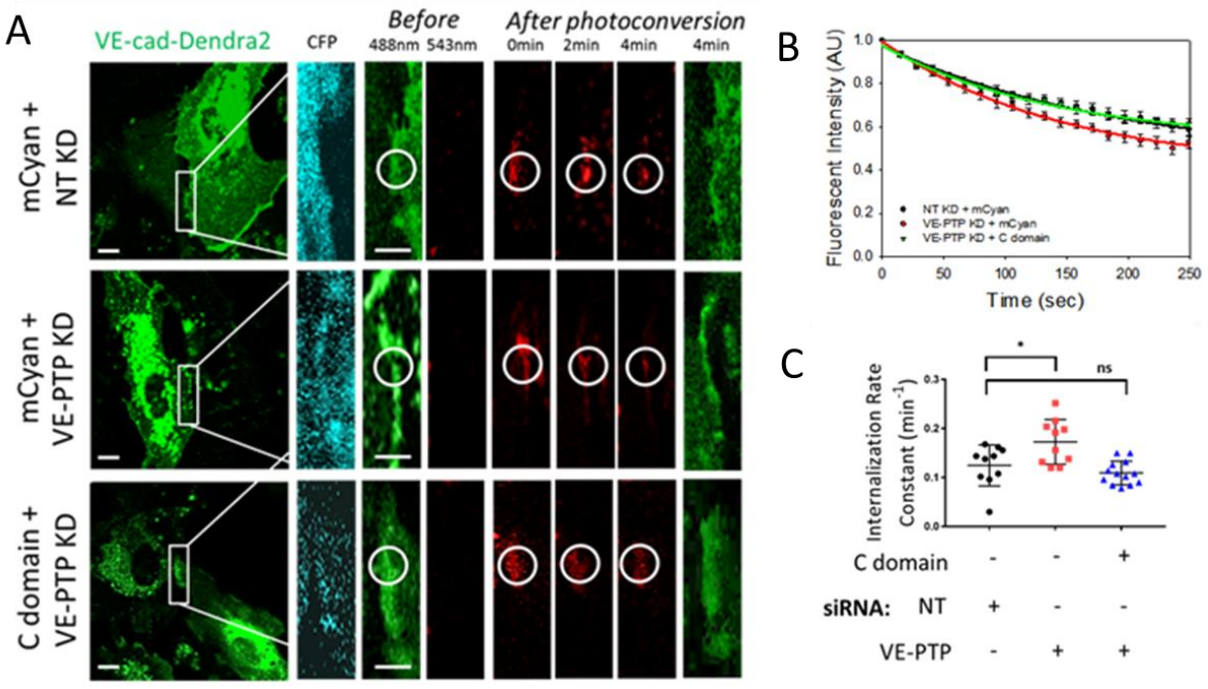

Figure 42. VE-PTP cytosolic domain rescues VE-cadherin internalization rate in VE-PTP-depleted endothelial monolayers.

(A) VE-cadherin-Dendra2 before (green) and after (red) photoconversion in HPAECs treated with of NT siRNA or VE-PTP siRNA and overexpressing mCyan or HPAECs treated with VE-PTP siRNA and expressing VE-PTP cytosolic (C) domain. Scale bars, 5μm. (B) VE-cadherin internalization rate curves for groups in A; mean ± SEM; n=10-13 junctions from 3 independent experiments. (C) Internalization rate constants calculated from B were 0.12 ± 0.01 min^{-1} in NT siRNA treated cells, 0.17 ± 0.01 min^{-1} in VE-PTP depleted cells, or 0.11 ± 0.01 min^{-1} in VE-PTP -depleted cells overexpressing VE-PTP C domain; mean ± SEM; n=10-13 junctions from 3 independent experiments; *, $p<0.05$; one-way ANOVA.

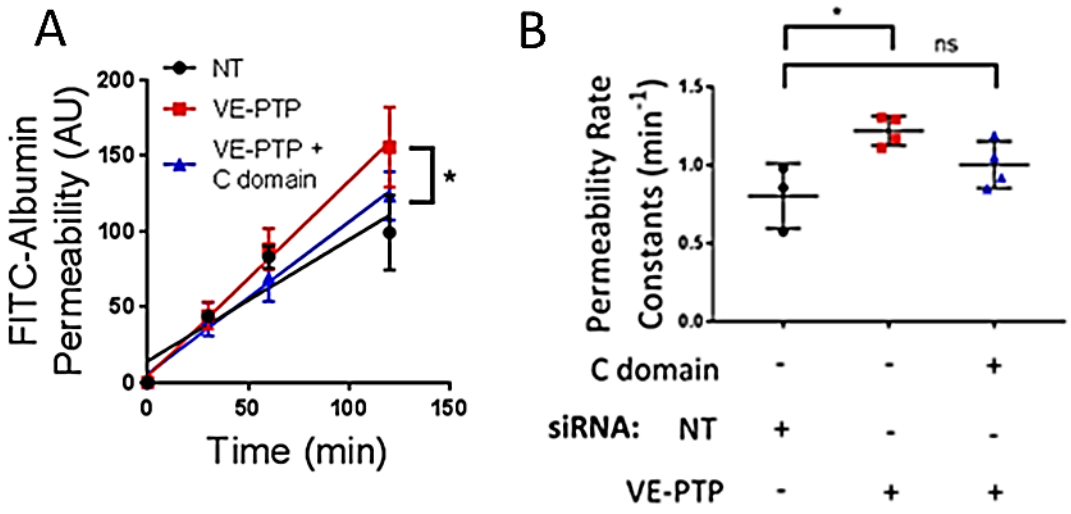

Figure 43. VE-PTP cytosolic domain rescues endothelial permeability in VE-PTP-depleted endothelial monolayers.
(A) Permeability of HPAEC monolayers to FITC-conjugated albumin in HPAECs treated with of NT siRNA or VE-PTP siRNA and overexpressing mCyan or HPAECs treated with VE-PTP siRNA and expressing VE-PTP cytosolic (C) domain; n=3-4, *, $p<0.05$; one-way ANOVA. (B) Permeability rate constants from A were 0.80 ± 0.12 min^{-1} in NT siRNA-treated cells, 1.22 ± 0.05 min^{-1} VE-PTP depletion or 1.00 ± 0.07 min^{-1} in cells overexpressing VE-PTP domain and on the background of VE-PTP depletion; mean ± SEM; n=3-4, *, $p<0.05$; one-way ANOVA.

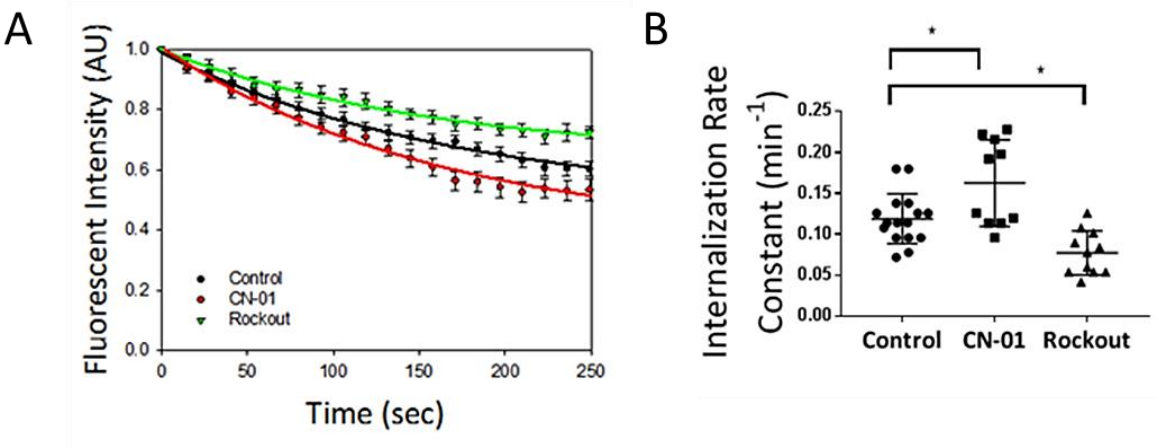

Figure 44. Effect of Rho signaling on VE-cadherin internalization rate at AJs.
VE-cadherin-Dendra2 internalization curves (A) and internalization rate constants (B) in HPAECs treated with vehicle, or 50 µM Rho activator (CN-01), or 50 µM ROCK inhibitor (Rockout); mean ± SEM; n=8-16 junctions from 3 independent experiments; *, $p<0.05$; one-way ANOVA.

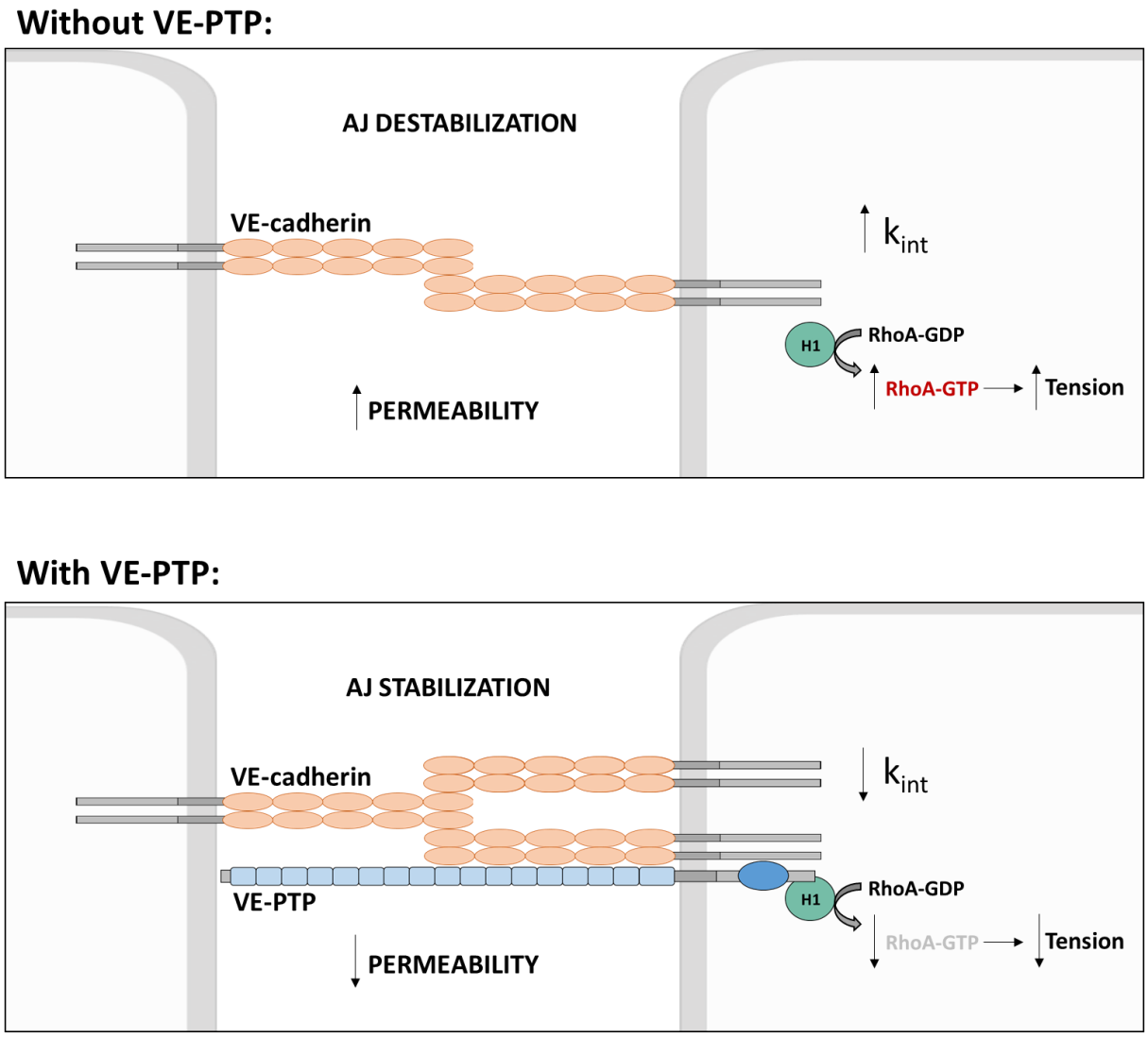

Figure 45. VE-PTP Inhibits GEF-H1 to Stabilize VE-cadherin Junctions in Endothelial Cells. We demonstrate a novel function of VE-PTP in stabilizing VE-cadherin junctions in the quiescent confluent endothelial monolayer. In the absence of VE-PTP, there is high GEF-H1 activity at VE-cadherin junctions which results in increased RhoA activity and tension at AJs. The tension applied to VE-cadherin increases VE-cadherin internalization rate and increases endothelial permeability. In the presence of VE-PTP, VE-PTP serves as a scaffold through direct interaction with GEF-H1 and inhibits its binding to RhoA, thus reducing RhoA activity and tension at VE-cadherin junctions. VE-PTP promotes endothelial barrier stability by reducing the rate of VE-cadherin internalization and restricting endothelial permeability. This is an essential factor regulating the stability of AJs in vessels.

5. DISCUSSION AND CONCLUSION

VE-PTP acts as a scaffold in the resting endothelium

VE-cadherin adhesion exhibits steady-state kinetics, an inherently dynamic process, which is responsible for the integrity of the endothelial barrier. VE-cadherin's kinetics, or dynamics, involve both the k_{on} rate and k_{off} rate. The $k_{on,}$ rate is the recruitment of VE-cadherin to the membrane. The k_{off} rate is the movement of VE-cadherin from the adherens junction, where the VE-cadherin undergoes internalization as well as lateral movement and displacement. VE-cadherin internalization, however, is the major player determining k_{off} (Daneshjou et al., 2015).

The interaction between VE-PTP, the receptor-like, transmembrane protein tyrosine phosphatase (Alonso et al., 2004; Fachinger et al., 1999), and VE-cadherin, form a critical complex to maintain the endothelial barrier in the resting state. In this thesis, we have discovered that VE-PTP plays a vital part in VE-cadherin's steady state kinetics within the resting, confluent endothelium. Immunofluorescent staining experiments indicated that VE-PTP knockdown decreases VE-cadherin at the junction. Because the density of VE-cadherin determines its dynamic nature at the junction (Abu Taha et al., 2014; Huveneers et al., 2012), this suggests that VE-PTP plays a significant role in maintaining VE-cadherin junctional density through decreasing VE-cadherin's internalization rate in the resting endothelium.

Through a series of Dendra2 experiments, we have established the role of VE-PTP's various domains in stabilizing VE-cadherin adhesion. VE-PTP contains an extracellular domain consisting of 17 fibronectin-like repeats, a transmembrane domain, and an intracellular phosphatase domain. Both WT (full-length) and Δ16FN (removal of first 16 fibronectins) VE-PTP constructs stabilized VE-cadherin through reducing VE-cadherin internalization rate, however deletion of the 17^{th} fibronectin domain abolished that stabilization (ΔN). Because the

17th fibronectin-like domain of VE-PTP has been found to be the interaction point at which VE-cadherin binds (Nawroth et al., 2002), these experiments suggest that in the resting state, VE-PTP needs to interact with VE-cadherin to exert its effect on VE-cadherin internalization. However, the effect of ΔN VE-PTP is still inconclusive, because its localization at VE-cadherin junctions was visually lower than the other VE-PTP constructs tested. This may be because ΔN is more disbursed throughout the junction suggesting that VE-cadherin is not anchoring it there. Dendra2 experiments therefore may not have accurately shown the true effect of ΔN on VE-cadherin internalization. Further experiments will need to elucidate if ΔN can indeed reduce VE-cadherin internalization rate if there is sufficient expression at the VE-cadherin junction. Using ΔN in viral form may be a good method to ensure sufficient expression at the endothelial barrier.

Phosphorylation and dephosphorylation of VE-cadherin's tyrosine residues have been established as crucial sites for VE-cadherin regulation in the stimulated endothelium, however, until now, no studies have investigated how crucial these sites are in the resting endothelium. Knockdown of VE-PTP and inhibition of VE-PTP phosphatase activity in previous studies had no effect on the phosphorylation state of VE-cadherin (Gurnik et al., 2016; Nottebaum et al., 2008). In support of these findings, VE-PTP overexpression in CHO cells expressing GFP-VE-cadherin had no effect on Y658 and Y685 phosphorylation state. Additionally, overexpression of a phosphatase inactive VE-PTP mutant was able to stabilize VE-cadherin through decreased VE-cadherin internalization. Furthermore, treatment of resting endothelial cells with AKB-9785, a specific VE-PTP phosphatase inhibitor, had no effect on the VE-cadherin internalization rate. These studies collectively suggest that VE-PTP phosphatase activity is minimally important in the resting endothelium.

Although, we found no change in the VE-cadherin phosphorylation state, it is still possible that VE-PTP's phosphatase function is important in the phosphorylation state of other proteins. The catenins which interact with VE-cadherin could play a role in VE-PTP's effect on VE-cadherin internalization. Plakoglobin is a probable candidate if this is true. In previous studies, plakoglobin and not β-catenin was shown to be a key player in maintaining the endothelial barrier (Nottebaum et al., 2008). Further studies need to establish the role of plakoglobin in VE-cadherin dynamics to answer this question.

Deleting the VE-PTP phosphatase domain did not have a stabilizing effect on VE-cadherin. This suggests that the VE-PTP phosphatase domain itself is important to stabilize VE-cadherin, even though VE-PTP's phosphatase activity may be minimally important. Therefore, we have demonstrated that VE-PTP has the ability to serve as a scaffold to another protein which can indirectly stabilize VE-cadherin internalization rate.

The scaffolding role of VE-PTP allows the possibility that other phosphatases could behave in this manner under resting conditions. In this regard, VE-PTP resembles PTP-PEST, a cytosolic member of the PTP family, which also forms protein complexes independent of its catalytic activity (Davidson and Veillette, 2001). In our studies, we investigated VE-PTP's intracellular domain in its entirety. Future studies will need to determine the importance of smaller domains within the cytosolic region. This would lead to answering more specific questions about determining the importance of the catalytic domain and flanking non-catalytic domains.

VE-PTP binds to GEF-H1 to inhibit RhoA activity and tension at VE-cadherin junctions

Through a series of immunoprecipitation experiments and subsequent mass spectrometry analyses, we found that VE-PTP binds to and inhibits a guanine nucleotide exchange factor for

RhoA, GEF-H1 (Krendel et al., 2002; Ren et al., 1998). GEF-H1 promotes the exchange of RhoA GDP to GTP leading to activation of RhoA (Krendel et al., 2002; Ren et al., 1998). Our data demonstrate that binding to VE-PTP inhibits GEF-H1 activity because overexpression of full length or the cytosolic portion of VE-PTP significantly reduced GEF-H1 binding to RhoA and consequently inhibited RhoA activity at endothelial AJs. On the contrary, depletion of VE-PTP resulted in activation of RhoA specifically at AJs and not in cytosol. This finding suggests that VE-PTP provides spatial inhibition of RhoA at the AJs. This is similar to the tight junction protein cingulin in epithelial cells where interaction with GEF-H1 inhibits RhoA activity at TJs (Aijaz et al., 2005).

Exactly how VE-PTP regulates GEF-H1 activity remains unknown. Previous work has demonstrated that GEF-H1 activity is regulated by protein-protein interaction (Aijaz et al., 2005; Krendel et al., 2002; Ren et al., 1998) as well as by phosphorylation at serine and threonine residues (Birkenfeld et al., 2007; Fujishiro et al., 2008; von Thun et al., 2013; Zenke et al., 2004). We found that VE-PTP did not dephosphorylate GEF-H1. Based on our data we propose that binding to VE-PTP stabilizes GEF-H1 in its inactive conformation which is unable to bind RhoA. This mechanism is similar to interaction with microtubules and cingulin (Aijaz et al., 2005; Krendel et al., 2002; Ren et al., 1998), both known to inhibit GEF-H1 ability to activate RhoA (Aijaz et al., 2005; Krendel et al., 2002; Ren et al., 1998).

Because of the mechanistic similarity to cingulin-mediated GEF-H1 inhibition at the tight junction, we investigated the role of cingulin in VE-cadherin junctional expression. We performed immunoprecipitation and western blot experiments on cells depleted of VE-PTP and determined VE-cadherin expression compared to control. Cingulin protein expression was not significantly affected in VE-PTP-depleted cells and had no effect on the junctional expression of VE-cadherin.

These results indicate that cingulin does not play a role in our particular mechanism, however, future studies should determine if there's crosstalk between the VE-cadherin junctions and tight junctions.

We have shown previously that RhoA destabilizes AJs *via* actomyosin-dependent increase in tension applied to VE-cadherin adhesion (Daneshjou et al., 2015; Yamada and Nelson, 2007). This generates forces which disrupts VE-cadherin *trans*-interactions and induces VE-cadherin internalization (Daneshjou et al., 2015). The spatial inhibition of the RhoA/ROCK pathway at AJs reduced this tension and stabilized VE-cadherin junctions (Daneshjou et al., 2015). Here, we describe a novel mechanism which is responsible for inhibiting RhoA signaling at AJs. VE-PTP interaction with GEF-H1 provides a constitutive mechanism modulating tension across VE-cadherin junctions in resting endothelial monolayers. Knockdown of VE-PTP increased the interaction of GEF-H1 with RhoA leading to increased tension across VE-cadherin junctions whereas overexpression of either VE-PTP or phosphatase inactive mutant reduced the tension applied to VE-cadherin junctions further supporting the proposed phosphatase-independent mechanism of GEF-H1 inhibition in resting endothelial monolayers. Interestingly, WT VE-PTP, but not a phosphatase inactive mutant, reduced tension in endothelial monolayers challenged with α-thrombin indicating that this described mechanism functions in a context-dependent manner. Collectively, our results support the model that the control of RhoA activity at VE-cadherin junctions and the resultant changes in actomyosin tension are the key regulators of AJ stability (Daneshjou et al., 2015).

Whether activation of the endothelium with thrombin will exhibit a higher importance for VE-PTP phosphatase activity in other systems needs to be elucidated. In our studies, we only tested VE-PTP phosphatase importance when analyzing VE-cadherin tension. Whether this holds

true for RhoA activity with the RhoA biosensor or in Dendra2 experiments, would be an interesting avenue to explore.

As stated previously, VE-cadherin molecules are continuously exchanged between junctional and cytosolic pools to remodel VE-cadherin junctions and maintain steady state homeostasis (Daneshjou et al., 2015; Dorland et al., 2016; Kruse et al., 2018; Xiao et al., 2003; Xiao et al., 2005). We previously established a relationship between tension across VE-cadherin adhesion and VE-cadherin internalization rate at AJs (Daneshjou et al., 2015). Here we extend this concept by describing a molecular mechanism providing control of VE-cadherin internalization at AJs in the quiescent endothelial barrier. Knockdown of VE-PTP increased VE-cadherin internalization rate and endothelial permeability, whereas knockdown of GEF-H1 or overexpression of cytosolic domain of VE-PTP, responsible for the interaction with GEF-H1, restored VE-cadherin internalization rate and reduced endothelial permeability. While depleting GEF-H1 might have broader effects on endothelial function through re-organization of the actin cytoskeleton (Birukova et al., 2006; Birukova et al., 2010; Krendel et al., 2002), our data demonstrate a significant role of GEF-H1 at the endothelial barrier.

Interestingly, depletion or overexpression of VE-PTP have no effect on Rac1 activity at AJs suggesting specificity of RhoA signaling. While RhoA is also known to be implicated in regulating the cell-cell adhesion by antagonizing Rac1 signaling in endothelial cells (Shcherbakova et al., 2018; Vouret-Craviari et al., 2002; Wojciak-Stothard et al., 2001), our data suggests that these proteins have no effect on the rate of VE-cadherin internalization in resting monolayers. Induction of Rac1 activity reduces VE-cadherin internalization rate (Daneshjou et al., 2015) and inversely, VE-cadherin adhesion can induce Rac1 through recruiting RacGEFs. Activation of Rac1 can induce p190RhoGAP thereby inhibiting RhoA activity. Because our

studies indicate that VE-PTP has no effect on Rac1, VE-PTP therefore does not contribute to this pathway. In this thesis, we have discovered that VE-PTP impacts RhoA signaling through inhibiting GEF-H1, a novel mechanism.

Other RhoGEFs, such as p115RhoGEF (Schmidt et al., 2013), have been shown to be important in the regulation of RhoA signaling in the endothelium. Deletion of endothelial FAK facilitates the interaction between p115RhoGEF and RhoA and plays a role in maintaining the endothelial barrier through assisting in the Rac1 and RhoA balance. In our studies, deletion of p115RhoGEF had no effect on VE-cadherin internalization rate. This suggests that VE-PTP-mediated barrier maintenance is specific to GEF-H1, however, it is possible that there are other RhoGEFs at play that were not tested. Further studies should investigate a larger pool of RhoGEFs to determine the full scope.

Whether VE-PTP specifically inhibits GEF-H1 at the VE-cadherin junction remains under scrutiny. Our studies have alluded to GEF-H1 regulation at the AJ. Immunostaining experiments indicated that VE-PTP knockdown reduced GEF-H1 at the VE-cadherin mask, however, because the GEF-H1 staining was relatively non-specific, these results need to be further investigated. Future studies will need to focus on implementing better tools for visualizing GEF-H1 distribution within the endothelium.

Knockdown of GEF-H1 affected RhoA and VE-cadherin tension specifically at the VE-cadherin junction. This suggests that GEF-H1 does effect RhoA activity at the AJ, but does not rule out the possibility that GEF-H1 can work at a distance. Previous studies investigating RhoA's spatiotemporal activity at the junction found an absence of localized RhoA activity at the disassembling junction (Szulcek et al., 2013). This suggests that the effect of RhoA signaling on VE-cadherin internalization rate and tension, for example, may operate at a distance. Indeed,

global inhibition of RhoA activity reduced VE-cadherin internalization whereas activation of RhoA increased VE-cadherin internalization indicating that global changes in RhoA can affect the VE-cadherin steady-state kinetics in the resting endothelium.

Conclusion

In conclusion, we demonstrate a novel function of VE-PTP in stabilizing VE-cadherin junctions in the quiescent endothelial monolayer. VE-PTP serves a scaffolding function through directly interacting with GEF-H1 and inhibiting its binding to RhoA, thus reducing RhoA activity and tension at VE-cadherin junctions. The decreased tension at VE-cadherin junctions reduces the rate of VE-cadherin internalization and is a primary factor regulating junctional stability (Figure 45).

6. FUTURE DIRECTIONS

One important question is the extent at which VE-PTP's phosphatase activity is important in the stimulated endothelium. We used thrombin to determine this importance in VE-cadherin tension, however, this wasn't investigated in terms of VE-cadherin dynamics or RhoA activity. Although ablation of VE-PTP's phosphatase activity can maintain VE-cadherin junctional integrity, it would be interesting to see if VE-PTP loses its ability to protect VE-cadherin dynamics and RhoA activity levels in the stimulated endothelium.

The dynamics of VE-PTP could also play a role in the mechanism described in this thesis. VE-PTP-Dendra2 would be a valuable tool to shed light on VE-PTP dynamics in the resting vs. stimulated endothelium. It would be worth it to investigate changes in VE-PTP dynamics of the various VE-PTP constructs, which would elucidate the importance of each domain in VE-PTP's movement at the endothelial barrier. This would be particularly interesting in the case of ΔN VE-PTP due to its inability to localize well at VE-cadherin junctions.

Furthermore, investigations into any subdomains within VE-PTP's intracellular domain would be very interesting to pursue so as to determine the essence of its non-catalytic (scaffolding) function versus catalytic function. Binding assays with GEF-H1's C terminal domain and various constructs of VE-PTP's intracellular domain would begin to answer this question. Additionally, performing immunofluorescent studies to look at the localization of VE-PTP's various intracellular domain constructs could elucidate binding partners and the importance of each domain in intracellular localization.

As stated in the discussion, further determination of GEF-H1 localization would be a valuable future study in elucidating whether GEF-H1 indeed functions solely at junctions to regulate RhoA activity at VE-cadherin junctions, or if GEF-H1 can function from a distance. High

resolution microscopy would be needed to determine intimate placement of GEF-H1 in cells depleted of VE-PTP, as well as interaction between VE-PTP and GEF-H1. Viral constructs would likely be needed for sufficient expression in endothelial cells.

Another important question is whether changes in VE-PTP localization due to the inflammatory state result in a higher interaction with its other major binding partner, Tie2 kinase. Although we did not investigate the role of Tie2 in our studies, this would be an interesting investigation to take on. Despite the long-standing notion that tyrosine phosphatases protect endothelial barrier function by maintaining VE-cadherin and associated catenin proteins in dephosphorylated states, VE-PTP has a dual role in regulating the permeability of the endothelial vessel wall through its direct interaction with VE-cadherin and Tie2(Frye et al., 2015; Hayashi et al., 2013). Depending on the intracellular context, VE-PTP has the capacity to both stabilize and destabilize AJs. It promotes endothelial barrier function by dephosphorylating VE-cadherin, but weakens the endothelial barrier by dephosphorylating Tie2 and inhibiting Ang1/Tie2 signaling(Frye et al., 2015; Gong et al., 2015; Hayashi et al., 2013; Nawroth et al., 2002; Shen et al., 2014). Elucidating VE-PTP's dual role would be an intriguing endeavor.

Collectively, the above studies would have great importance in furthering our understanding of how VE-PTP functions under many different hats and how this translates to a disease state. How VE-PTP transforms between different endothelial states could potentially lead to therapeutic advances in preventative medicine.

7. REFERENCES

Abiko, H., S. Fujiwara, K. Ohashi, R. Hiatari, T. Mashiko, N. Sakamoto, M. Sato, and K. Mizuno. 2015. Rho guanine nucleotide exchange factors involved in cyclic-stretch-induced reorientation of vascular endothelial cells. *J Cell Sci*. 128:1683-1695.

Abu Taha, A., M. Taha, J. Seebach, and H.J. Schnittler. 2014. ARP2/3-mediated junction-associated lamellipodia control VE-cadherin-based cell junction dynamics and maintain monolayer integrity. *Mol Biol Cell*. 25:245-256.

Aijaz, S., F. D'Atri, S. Citi, M.S. Balda, and K. Matter. 2005. Binding of GEF-H1 to the tight junction-associated adaptor cingulin results in inhibition of Rho signaling and G1/S phase transition. *Dev Cell*. 8:777-786.

Allingham, M.J., J.D. van Buul, and K. Burridge. 2007. ICAM-1-mediated, Src- and Pyk2-dependent vascular endothelial cadherin tyrosine phosphorylation is required for leukocyte transendothelial migration. *J Immunol*. 179:4053-4064.

Alonso, A., J. Sasin, N. Bottini, I. Friedberg, I. Friedberg, A. Osterman, A. Godzik, T. Hunter, J. Dixon, and T. Mustelin. 2004. Protein tyrosine phosphatases in the human genome. *Cell*. 117:699-711.

Andriopoulou, P., P. Navarro, A. Zanetti, M.G. Lampugnani, and E. Dejana. 1999. Histamine induces tyrosine phosphorylation of endothelial cell-to-cell adherens junctions. *Arterioscler Thromb Vasc Biol*. 19:2286-2297.

Angelini, D.J., S.W. Hyun, D.N. Grigoryev, P. Garg, P. Gong, I.S. Singh, A. Passaniti, J.D. Hasday, and S.E. Goldblum. 2006. TNF-alpha increases tyrosine phosphorylation of vascular endothelial cadherin and opens the paracellular pathway through fyn activation in human lung endothelia. *Am J Physiol Lung Cell Mol Physiol*. 291:L1232-1245.

Bakal, C.J., D. Finan, J. LaRose, C.D. Wells, G. Gish, S. Kulkarni, P. DeSepulveda, A. Wilde, and R. Rottapel. 2005. The Rho GTP exchange factor Lfc promotes spindle assembly in early mitosis. *Proc Natl Acad Sci U S A*. 102:9529-9534.

Balsamo, J., C. Arregui, T. Leung, and J. Lilien. 1998. The nonreceptor protein tyrosine phosphatase PTP1B binds to the cytoplasmic domain of N-cadherin and regulates the cadherin-actin linkage. *J Cell Biol*. 143:523-532.

Baumeister, U., R. Funke, K. Ebnet, H. Vorschmitt, S. Koch, and D. Vestweber. 2005. Association of Csk to VE-cadherin and inhibition of cell proliferation. *EMBO J*. 24:1686-1695.

Baumer, S., L. Keller, A. Holtmann, R. Funke, B. August, A. Gamp, H. Wolburg, K. Wolburg-Buchholz, U. Deutsch, and D. Vestweber. 2006. Vascular endothelial cell-specific phosphotyrosine phosphatase (VE-PTP) activity is required for blood vessel development. *Blood*. 107:4754-4762.

Beltran, P.J., and J.L. Bixby. 2003. Receptor protein tyrosine phosphatases as mediators of cellular adhesion. *Front Biosci*. 8:d87-99.

Birkenfeld, J., P. Nalbant, B.P. Bohl, O. Pertz, K.M. Hahn, and G.M. Bokoch. 2007. GEF-H1 modulates localized RhoA activation during cytokinesis under the control of mitotic kinases. *Dev Cell*. 12:699-712.

Birkenfeld, J., P. Nalbant, S.H. Yoon, and G.M. Bokoch. 2008. Cellular functions of GEF-H1, a microtubule-regulated Rho-GEF: is altered GEF-H1 activity a crucial determinant of disease pathogenesis? *Trends Cell Biol*. 18:210-219.

Birukova, A.A., D. Adyshev, B. Gorshkov, G.M. Bokoch, K.G. Birukov, and A.D. Verin. 2006. GEF-H1 is involved in agonist-induced human pulmonary endothelial barrier dysfunction. *Am J Physiol Lung Cell Mol Physiol*. 290:L540-548.

Birukova, A.A., P. Fu, J. Xing, B. Yakubov, I. Cokic, and K.G. Birukov. 2010. Mechanotransduction by GEF-H1 as a novel mechanism of ventilator-induced vascular endothelial permeability. *Am J Physiol Lung Cell Mol Physiol*. 298:L837-848.

Birukova, A.A., K. Smurova, K.G. Birukov, P. Usatyuk, F. Liu, K. Kaibuchi, A. Ricks-Cord, V. Natarajan, I. Alieva, J.G. Garcia, and A.D. Verin. 2004. Microtubule disassembly induces cytoskeletal remodeling and lung vascular barrier dysfunction: role of Rho-dependent mechanisms. *J Cell Physiol*. 201:55-70.

Bishop, A.L., and A. Hall. 2000. Rho GTPases and their effector proteins. *Biochem J*. 348 Pt 2:241-255.

Braga, V.M., L.M. Machesky, A. Hall, and N.A. Hotchin. 1997. The small GTPases Rho and Rac are required for the establishment of cadherin-dependent cell-cell contacts. *J Cell Biol*. 137:1421-1431.

Breviario, F., L. Caveda, M. Corada, I. Martin-Padura, P. Navarro, J. Golay, M. Introna, D. Gulino, M.G. Lampugnani, and E. Dejana. 1995. Functional properties of human vascular endothelial cadherin (7B4/cadherin-5), an endothelium-specific cadherin. *Arterioscler Thromb Vasc Biol*. 15:1229-1239.

Broermann, A., M. Winderlich, H. Block, M. Frye, J. Rossaint, A. Zarbock, G. Cagna, R. Linnepe, D. Schulte, A.F. Nottebaum, and D. Vestweber. 2011. Dissociation of VE-PTP from VE-cadherin is required for leukocyte extravasation and for VEGF-induced vascular permeability in vivo. *J Exp Med*. 208:2393-2401.

Butler, J.P., I.M. Tolic-Norrelykke, B. Fabry, and J.J. Fredberg. 2002. Traction fields, moments, and strain energy that cells exert on their surroundings. *Am J Physiol Cell Physiol*. 282:C595-605.

Cain, R.J., B. Vanhaesebroeck, and A.J. Ridley. 2010. The PI3K p110alpha isoform regulates endothelial adherens junctions via Pyk2 and Rac1. *J Cell Biol*. 188:863-876.

Callow, M.G., S. Zozulya, M.L. Gishizky, B. Jallal, and T. Smeal. 2005. PAK4 mediates morphological changes through the regulation of GEF-H1. *J Cell Sci*. 118:1861-1872.

Carman, C.V., and T.A. Springer. 2004. A transmigratory cup in leukocyte diapedesis both through individual vascular endothelial cells and between them. *J Cell Biol*. 167:377-388.

Carra, S., E. Foglia, S. Cermenati, E. Bresciani, C. Giampietro, C. Lora Lamia, E. Dejana, M. Beltrame, and F. Cotelli. 2012. Ve-ptp modulates vascular integrity by promoting adherens junction maturation. *PLoS One*. 7:e51245.

Chesla, S.E., P. Selvaraj, and C. Zhu. 1998. Measuring two-dimensional receptor-ligand binding kinetics by micropipette. *Biophys J*. 75:1553-1572.

Chiasson, C.M., K.B. Wittich, P.A. Vincent, V. Faundez, and A.P. Kowalczyk. 2009. p120-catenin inhibits VE-cadherin internalization through a Rho-independent mechanism. *Mol Biol Cell*. 20:1970-1980.

Chien, Y.H., N. Jiang, F. Li, F. Zhang, C. Zhu, and D. Leckband. 2008. Two stage cadherin kinetics require multiple extracellular domains but not the cytoplasmic region. *J Biol Chem*. 283:1848-1856.

Chudakov, D.M., S. Lukyanov, and K.A. Lukyanov. 2007. Using photoactivatable fluorescent protein Dendra2 to track protein movement. *Biotechniques*. 42:553, 555, 557 passim.

Cohen, D.M., M.T. Yang, and C.S. Chen. 2013. Measuring cell-cell tugging forces using bowtie-patterned mPADs (microarray post detectors). *Methods Mol Biol*. 1066:157-168.

Collares-Buzato, C.B., M.A. Jepson, N.L. Simmons, and B.H. Hirst. 1998. Increased tyrosine phosphorylation causes redistribution of adherens junction and tight junction proteins and perturbs paracellular barrier function in MDCK epithelia. *Eur J Cell Biol*. 76:85-92.

Conway, D.E., M.T. Breckenridge, E. Hinde, E. Gratton, C.S. Chen, and M.A. Schwartz. 2013. Fluid shear stress on endothelial cells modulates mechanical tension across VE-cadherin and PECAM-1. *Curr Biol*. 23:1024-1030.

Daneshjou, N., N. Sieracki, G.P. van Nieuw Amerongen, D.E. Conway, M.A. Schwartz, Y.A. Komarova, and A.B. Malik. 2015. Rac1 functions as a reversible tension modulator to stabilize VE-cadherin trans-interaction. *J Cell Biol*. 209:181.

Davidson, D., and A. Veillette. 2001. PTP-PEST, a scaffold protein tyrosine phosphatase, negatively regulates lymphocyte activation by targeting a unique set of substrates. *EMBO J*. 20:3414-3426.

Davis, M.A., R.C. Ireton, and A.B. Reynolds. 2003. A core function for p120-catenin in cadherin turnover. *J Cell Biol*. 163:525-534.

Dejana, E., F. Orsenigo, and M.G. Lampugnani. 2008. The role of adherens junctions and VE-cadherin in the control of vascular permeability. *J Cell Sci*. 121:2115-2122.

Del Vecchio, P.J., A. Siflinger-Birnboim, J.M. Shepard, R. Bizios, J.A. Cooper, and A.B. Malik. 1987. Endothelial monolayer permeability to macromolecules. *Fed Proc*. 46:2511-2515.

Dominguez, M.G., V.C. Hughes, L. Pan, M. Simmons, C. Daly, K. Anderson, I. Noguera-Troise, A.J. Murphy, D.M. Valenzuela, S. Davis, G. Thurston, G.D. Yancopoulos, and N.W. Gale. 2007. Vascular endothelial tyrosine phosphatase (VE-PTP)-null mice undergo vasculogenesis but die embryonically because of defects in angiogenesis. *Proc Natl Acad Sci U S A*. 104:3243-3248.

Dorland, Y.L., T.S. Malinova, A.M. van Stalborch, A.G. Grieve, D. van Geemen, N.S. Jansen, B.J. de Kreuk, K. Nawaz, J. Kole, D. Geerts, R.J. Musters, J. de Rooij, P.L. Hordijk, and S. Huveneers. 2016. The F-BAR protein pacsin2 inhibits asymmetric VE-cadherin internalization from tensile adherens junctions. *Nat Commun*. 7:12210.

Eliceiri, B.P., R. Paul, P.L. Schwartzberg, J.D. Hood, J. Leng, and D.A. Cheresh. 1999. Selective requirement for Src kinases during VEGF-induced angiogenesis and vascular permeability. *Mol Cell*. 4:915-924.

Esser, S., M.G. Lampugnani, M. Corada, E. Dejana, and W. Risau. 1998. Vascular endothelial growth factor induces VE-cadherin tyrosine phosphorylation in endothelial cells. *J Cell Sci*. 111 (Pt 13):1853-1865.

Fachinger, G., U. Deutsch, and W. Risau. 1999. Functional interaction of vascular endothelial-protein-tyrosine phosphatase with the angiopoietin receptor Tie-2. *Oncogene*. 18:5948-5953.

Feng, D., J.A. Nagy, K. Pyne, H.F. Dvorak, and A.M. Dvorak. 1998. Neutrophils emigrate from venules by a transendothelial cell pathway in response to FMLP. *J Exp Med*. 187:903-915.

Frye, M., M. Dierkes, V. Kuppers, M. Vockel, J. Tomm, D. Zeuschner, J. Rossaint, A. Zarbock, G.Y. Koh, K. Peters, A.F. Nottebaum, and D. Vestweber. 2015. Interfering with VE-PTP stabilizes endothelial junctions in vivo via Tie-2 in the absence of VE-cadherin. *J Exp Med*. 212:2267-2287.

Fujishiro, S.H., S. Tanimura, S. Mure, Y. Kashimoto, K. Watanabe, and M. Kohno. 2008. ERK1/2 phosphorylate GEF-H1 to enhance its guanine nucleotide exchange activity toward RhoA. *Biochem Biophys Res Commun*. 368:162-167.

Fujita, S., R.K. Puri, Z.X. Yu, W.D. Travis, and V.J. Ferrans. 1991. An ultrastructural study of in vivo interactions between lymphocytes and endothelial cells in the pathogenesis of the vascular leak syndrome induced by interleukin-2. *Cancer*. 68:2169-2174.

Gavard, J., and J.S. Gutkind. 2006. VEGF controls endothelial-cell permeability by promoting the beta-arrestin-dependent endocytosis of VE-cadherin. *Nat Cell Biol*. 8:1223-1234.

Gebbink, M.F., O. Kranenburg, M. Poland, F.P. van Horck, B. Houssa, and W.H. Moolenaar. 1997. Identification of a novel, putative Rho-specific GDP/GTP exchange factor and a RhoA-binding protein: control of neuronal morphology. *J Cell Biol*. 137:1603-1613.

Gong, H., X. Gao, S. Feng, M.R. Siddiqui, A. Garcia, M.G. Bonini, Y. Komarova, S.M. Vogel, D. Mehta, and A.B. Malik. 2014. Evidence of a common mechanism of disassembly of adherens junctions through Galpha13 targeting of VE-cadherin. *J Exp Med*. 211:579-591.

Gong, H., J. Rehman, H. Tang, K. Wary, M. Mittal, P. Chaturvedi, Y.Y. Zhao, Y.A. Komarova, S.M. Vogel, and A.B. Malik. 2015. HIF2alpha signaling inhibits adherens junctional disruption in acute lung injury. *J Clin Invest*. 125:652-664.

Grazia Lampugnani, M., A. Zanetti, M. Corada, T. Takahashi, G. Balconi, F. Breviario, F. Orsenigo, A. Cattelino, R. Kemler, T.O. Daniel, and E. Dejana. 2003. Contact inhibition of VEGF-induced proliferation requires vascular endothelial cadherin, beta-catenin, and the phosphatase DEP-1/CD148. *J Cell Biol*. 161:793-804.

Gurnik, S., K. Devraj, J. Macas, M. Yamaji, J. Starke, A. Scholz, K. Sommer, M. Di Tacchio, R. Vutukuri, H. Beck, M. Mittelbronn, C. Foerch, W. Pfeilschifter, S. Liebner, K.G. Peters, K.H. Plate, and Y. Reiss. 2016. Angiopoietin-2-induced blood-brain barrier compromise and increased stroke size are rescued by VE-PTP-dependent restoration of Tie2 signaling. *Acta Neuropathol*. 131:753-773.

Han, J., G. Zhang, E.J. Welch, Y. Liang, J. Fu, S.M. Vogel, C.A. Lowell, X. Du, D.A. Cheresh, A.B. Malik, and Z. Li. 2013. A critical role for Lyn kinase in strengthening endothelial integrity and barrier function. *Blood*. 122:4140-4149.

Hart, M.J., X. Jiang, T. Kozasa, W. Roscoe, W.D. Singer, A.G. Gilman, P.C. Sternweis, and G. Bollag. 1998. Direct stimulation of the guanine nucleotide exchange activity of p115 RhoGEF by Galpha13. *Science*. 280:2112-2114.

Hayashi, M., A. Majumdar, X. Li, J. Adler, Z. Sun, S. Vertuani, C. Hellberg, S. Mellberg, S. Koch, A. Dimberg, G.Y. Koh, E. Dejana, H.G. Belting, M. Affolter, G. Thurston, L. Holmgren, D. Vestweber, and L. Claesson-Welsh. 2013. VE-PTP regulates VEGFR2 activity in stalk cells to establish endothelial cell polarity and lumen formation. *Nat Commun*. 4:1672.

Herbrand, U., and M.R. Ahmadian. 2006. p190-RhoGAP as an integral component of the Tiam1/Rac1-induced downregulation of Rho. *Biol Chem*. 387:311-317.

Holinstat, M., D. Mehta, T. Kozasa, R.D. Minshall, and A.B. Malik. 2003. Protein kinase Calpha-induced p115RhoGEF phosphorylation signals endothelial cytoskeletal rearrangement. *J Biol Chem*. 278:28793-28798.

Holsinger, L.J., K. Ward, B. Duffield, J. Zachwieja, and B. Jallal. 2002. The transmembrane receptor protein tyrosine phosphatase DEP1 interacts with p120(ctn). *Oncogene*. 21:7067-7076.

Hou, W.H., I.H. Liu, C.C. Tsai, F.E. Johnson, S.S. Huang, and J.S. Huang. 2011. CRSBP-1/LYVE-1 ligands disrupt lymphatic intercellular adhesion by inducing tyrosine phosphorylation and internalization of VE-cadherin. *J Cell Sci*. 124:1231-1244.

Huveneers, S., J. Oldenburg, E. Spanjaard, G. van der Krogt, I. Grigoriev, A. Akhmanova, H. Rehmann, and J. de Rooij. 2012. Vinculin associates with endothelial VE-cadherin junctions to control force-dependent remodeling. *J Cell Biol*. 196:641-652.

Johnson, D.S., and Y.H. Chen. 2012. Ras family of small GTPases in immunity and inflammation. *Curr Opin Pharmacol*. 12:458-463.

Kakiashvili, E., P. Speight, F. Waheed, R. Seth, M. Lodyga, S. Tanimura, M. Kohno, O.D. Rotstein, A. Kapus, and K. Szaszi. 2009. GEF-H1 mediates tumor necrosis factor-alpha-induced Rho activation and myosin phosphorylation: role in the regulation of tubular paracellular permeability. *J Biol Chem*. 284:11454-11466.

Kofler, R., and G. Wick. 1977. Some methodologic aspects of the chromium chloride method for coupling antigen to erythrocytes. *J Immunol Methods*. 16:201-209.

Komarova, Y.A., K. Kruse, D. Mehta, and A.B. Malik. 2017. Protein Interactions at Endothelial Junctions and Signaling Mechanisms Regulating Endothelial Permeability. *Circ Res*. 120:179-206.

Kozasa, T., X. Jiang, M.J. Hart, P.M. Sternweis, W.D. Singer, A.G. Gilman, G. Bollag, and P.C. Sternweis. 1998. p115 RhoGEF, a GTPase activating protein for Galpha12 and Galpha13. *Science*. 280:2109-2111.

Krendel, M., F.T. Zenke, and G.M. Bokoch. 2002. Nucleotide exchange factor GEF-H1 mediates cross-talk between microtubules and the actin cytoskeleton. *Nat Cell Biol*. 4:294-301.

Krueger, N.X., and H. Saito. 1992. A human transmembrane protein-tyrosine-phosphatase, PTP zeta, is expressed in brain and has an N-terminal receptor domain homologous to carbonic anhydrases. *Proc Natl Acad Sci U S A*. 89:7417-7421.

Krueger, N.X., M. Streuli, and H. Saito. 1990. Structural diversity and evolution of human receptor-like protein tyrosine phosphatases. *EMBO J*. 9:3241-3252.

Kruse, K., Q.S. Lee, Y. Sun, J. Klomp, X. Yang, F. Huang, M.Y. Sun, S. Zhao, Z. Hong, S.M. Vogel, J.W. Shin, D.E. Leckband, L.M. Tai, A.B. Malik, and Y.A. Komarova. 2018. N-cadherin signaling via Trio assembles adherens junctions to restrict endothelial permeability. *J Cell Biol*.

Kurokawa, K., and M. Matsuda. 2005. Localized RhoA activation as a requirement for the induction of membrane ruffling. *Mol Biol Cell*. 16:4294-4303.

Lampugnani, M.G., M. Corada, P. Andriopoulou, S. Esser, W. Risau, and E. Dejana. 1997. Cell confluence regulates tyrosine phosphorylation of adherens junction components in endothelial cells. *J Cell Sci*. 110 (Pt 17):2065-2077.

Lampugnani, M.G., M. Corada, L. Caveda, F. Breviario, O. Ayalon, B. Geiger, and E. Dejana. 1995. The molecular organization of endothelial cell to cell junctions: differential association of plakoglobin, beta-catenin, and alpha-catenin with vascular endothelial cadherin (VE-cadherin). *J Cell Biol*. 129:203-217.

Lampugnani, M.G., A. Zanetti, F. Breviario, G. Balconi, F. Orsenigo, M. Corada, R. Spagnuolo, M. Betson, V. Braga, and E. Dejana. 2002. VE-cadherin regulates endothelial actin activating Rac and increasing membrane association of Tiam. *Mol Biol Cell*. 13:1175-1189.

Lansbergen, G., Y. Komarova, M. Modesti, C. Wyman, C.C. Hoogenraad, H.V. Goodson, R.P. Lemaitre, D.N. Drechsel, E. van Munster, T.W. Gadella, Jr., F. Grosveld, N. Galjart,

G.G. Borisy, and A. Akhmanova. 2004. Conformational changes in CLIP-170 regulate its binding to microtubules and dynactin localization. *J Cell Biol*. 166:1003-1014.

Lee, W.L., and A.S. Slutsky. 2010. Sepsis and endothelial permeability. *N Engl J Med*. 363:689-691.

Li, X., N. Padhan, E.O. Sjostrom, F.P. Roche, C. Testini, N. Honkura, M. Sainz-Jaspeado, E. Gordon, K. Bentley, A. Philippides, V. Tolmachev, E. Dejana, R.V. Stan, D. Vestweber, K. Ballmer-Hofer, C. Betsholtz, K. Pietras, L. Jansson, and L. Claesson-Welsh. 2016. VEGFR2 pY949 signalling regulates adherens junction integrity and metastatic spread. *Nat Commun*. 7:11017.

Liebner, S., U. Kniesel, H. Kalbacher, and H. Wolburg. 2000. Correlation of tight junction morphology with the expression of tight junction proteins in blood-brain barrier endothelial cells. *Eur J Cell Biol*. 79:707-717.

Lilien, J., and J. Balsamo. 2005. The regulation of cadherin-mediated adhesion by tyrosine phosphorylation/dephosphorylation of beta-catenin. *Curr Opin Cell Biol*. 17:459-465.

Liu, Y., C. Collins, W.B. Kiosses, A.M. Murray, M. Joshi, T.R. Shepherd, E.J. Fuentes, and E. Tzima. 2013. A novel pathway spatiotemporally activates Rac1 and redox signaling in response to fluid shear stress. *J Cell Biol*. 201:863-873.

MacNevin, C.J., A. Toutchkine, D.J. Marston, C.W. Hsu, D. Tsygankov, L. Li, B. Liu, T. Qi, D.V. Nguyen, and K.M. Hahn. 2016. Ratiometric Imaging Using a Single Dye Enables Simultaneous Visualization of Rac1 and Cdc42 Activation. *J Am Chem Soc*. 138:2571-2575.

Majno, G., and G.E. Palade. 1961. Studies on inflammation. 1. The effect of histamine and serotonin on vascular permeability: an electron microscopic study. *J Biophys Biochem Cytol*. 11:571-605.

Mamdouh, Z., A. Mikhailov, and W.A. Muller. 2009. Transcellular migration of leukocytes is mediated by the endothelial lateral border recycling compartment. *J Exp Med*. 206:2795-2808.

Matsuyoshi, N., M. Hamaguchi, S. Taniguchi, A. Nagafuchi, S. Tsukita, and M. Takeichi. 1992. Cadherin-mediated cell-cell adhesion is perturbed by v-src tyrosine phosphorylation in metastatic fibroblasts. *J Cell Biol*. 118:703-714.

Miyashita, Y., and M. Ozawa. 2007. Increased internalization of p120-uncoupled E-cadherin and a requirement for a dileucine motif in the cytoplasmic domain for endocytosis of the protein. *J Biol Chem*. 282:11540-11548.

Monaghan-Benson, E., and K. Burridge. 2013. VE-cadherin status as an indicator of microvascular permeability. *Methods Mol Biol*. 1046:335-342.

Muhamed, I., J. Wu, P. Sehgal, X. Kong, A. Tajik, N. Wang, and D.E. Leckband. 2016. E-cadherin-mediated force transduction signals regulate global cell mechanics. *J Cell Sci*. 129:1843-1854.

Nalbant, P., Y.C. Chang, J. Birkenfeld, Z.F. Chang, and G.M. Bokoch. 2009. Guanine nucleotide exchange factor-H1 regulates cell migration via localized activation of RhoA at the leading edge. *Mol Biol Cell*. 20:4070-4082.

Navarro, P., L. Caveda, F. Breviario, I. Mandoteanu, M.G. Lampugnani, and E. Dejana. 1995. Catenin-dependent and -independent functions of vascular endothelial cadherin. *J Biol Chem*. 270:30965-30972.

Nawroth, R., G. Poell, A. Ranft, S. Kloep, U. Samulowitz, G. Fachinger, M. Golding, D.T. Shima, U. Deutsch, and D. Vestweber. 2002. VE-PTP and VE-cadherin ectodomains

interact to facilitate regulation of phosphorylation and cell contacts. *EMBO J*. 21:4885-4895.

Niu, J., J. Profirovic, H. Pan, R. Vaiskunaite, and T. Voyno-Yasenetskaya. 2003. G Protein betagamma subunits stimulate p114RhoGEF, a guanine nucleotide exchange factor for RhoA and Rac1: regulation of cell shape and reactive oxygen species production. *Circ Res*. 93:848-856.

Nobes, C.D., and A. Hall. 1995. Rho, rac, and cdc42 GTPases regulate the assembly of multimolecular focal complexes associated with actin stress fibers, lamellipodia, and filopodia. *Cell*. 81:53-62.

Nottebaum, A.F., G. Cagna, M. Winderlich, A.C. Gamp, R. Linnepe, C. Polaschegg, K. Filippova, R. Lyck, B. Engelhardt, O. Kamenyeva, M.G. Bixel, S. Butz, and D. Vestweber. 2008. VE-PTP maintains the endothelial barrier via plakoglobin and becomes dissociated from VE-cadherin by leukocytes and by VEGF. *J Exp Med*. 205:2929-2945.

Nourshargh, S., P.L. Hordijk, and M. Sixt. 2010. Breaching multiple barriers: leukocyte motility through venular walls and the interstitium. *Nat Rev Mol Cell Biol*. 11:366-378.

Orsenigo, F., C. Giampietro, A. Ferrari, M. Corada, A. Galaup, S. Sigismund, G. Ristagno, L. Maddaluno, G.Y. Koh, D. Franco, V. Kurtcuoglu, D. Poulikakos, P. Baluk, D. McDonald, M. Grazia Lampugnani, and E. Dejana. 2012. Phosphorylation of VE-cadherin is modulated by haemodynamic forces and contributes to the regulation of vascular permeability in vivo. *Nat Commun*. 3:1208.

Pappenheimer, J.R., E.M. Renkin, and L.M. Borrero. 1951. Filtration, diffusion and molecular sieving through peripheral capillary membranes; a contribution to the pore theory of capillary permeability. *Am J Physiol*. 167:13-46.

Patel, M., and A.V. Karginov. 2014. Phosphorylation-mediated regulation of GEFs for RhoA. *Cell Adh Migr*. 8:11-18.

Pathak, R., V.D. Delorme-Walker, M.C. Howell, A.N. Anselmo, M.A. White, G.M. Bokoch, and C. Dermardirossian. 2012. The microtubule-associated Rho activating factor GEF-H1 interacts with exocyst complex to regulate vesicle traffic. *Dev Cell*. 23:397-411.

Patterson, K.I., T. Brummer, P.M. O'Brien, and R.J. Daly. 2009. Dual-specificity phosphatases: critical regulators with diverse cellular targets. *Biochem J*. 418:475-489.

Pertz, O., L. Hodgson, R.L. Klemke, and K.M. Hahn. 2006. Spatiotemporal dynamics of RhoA activity in migrating cells. *Nature*. 440:1069-1072.

Piedra, J., S. Miravet, J. Castano, H.G. Palmer, N. Heisterkamp, A. Garcia de Herreros, and M. Dunach. 2003. p120 Catenin-associated Fer and Fyn tyrosine kinases regulate beta-catenin Tyr-142 phosphorylation and beta-catenin-alpha-catenin Interaction. *Mol Cell Biol*. 23:2287-2297.

Potter, M.D., S. Barbero, and D.A. Cheresh. 2005. Tyrosine phosphorylation of VE-cadherin prevents binding of p120- and beta-catenin and maintains the cellular mesenchymal state. *J Biol Chem*. 280:31906-31912.

Quaggin, S.N.H.A., Chicago, Illinois, 60614, US). 2017. VE-PTP KNOCKOUT. MANNIN RESEARCH INC. (629 Eastern Avenue, Ste C300Toronto, Ontario M4M 1E4, CA).

Radeva, M.Y., and J. Waschke. 2018. Mind the gap: mechanisms regulating the endothelial barrier. *Acta Physiol (Oxf)*. 222.

Raftopoulou, M., and A. Hall. 2004. Cell migration: Rho GTPases lead the way. *Dev Biol*. 265:23-32.

Ren, Y., R. Li, Y. Zheng, and H. Busch. 1998. Cloning and characterization of GEF-H1, a microtubule-associated guanine nucleotide exchange factor for Rac and Rho GTPases. *J Biol Chem*. 273:34954-34960.

Ridley, A.J., and A. Hall. 1992. The small GTP-binding protein rho regulates the assembly of focal adhesions and actin stress fibers in response to growth factors. *Cell*. 70:389-399.

Rojas, A.M., G. Fuentes, A. Rausell, and A. Valencia. 2012. The Ras protein superfamily: evolutionary tree and role of conserved amino acids. *J Cell Biol*. 196:189-201.

Samarin, S.N., A.I. Ivanov, G. Flatau, C.A. Parkos, and A. Nusrat. 2007. Rho/Rho-associated kinase-II signaling mediates disassembly of epithelial apical junctions. *Mol Biol Cell*. 18:3429-3439.

Schmidt, T.T., M. Tauseef, L. Yue, M.G. Bonini, J. Gothert, T.L. Shen, J.L. Guan, S. Predescu, R. Sadikot, and D. Mehta. 2013. Conditional deletion of FAK in mice endothelium disrupts lung vascular barrier function due to destabilization of RhoA and Rac1 activities. *Am J Physiol Lung Cell Mol Physiol*. 305:L291-300.

Schossleitner, K., S. Rauscher, M. Groger, H.P. Friedl, R. Finsterwalder, A. Habertheuer, M. Sibilia, C. Brostjan, D. Fodinger, S. Citi, and P. Petzelbauer. 2016. Evidence That Cingulin Regulates Endothelial Barrier Function In Vitro and In Vivo. *Arterioscler Thromb Vasc Biol*. 36:647-654.

Schulte, D., V. Kuppers, N. Dartsch, A. Broermann, H. Li, A. Zarbock, O. Kamenyeva, F. Kiefer, A. Khandoga, S. Massberg, and D. Vestweber. 2011. Stabilizing the VE-cadherin-catenin complex blocks leukocyte extravasation and vascular permeability. *EMBO J*. 30:4157-4170.

Schumacher, M.A., J.L. Todd, A.E. Rice, K.G. Tanner, and J.M. Denu. 2002. Structural basis for the recognition of a bisphosphorylated MAP kinase peptide by human VHR protein Phosphatase. *Biochemistry*. 41:3009-3017.

Shashikanth, N., Y.I. Petrova, S. Park, J. Chekan, S. Maiden, M. Spano, T. Ha, B.M. Gumbiner, and D.E. Leckband. 2015. Allosteric Regulation of E-Cadherin Adhesion. *J Biol Chem*. 290:21749-21761.

Shcherbakova, D.M., N. Cox Cammer, T.M. Huisman, V.V. Verkhusha, and L. Hodgson. 2018. Direct multiplex imaging and optogenetics of Rho GTPases enabled by near-infrared FRET. *Nat Chem Biol*. 14:591-600.

Shen, J., M. Frye, B.L. Lee, J.L. Reinardy, J.M. McClung, K. Ding, M. Kojima, H. Xia, C. Seidel, R. Lima e Silva, A. Dong, S.F. Hackett, J. Wang, B.W. Howard, D. Vestweber, C.D. Kontos, K.G. Peters, and P.A. Campochiaro. 2014. Targeting VE-PTP activates TIE2 and stabilizes the ocular vasculature. *J Clin Invest*. 124:4564-4576.

Siflinger-Birnboim, A., P.J. Del Vecchio, J.A. Cooper, F.A. Blumenstock, J.M. Shepard, and A.B. Malik. 1987. Molecular sieving characteristics of the cultured endothelial monolayer. *J Cell Physiol*. 132:111-117.

Soni, D., S.C. Regmi, D.M. Wang, A. DebRoy, Y.Y. Zhao, S.M. Vogel, A.B. Malik, and C. Tiruppathi. 2017. Pyk2 phosphorylation of VE-PTP downstream of STIM1-induced Ca(2+) entry regulates disassembly of adherens junctions. *Am J Physiol Lung Cell Mol Physiol*. 312:L1003-L1017.

Souma, T., B.R. Thomson, S. Heinen, I. Anna Carota, S. Yamaguchi, T. Onay, P. Liu, A.K. Ghosh, C. Li, V. Eremina, Y.K. Hong, A.N. Economides, D. Vestweber, K.G. Peters, J. Jin, and S.E. Quaggin. 2018. Context-dependent functions of angiopoietin 2 are

determined by the endothelial phosphatase VEPTP. *Proc Natl Acad Sci U S A*. 115:1298-1303.

Stockton, R.A., R. Shenkar, I.A. Awad, and M.H. Ginsberg. 2010. Cerebral cavernous malformations proteins inhibit Rho kinase to stabilize vascular integrity. *J Exp Med*. 207:881-896.

Sui, X.F., T.D. Kiser, S.W. Hyun, D.J. Angelini, R.L. Del Vecchio, B.A. Young, J.D. Hasday, L.H. Romer, A. Passaniti, N.K. Tonks, and S.E. Goldblum. 2005. Receptor protein tyrosine phosphatase micro regulates the paracellular pathway in human lung microvascular endothelia. *Am J Pathol*. 166:1247-1258.

Szulcek, R., C.M. Beckers, J. Hodzic, J. de Wit, Z. Chen, T. Grob, R.J. Musters, R.D. Minshall, V.W. van Hinsbergh, and G.P. van Nieuw Amerongen. 2013. Localized RhoA GTPase activity regulates dynamics of endothelial monolayer integrity. *Cardiovasc Res*. 99:471-482.

Tabdili, H., A.K. Barry, M.D. Langer, Y.H. Chien, Q. Shi, K.J. Lee, S. Lu, and D.E. Leckband. 2012a. Cadherin point mutations alter cell sorting and modulate GTPase signaling. *J Cell Sci*. 125:3299-3309.

Tabdili, H., M. Langer, Q. Shi, Y.C. Poh, N. Wang, and D. Leckband. 2012b. Cadherin-dependent mechanotransduction depends on ligand identity but not affinity. *J Cell Sci*. 125:4362-4371.

Takahashi, K., R. Kim, C. Lauhan, Y. Park, N.G. Nguyen, D. Vestweber, M.G. Dominguez, D.M. Valenzuela, A.J. Murphy, G.D. Yancopoulos, N.W. Gale, and T. Takahashi. 2017. Expression of receptor-type protein tyrosine phosphatase in developing and adult renal vasculature. *PLoS One*. 12:e0177192.

Takeichi, M., and S. Nakagawa. 2001. Cadherin-dependent cell-cell adhesion. *Curr Protoc Cell Biol*. Chapter 9:Unit 9 3.

Thurston, G., C. Suri, K. Smith, J. McClain, T.N. Sato, G.D. Yancopoulos, and D.M. McDonald. 1999. Leakage-resistant blood vessels in mice transgenically overexpressing angiopoietin-1. *Science*. 286:2511-2514.

Tiganis, T., and A.M. Bennett. 2007. Protein tyrosine phosphatase function: the substrate perspective. *Biochem J*. 402:1-15.

Timmerman, I., M. Hoogenboezem, A.M. Bennett, D. Geerts, P.L. Hordijk, and J.D. van Buul. 2012. The tyrosine phosphatase SHP2 regulates recovery of endothelial adherens junctions through control of beta-catenin phosphorylation. *Mol Biol Cell*. 23:4212-4225.

Tonks, N.K. 2006. Protein tyrosine phosphatases: from genes, to function, to disease. *Nat Rev Mol Cell Biol*. 7:833-846.

Tornavaca, O., M. Chia, N. Dufton, L.O. Almagro, D.E. Conway, A.M. Randi, M.A. Schwartz, K. Matter, and M.S. Balda. 2015. ZO-1 controls endothelial adherens junctions, cell-cell tension, angiogenesis, and barrier formation. *J Cell Biol*. 208:821-838.

Tsai, C.F., Y.T. Wang, Y.R. Chen, C.Y. Lai, P.Y. Lin, K.T. Pan, J.Y. Chen, K.H. Khoo, and Y.J. Chen. 2008. Immobilized metal affinity chromatography revisited: pH/acid control toward high selectivity in phosphoproteomics. *J Proteome Res*. 7:4058-4069.

Tse, J.R., and A.J. Engler. 2010. Preparation of hydrogel substrates with tunable mechanical properties. *Curr Protoc Cell Biol*. Chapter 10:Unit 10 16.

Ukropec, J.A., M.K. Hollinger, S.M. Salva, and M.J. Woolkalis. 2000. SHP2 association with VE-cadherin complexes in human endothelial cells is regulated by thrombin. *J Biol Chem*. 275:5983-5986.

van Buul, J.D., D. Geerts, and S. Huveneers. 2014. Rho GAPs and GEFs: controling switches in endothelial cell adhesion. *Cell Adh Migr*. 8:108-124.

van Nieuw Amerongen, G.P., C.M. Beckers, I.D. Achekar, S. Zeeman, R.J. Musters, and V.W. van Hinsbergh. 2007. Involvement of Rho kinase in endothelial barrier maintenance. *Arterioscler Thromb Vasc Biol*. 27:2332-2339.

van Nieuw Amerongen, G.P., S. van Delft, M.A. Vermeer, J.G. Collard, and V.W. van Hinsbergh. 2000. Activation of RhoA by thrombin in endothelial hyperpermeability: role of Rho kinase and protein tyrosine kinases. *Circ Res*. 87:335-340.

Vandenbroucke St Amant, E., M. Tauseef, S.M. Vogel, X.P. Gao, D. Mehta, Y.A. Komarova, and A.B. Malik. 2012. PKCalpha activation of p120-catenin serine 879 phospho-switch disassembles VE-cadherin junctions and disrupts vascular integrity. *Circ Res*. 111:739-749.

Vestweber, D. 2008. VE-cadherin: the major endothelial adhesion molecule controlling cellular junctions and blood vessel formation. *Arterioscler Thromb Vasc Biol*. 28:223-232.

Vestweber, D. 2012. Relevance of endothelial junctions in leukocyte extravasation and vascular permeability. *Ann N Y Acad Sci*. 1257:184-192.

Vestweber, D., F. Wessel, and A.F. Nottebaum. 2014. Similarities and differences in the regulation of leukocyte extravasation and vascular permeability. *Semin Immunopathol*. 36:177-192.

Vetter, I.R., and A. Wittinghofer. 2001. The guanine nucleotide-binding switch in three dimensions. *Science*. 294:1299-1304.

Vockel, M., and D. Vestweber. 2013. How T cells trigger the dissociation of the endothelial receptor phosphatase VE-PTP from VE-cadherin. *Blood*. 122:2512-2522.

Volberg, T., Y. Zick, R. Dror, I. Sabanay, C. Gilon, A. Levitzki, and B. Geiger. 1992. The effect of tyrosine-specific protein phosphorylation on the assembly of adherens-type junctions. *EMBO J*. 11:1733-1742.

von Thun, A., C. Preisinger, O. Rath, J.P. Schwarz, C. Ward, N. Monsefi, J. Rodriguez, A. Garcia-Munoz, M. Birtwistle, W. Bienvenut, K.I. Anderson, W. Kolch, and A. von Kriegsheim. 2013. Extracellular signal-regulated kinase regulates RhoA activation and tumor cell plasticity by inhibiting guanine exchange factor H1 activity. *Mol Cell Biol*. 33:4526-4537.

Vouret-Craviari, V., C. Bourcier, E. Boulter, and E. van Obberghen-Schilling. 2002. Distinct signals via Rho GTPases and Src drive shape changes by thrombin and sphingosine-1-phosphate in endothelial cells. *J Cell Sci*. 115:2475-2484.

Wallez, Y., F. Cand, F. Cruzalegui, C. Wernstedt, S. Souchelnytskyi, I. Vilgrain, and P. Huber. 2007. Src kinase phosphorylates vascular endothelial-cadherin in response to vascular endothelial growth factor: identification of tyrosine 685 as the unique target site. *Oncogene*. 26:1067-1077.

Weis, S., S. Shintani, A. Weber, R. Kirchmair, M. Wood, A. Cravens, H. McSharry, A. Iwakura, Y.S. Yoon, N. Himes, D. Burstein, J. Doukas, R. Soll, D. Losordo, and D. Cheresh. 2004. Src blockade stabilizes a Flk/cadherin complex, reducing edema and tissue injury following myocardial infarction. *J Clin Invest*. 113:885-894.

Wennerberg, K., K.L. Rossman, and C.J. Der. 2005. The Ras superfamily at a glance. *J Cell Sci*. 118:843-846.

Wessel, F., M. Winderlich, M. Holm, M. Frye, R. Rivera-Galdos, M. Vockel, R. Linnepe, U. Ipe, A. Stadtmann, A. Zarbock, A.F. Nottebaum, and D. Vestweber. 2014. Leukocyte

extravasation and vascular permeability are each controlled in vivo by different tyrosine residues of VE-cadherin. *Nat Immunol*. 15:223-230.

Wildenberg, G.A., M.R. Dohn, R.H. Carnahan, M.A. Davis, N.A. Lobdell, J. Settleman, and A.B. Reynolds. 2006. p120-catenin and p190RhoGAP regulate cell-cell adhesion by coordinating antagonism between Rac and Rho. *Cell*. 127:1027-1039.

Winderlich, M., L. Keller, G. Cagna, A. Broermann, O. Kamenyeva, F. Kiefer, U. Deutsch, A.F. Nottebaum, and D. Vestweber. 2009. VE-PTP controls blood vessel development by balancing Tie-2 activity. *J Cell Biol*. 185:657-671.

Wojciak-Stothard, B., S. Potempa, T. Eichholtz, and A.J. Ridley. 2001. Rho and Rac but not Cdc42 regulate endothelial cell permeability. *J Cell Sci*. 114:1343-1355.

Woodfin, A., M.B. Voisin, M. Beyrau, B. Colom, D. Caille, F.M. Diapouli, G.B. Nash, T. Chavakis, S.M. Albelda, G.E. Rainger, P. Meda, B.A. Imhof, and S. Nourshargh. 2011. The junctional adhesion molecule JAM-C regulates polarized transendothelial migration of neutrophils in vivo. *Nat Immunol*. 12:761-769.

Xiao, K., D.F. Allison, M.D. Kottke, S. Summers, G.P. Sorescu, V. Faundez, and A.P. Kowalczyk. 2003. Mechanisms of VE-cadherin processing and degradation in microvascular endothelial cells. *J Biol Chem*. 278:19199-19208.

Xiao, K., J. Garner, K.M. Buckley, P.A. Vincent, C.M. Chiasson, E. Dejana, V. Faundez, and A.P. Kowalczyk. 2005. p120-Catenin regulates clathrin-dependent endocytosis of VE-cadherin. *Mol Biol Cell*. 16:5141-5151.

Xu, Y., and G.J. Fisher. 2012. Receptor type protein tyrosine phosphatases (RPTPs) - roles in signal transduction and human disease. *J Cell Commun Signal*. 6:125-138.

Yamada, S., and W.J. Nelson. 2007. Localized zones of Rho and Rac activities drive initiation and expansion of epithelial cell-cell adhesion. *J Cell Biol*. 178:517-527.

Yamahashi, Y., Y. Saito, N. Murata-Kamiya, and M. Hatakeyama. 2011. Polarity-regulating kinase partitioning-defective 1b (PAR1b) phosphorylates guanine nucleotide exchange factor H1 (GEF-H1) to regulate RhoA-dependent actin cytoskeletal reorganization. *J Biol Chem*. 286:44576-44584.

Yang, M.T., J. Fu, Y.K. Wang, R.A. Desai, and C.S. Chen. 2011. Assaying stem cell mechanobiology on microfabricated elastomeric substrates with geometrically modulated rigidity. *Nat Protoc*. 6:187-213.

Yeh, Y.T., R. Serrano, J. Francois, J.J. Chiu, Y.J. Li, J.C. Del Alamo, S. Chien, and J.C. Lasheras. 2018. Three-dimensional forces exerted by leukocytes and vascular endothelial cells dynamically facilitate diapedesis. *Proc Natl Acad Sci U S A*. 115:133-138.

Young, B.A., X. Sui, T.D. Kiser, S.W. Hyun, P. Wang, S. Sakarya, D.J. Angelini, K.L. Schaphorst, J.D. Hasday, A.S. Cross, L.H. Romer, A. Passaniti, and S.E. Goldblum. 2003. Protein tyrosine phosphatase activity regulates endothelial cell-cell interactions, the paracellular pathway, and capillary tube stability. *Am J Physiol Lung Cell Mol Physiol*. 285:L63-75.

Yuan, S.Y., and R.R. Rigor. 2010. *In* Regulation of Endothelial Barrier Function, San Rafael (CA).

Zenke, F.T., M. Krendel, C. DerMardirossian, C.C. King, B.P. Bohl, and G.M. Bokoch. 2004. p21-activated kinase 1 phosphorylates and regulates 14-3-3 binding to GEF-H1, a microtubule-localized Rho exchange factor. *J Biol Chem*. 279:18392-18400.

Zhao, Y., K.K. Ting, J. Li, V.C. Cogger, J. Chen, A. Johansson-Percival, S.F. Ngiow, J. Holst, G. Grau, S. Goel, T. Muller, E. Dejana, G. McCaughan, M.J. Smyth, R. Ganss, M.A.

Vadas, and J.R. Gamble. 2017. Targeting Vascular Endothelial-Cadherin in Tumor-Associated Blood Vessels Promotes T-cell-Mediated Immunotherapy. *Cancer Res*. 77:4434-4447.

8. VITA

NAME — Vanessa V. Juettner

EDUCATION — Ph.D. Pharmacology, University of Illinois, Chicago, IL, 2019

HONORS — NIH Lung Biology Training Grant, University of Illinois at Chicago, 2015-2017

PUBLICATIONS

Juettner VV, Kruse K, Dan A, Vu V, Khan Y, Le J, Leckband D, Komarova YA and Malik AB. "VE-PTP Interaction with GEF-H1 Stabilizes VE-cadherin Junctions and Basal Endothelial Permeability" *Journal of Cell Biology*, In Press.

Garcia AN*, **Juettner VV***, Vogel SM, Gao X, Komarova YA and Malik AB. "IQGAP1 through activation of the RhoGTPase Cdc42 promotes resolution of vascular injury". *Journal of Biological Chemistry,* In Preparation.

Juettner VV, Komarova YA, and Malik AB. "Two Faces of Janus: The Dual Role of VE-PTP in regulating the Adherens Junctions" *Circ. Res*., In Preparation.

Pearson RM, **Juettner VV**. "Biomolecular corona on nanoparticles: a survey of recent literature and its implications in targeted drug delivery." *Frontiers in Chemistry*, November 2014.

ABSTRACTS

Juettner V, Dan A, Leckband D, Komarova Y, Malik AB. VE-PTP Functions as a Scaffold to Stabilize the AJ and Endothelial Barrier. FASEB J, April 2018 32:1 699.14. Experimental Biology, San Diego, CA.

Juettner V, Dan A, Leckband D, Komarova Y, Malik AB. VE-PTP Scaffold Function in Adherens Junction Stabilization ASCB EMBO, December 2017. ASCB, Philadelphia, PA.

Juettner V, Dan A, Leckband D, Komarova Y, Malik AB. The Role of VE-PTP in Stabilizing the Adherens Junction Vasculata, July 2017.

Juettner V, Dan A, Leckband D, Komarova Y, Malik AB. The Role of VE-PTP Scaffold in Stabilizing the Adherens Junction FASEB J, April 2017 31:1 1065.2. Experimental Biology, Chicago, IL.